ALLAN DE AMORIM DOS SANTOS

AUXILIATED CELLULASE PRETREATMENT FOR OPTIMIZATION OF CELLULOSE NANOFIBRILS OBTENTION

LAVRAS-MG
2019

ALLAN DE AMORIM DOS SANTOS

AUXILIATED CELLULASE PRETREATMENT FOR OPTIMIZATION OF CELLULOSE NANOFIBRILS OBTENTION

Dissertação apresentada à Universidade Federal de Lavras, como parte das exigências do Programa de Pós-Graduação em Ciência e Tecnologia da Madeira, para a obtenção do título de Mestre.

Dr. Gustavo Henrique Denzin Tonoli
Orientador
Dra. Maria Alves Ferreira
Coorientadora

LAVRAS-MG
2019

Ficha catalográfica elaborada pelo Sistema de Geração de Ficha Catalográfica da Biblioteca Universitária da UFLA, com dados informados pelo(a) próprio(a) autor(a).

Santos, Allan de Amorim dos.
Auxiliated cellulase pretreatment for optimization of cellulose nanofibrils obtention / Allan de Amorim dos Santos. - 2019.
105 p. : il.

Orientador(a): Gustavo Henrique Denzin Tonoli.
Coorientador(a): Maria Alves Ferreira.
Dissertação (mestrado acadêmico) - Universidade Federal de Lavras, 2019.
Bibliografia.

1. Nanotecnologia florestal. 2. Hidrólise enzimática. 3. Nanocelulose. I. Tonoli, Gustavo Henrique Denzin. II. Ferreira, Maria Alves. III. Título.

ALLAN DE AMORIM DOS SANTOS

AUXILIATED CELLULASE PRETREATMENT FOR OPTIMIZATION OF CELLULOSE NANOFIBRILS OBTENTION

PRÉ-TRATAMENTO AUXILIADO POR CELULASE PARA OTIMIZAÇÃO DA OBTENÇÃO DE NANOFIBRILAS DE CELULOSE

Dissertação apresentada à Universidade Federal de Lavras, como parte das exigências do Programa de Pós-Graduação em Ciência e Tecnologia da Madeira, para a obtenção do título de Mestre.

APROVADA em 22 de fevereiro de 2019.

Dr. Gustavo Henrique Denzin Tonoli - UFLA
Dr. Rodrigo Teixeira Santos Freire - UFSJ
Dra. Maria Lúcia Bianchi - UFLA

Dr. Gustavo Henrique Denzin Tonoli
Orientador
Dr. Maria Alves Ferreira
Coorientadora

LAVRAS-MG
2019

Aos meus pais Reni e Maria das Dores.
À minha irmã Kátia e sobrinha Mariáh.

DEDICO

AGRADECIMENTOS

A Deus, onde baseio minha fé e que vem iluminando meu percurso.

À Universidade Federal de Lavras e ao Programa de Pós-Graduação em Ciência e Tecnologia da Madeira pela oportunidade de estudo de qualidade, onde o presente trabalho foi realizado com apoio da Coordenação de Aperfeiçoamento de Pessoal de Nível Superior – Brasil (CAPES) – Código de Financiamento 001.

Aos professores e técnicos do Departamento de Ciências florestais, pelo ensinamento ao longo do mestrado.

Ao Renato Augusto Pereira Damásio, representando a Klabin S.A. pelos esclarecimentos e pelo apoio.

Ao professor Gustavo Henrique Denzin Tonoli, pela orientação, calma e confiança. À professora Maria Alves Ferreira pela coorientação e também a toda banca avaliadora.

Aos meus pais Reni e Maria, minha irmã Kátia, e sobrinha Mariáh. Vocês são minha base e meu norte.

Aos amigos do Laboratório de Nanotecnologia florestal, Luiz Eduardo, Matheus, Maressa, Maryella, Luiza, Lays, Alisson, Lívia, Jordão, Maria, Caio, Fernanda, Rafaela, Breno, Mayck e Joice. Vocês deixaram esse período mais leve e me ensinaram muito. Também aos amigos da CTM, principalmente a galera do mestrado (2017/2).

Aos amigos do 101 (Luciano, Isaac, Chimba e Carol). Aos amigos da Pensão (Lucas, Daniel, Nathy, Aninha, Mayara, Paulinha e Elesandra).

Às POC's Willian, Guga, Amém, Bário e Vlad. Não teria sido tão bom esse período se vocês não estivessem ao meu lado.

Às amigas Brenda, Bruna e Laís, que mesmo à distância me confortavam e ajudavam a aguentar os trancos e barrancos.

Aos amigos de Reduto, Viçosa e do intercâmbio, Buteco, Medalha e 2321. E às demais pessoas que não mencionei, mas me ajudaram na construção desse trabalho.

Não há palavras suficientes que expressem minha gratidão a vocês.

Obrigado!

RESUMO

Materiais em escala nanométrica têm ganhado destaque no meio científico e tecnológico por possuírem suas propriedades físicas e químicas potencializadas. Entre estes, têm-se as celuloses nanoestruturadas, como as nanofibrilas e os nanocristais, que possuem um potencial de redução de impactos ambientais por serem de fonte renovável e substituir materiais poliméricos derivados do petróleo. Entretanto, a obtenção de nanofibrilas de celulose pelo processo mecânico consome muita energia elétrica. A ação de enzimas celulases pode facilitar a desfibrilação de polpas devido à clivagem que provocam na cadeia celulósica, reduzindo assim o consumo energético. Portanto, objetivou-se estudar o efeito de pré-tratamento enzimático para facilitar a obtenção de nanofibrilas a partir de polpas comerciais branqueadas e não branqueadas de *Eucalyptus* sp. e *Pinus* sp. a baixo consumo energético. Para realização da hidrólise enzimática foram utilizados complexos celulolíticos com atividade de endoglucanase (enzima A e enzima B), com concentração de 3% de polpa em suspensão, 50°C e 2 h de tempo de reação. Nanofibrilas de celulose foram obtidas pelo processo mecânico utilizando moinho desfibrilador, com 5 passagens e concentração de 2%, avaliando o consumo energético de cada tratamento. Foi analisada a morfologia das nanofibrilas de celulose por imagens obtidas de microscópio de luz (LM) e microscópio eletrônico de transmissão (TEM). Foram analisadas a turbidez, estabilidade em água e potencial zeta das nanofibrilas de celulose, bem como a confecção de filmes nanoestruturados, a fim de obter valores de resistência mecânica das nanofibrilas de celulose. O pré-tratamento enzimático diminuiu o consumo energético de polpas branqueadas em 58%, ao passo que para polpas não branqueadas a diminuição alcançou 55%. Mesmo com aplicação de celulase, encontrou-se dificultada de na desfibrilação da polpa quimiotermomecânica (CTMP). As suspensões de nanofibrilas apresentaram maior estabilidade em água com a aplicação do pré-tratamento enzimático, assim como houve um aumento na resistência mecânica dos filmes formados. A enzima A mostrou melhor desempenho para polpas branqueadas; além de diminuir o consumo em 58%, gerou nanofibrilas com diâmetro mediano de 24 variando entre 12 nm e 79 nm. A enzima B mostrou resultados mais significativos para polpa não branqueada, em que gerou diâmetro mediano de nanofibrilas de 22 variando entre 13 nm e 66 nm, e completa estabilidade da suspensão em água no ciclo de formação de gel pelo desfibrilador. Diante do exposto, espera-se melhorar a obtenção e qualidade de produtos celulósicos nanoestruturados para aplicação em vários produtos no mercado.

Palavras-chave: Nanotecnologia florestal. Hidrólise enzimática. Nanofibras. Nanocelulose. Fibras lignocelulósicas.

ABSTRACT

Materials at nanometric scale have gained prominence in the scientific and technological environment because they have their physical and chemical properties enhanced. Among these are nanostructured celluloses, such as nanofibrils and nanocrystals, which have the potential to reduce environmental impacts because they are formed from a renewable source and due to the possibility to replace polymeric materials derived from petroleum. However, the production of cellulose nanofibrils by the mechanical process consumes a lot of electrical energy. The action of cellulase enzymes may facilitate the defibrillation of pulps due to the cleavage they cause in the cellulosic chain, thus reducing energy consumption. The aim of this work was to study the effect of enzymatic pretreatment to facilitate the production of nanofibrils from bleached and unbleached commercial pulps of *Eucalyptus* sp. and *Pinus* sp. at low energy consumption. In order to carry out the enzymatic hydrolysis, cellulolytic complexes with endoglucanase activity were used (enzyme A and enzyme B), with a concentration of 3% pulp in suspension, 50 ° C and 2 h of reaction time. Cellulose nanofibrils were obtained by mechanical process using a defibrillator mill, with 5 cycles and 2% concentration, evaluating the energy consumption of each pretreatment. The morphology of cellulose nanofibrils was analyzed by light microscopy (LM) and transmission electron microscopy (TEM). It was analyzed the turbidity, stability in water and zeta potential of cellulose nanofibrils suspensions as well as the preparation of nanostructured films in order to obtain mechanical resistance values of cellulose nanofibrils. Enzymatic pretreatment decreased the energetic consumption of bleached pulps by 58%, whereas for unbleached pulps the decrease was 55%. Even with cellulase application, difficulty in defibrillation of chemithermomechanical pulp (CTMP) was observed. The suspensions of nanofibrils presented greater stability in water with the application of the enzymatic pretreatment, as well as there was an increase in the mechanical resistance of the films formed. Enzyme A showed better performance for bleached pulps, in addition to reducing consumption by 58%, generated nanofibrils with a median diameter of 24 with range between 12 nm and 79 nm. The enzyme B showed more significant results for unbleached pulp, in which it generated median nanofibrils diameter of 22 with range between 13 nm and 66 nm , and complete stability of the suspension in water in the gel formation cycle by the defibrillator. In view of the foregoing, it is expected to improve the procurement and quality of nanostructured cellulosic products for application in various products on the market.

Keywords: Forest nanotechnology. Enzymatic hydrolysis. Nanofibrils. Nanocellulose. Lignocellulosic fibers.

LISTA DE ILUSTRAÇÕES

PRIMEIRA PARTE

SEGUNDA PARTE

TERCEIRA PARTE

LISTA DE TABELAS

SEGUNDA PARTE

TERCEIRA PARTE

APÊNDICE

LISTA DE ABREVIATURAS

ºC	Graus Celsius
µg	Micrograma
A	Enzima A (endoglucanase monocomponente)
B	Enzima B (endoglucanase monocomponente)
B-Euc	Polpa de *Eucalyptus* sp. branqueada
B-Pin	Polpa de *Pinus* sp. branqueada
cm	Centímetro
cm^3	Centímetro cúbico
CTMP	Polpa quimiotermomomecânica
g	Grama
GPa	Gigapascal
h	Hora
kV	Quilovolt
kW	Quilowatt
L	Litro
LM	Microscopia de luz
mA	Miliampère
min	Minutos
mm	Milímetro
mV	Milivolt
MPa	Megapascal
NTU	Unidade de turbidez nefelométrica
rpm	Rotação por minuto
TEM	Microscopia eletrônica de transmissão
TEMPO; T	Oxidante 1-oxil-2,2,6,6-tetrametilpiperidina
ton	Tonelada
UB-Euc	Polpa de *Eucalyptus* sp. não branqueada
UB-Pin	Polpa de *Pinus* sp. não branqueada
v	Volume
w	Massa
WE	Pré-tratamento sem adição de enzima
XRD	Difração de raios-X

SUMÁRIO

APRESENTAÇÃO DESTA DISSERTAÇÃO

Essa dissertação é subdividida em quatro partes. A primeira parte é composta por introdução, objetivos, revisão de literatura e considerações finais da revisão de literatura. A revisão de literatura esclarece o conteúdo que será abordado nos 2 artigos apresentados, que são as duas próximas subdivisões da dissertação. As considerações finais da revisão de literatura resumem os principais aspectos levantados durante a revisão de literatura.

A segunda parte da dissertação contém o artigo que aborda a extração de nanofibrilas de celulose a partir de polpas branqueadas de *Eucalyptus* sp. e *Pinus* sp. após aplicação de celulase (atividade endoglucanase) como pré-tratamento enzimático. O pré-tratamento enzimático é comparado ao pré-tratamento utilizando o reagente TEMPO, considerado o mais eficiente atualmente, e também ao pré-tratamento sem adição de enzima.

A terceira subdivisão contém o artigo que aborda a extração de nanofibrilas de celulose, porém aplicada a polpas Kraft não branqueadas de *Eucalyptus* sp. e *Pinus* sp., e quimiotermomecânica (CTMP) de *Eucalyptus* sp. após aplicação de celulase.

A quarta e última parte traz a conclusão geral desta dissertação, trazendo os principais pontos observados e também sugestões para futuros trabalhos.

PRIMEIRA PARTE

1. INTRODUÇÃO

A utilização de produtos renováveis e biodegradáveis é uma solução sustentável frente a crescente utilização de produtos derivados do petróleo. Sua utilização busca diminuir os impactos ambientais negativos causados pela atividade da indústria petroquímica. Dentre os biopolímeros renováveis disponíveis, a celulose se destaca pela sua abundância, característica mecânica satisfatória, e pelo conhecimento já existente para sua obtenção e utilização. Nos setores papeleiro, moveleiro, têxtil, farmacêutico, médico e de construção civil, por exemplo, a celulose se destaca por agregar valor ao produto final, atuando como matéria prima base, reforço, aditivo ou fonte de energia.

Atualmente, a utilização da celulose em escala nanométrica tem chamado atenção devido à potencialização das suas características intrínsecas, gerando novos produtos ou melhorando produtos já existentes. Por possuir elevada superfície específica, baixa densidade,

alto módulo de resistência, biodegradabilidade e sua obtenção a partir de fontes renováveis, a nanocelulose vem se destacando como componente promissor na nanoengenharia.

Devido à heterogeneidade de materiais lignocelulósicos e da variedade nas formas de obtenção, as nanoceluloses possuem características diferenciadas entre si. As matérias primas mais comuns, atualmente, para produção de nanoceluloses são as polpas celulósicas comerciais, por apresentarem tecnologias bem estabelecidas.

Quanto à extração de nanoceluloses, a rota química de extração, por exemplo, gera materiais com maior cristalinidade, chamados de nanocristais de celulose, porém possui baixo rendimento e geram resíduos químicos. Por outro lado, rotas mecânicas de desfibrilação que possuem maior rendimento de extração, possuem alto consumo energético que inviabiliza sua produção em larga escala. Rotas biológicas, como a hidrólise enzimática, possuem maior especificidade na ação de desfibrilação, com a desvantagem de requerer maior tempo de obtenção.

Uma solução para superar os desafios de cada método é a combinação de tratamentos, utilizando pré-tratamentos, e assim viabilizando a produção em massa de nanoceluloses.

A rota mecânica por cisalhamento gera micro/nanofibrilas de celulose com alto rendimento, podendo alcançar 98% com alto consumo energético. Atualmente, tem-se buscado pré-tratamentos químicos e biológicos que modifiquem propriedades da polpa celulósica, e que auxiliem na diminuição do consumo energético. Além disso, tais pré-tratamentos podem melhorar as propriedades dos filmes gerados a partir das nanofibrilas de celulose.

O pré-tratamento enzimático, por sua vez, possui a vantagem de não produzir resíduos tóxicos ao ambiente, como alguns pré-tramentos químicos. Ainda, a utilização de enzimas auxilia no intumescimento da fibra e facilita o desprendimento de microfibrilas. A ação enzimática, apesar de conhecida, é complexa e age de forma singular em cada polpa celulósica.

2. OBJETIVOS

2.1 Objetivo geral

Otimizar a obtenção mecânica de nanofibrilas de celulose pela utilização de pré-tratamento enzimático com enzimas endoglucanase em polpas celulósicas comerciais a baixo consumo energético.

2.2 Objetivos específicos

a. Avaliar o efeito de pré-tratamento enzimático com enzima endoglucanase nas características químicas e morfológicas de polpas celulósicas.

b. Avaliar o consumo energético do processo mecânico de desfibrilação de polpas comerciais previamente tratadas com e sem enzimas.

c. Verificar o efeito de pré-tratamento enzimático de fibras de polpa celulósica em propriedades mecânicas e físicas de filmes gerados a partir de nanofibrilas de celulose.

d. Comparar as propriedades de resistência mecânica de nanofibrilas em diferentes passagens pelo microprocessador, principalmente entre a formação de gel e a última passagem.

3. REVISÃO DE LITERATURA

A fim de facilitar o entendimento do presente trabalho, a revisão de literatura foi dividida nos seguintes temas.

3.1 Materiais lignocelulósicos

Morfologicamente, materiais lignocelulósicos apresentam, de modo geral, células que possuem extremidades afiladas e pontiagudas, tecnologicamente chamadas de fibras (Burguer e Richter, 1991). Tais células possuem uma ultraestrutura compostas pela parede celular primária e parede celular secundária, sendo a parede secundária composta pelas camadas S1, S2 e S3 (Figura 1). Elas são unidas entre si pela lamela média (Burguer e Richter, 1991). As fibras são compostas de estruturas filamentosas chamadas de microfibrilas de celulose (Rowell, 1998; Silva, 2002), que formam ângulos com a direção longitudinal da planta que conferem às fibras características como elasticidade, dureza e resistência (Tienne et al., 2009). Essas características conferem propriedades que podem ser utilizadas nos setores têxteis, na indústria automotiva (John e Thomas, 2008) e como reforço na construção civil (Silva et al., 2015).

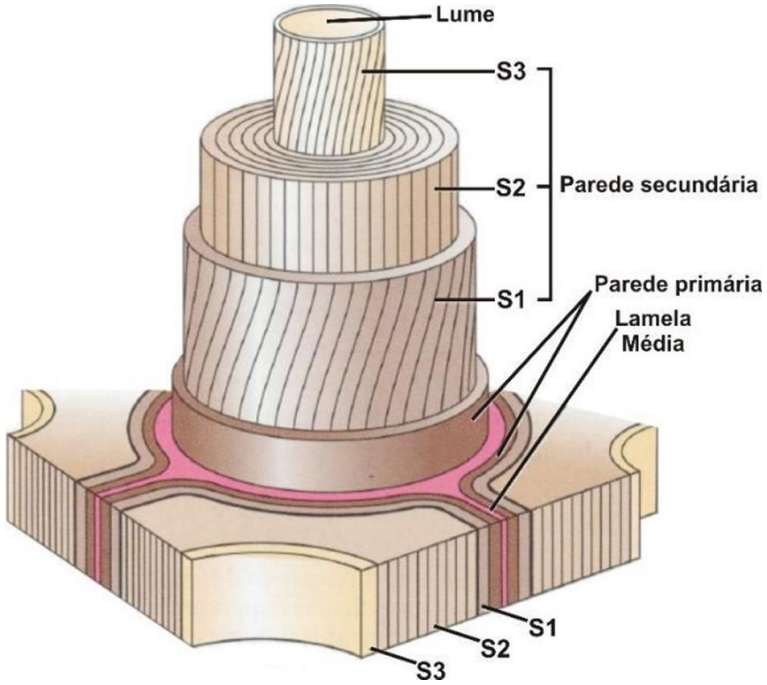

Figura 1. Ultraestrutura da parede celular. Fonte: Adaptado de Taiz e Zeiger (2002).

Quimicamente, os materiais lignocelulósicos têm como constituintes principais a holocelulose e a lignina. O termo holocelulose é aplicado à fração constituída por celulose e hemiceluloses (D'Almeida, 1998). Sua composição estrutural varia de acordo com as condições climáticas, condições de crescimento, espécies, gêneros, tecidos e maturidade da parede celular das plantas (Langan et al., 2014; Agbor et al., 2011).

Representando cerca de 10 a 25% em peso da biomassa lignocelulósica seca (Burhenne et al., 2013; Demirbas, 2015), a lignina possui maior concentração na lamela média, e existe uma menor concentração no interior da parede secundária. Possui função de ligação e fornece rigidez, resistência à compressão e resistência à decomposição da parede celular da planta. É um composto amorfo, tridimensional, de composição química bastante complexa, que se constitui de unidades de fenil propano, tendo sua cadeia altamente ramificada; é o componente mais hidrofóbico da madeira. Esta vem sendo estudada para a produção de biocombustíveis e produtos químicos a partir de materiais naturais (Azadi et al., 2013; Wang et al., 2013). Além disso, materiais à base de lignina também são aplicados em catálise, armazenamento de energia e remoção de poluentes (Liu et al., 2015).

Considerada indesejável para a produção de polpa celulósica, a lignina é retirada do material lignocelulósico pelos processos de polpação e branqueamento. Tais operações visam remover a maior parte possível de lignina sem causar dano apreciável às fibras. Entretanto, a existência de lignina residual na polpa concorre para que a fibra se torne mais rígida, o que

resulta em polpa com boas propriedades de resistência. Por outro lado, madeiras com alto teor de lignina exigem maior carga de produtos químicos para sua deslignificação durante a polpação (Alves, 2010).

Hemiceluloses são polissacarídeos que representam cerca de 20 a 35% da biomassa lignocelulósica (Burhenne et al., 2013; Demirbas, 2015; Li et al., 2015). São heteropolímeros compostos por cadeias curtas, lineares e ramificadas de diferentes tipos de monômeros, como pentoses e hexoses (Scheller e Ulvskov, 2010). Pentoses são monossacarídeos cujas unidades monoméricas contêm apenas cinco carbonos, constituindo principalmente as xilanas e arabinanas. As xilanas são encontradas principalmente em folhosas enquanto que as glucomananas são encontradas principalmente em madeiras de coníferas (Kapu e Trajano, 2014; Girio et al., 2010). As hemiceluloses aderem às fibrilas de celulose através de ligações de hidrogênio e interações de Van der Waals, e também fazem ligações cruzadas com a lignina (Kapu e Trajano, 2014).

Sabe-se que as hemiceluloses são constituintes desejáveis nas polpas celulósicas, aumentando o rendimento e apresentando efeitos benéficos na ligação interfibras e na resistência da celulose. Em virtude de suas qualidades desejáveis, a maior parte dos processos de obtenção de celulose procura remover o mínimo possível de hemiceluloses (Gomes, 2007). Estas podem ser hidrolisadas para a produção de etanol combustível e produtos químicos que podem ser usados por indústrias de alimentos, cosméticos e mineração (Kapu e Trajano, 2014; Girio et al., 2010).

Sendo o principal componente da parede celular, a celulose é um polissacarídeo linear com alto grau de polimerização. Representa cerca de 35 a 50% da parede celular (Burhenne et al., 2013; Demirbas, 2015; Li et al., 2015). As cadeias de celulose se unem por ligação de hidrogênio, determinando a maioria das propriedades das polpas celulósicas e seus produtos. Exerce influência na resistência individual da fibra e nas ligações entre as fibras e, associada com as hemiceluloses, determina as características da polpa celulósica, em termos de rendimento e de resistência (Barrichelo et al., 1984).

Existem ainda os extrativos, que são compostos que não fazem parte da constituição química da parede celular e incluem elevado número de compostos, muitos solúveis em água quente, álcool, benzeno e outros solventes neutros. Pertencem a diferentes grupos químicos, como as resinas, os açúcares, os taninos, os ácidos graxos, dentre outros, os quais influenciam nas propriedades da madeira (Almeida e Silva, 1990; Barrichelo et al., 1984; Foelkel et al., 1978; Oliveira, 1990). Os extrativos localizam-se nos canais resiníferos, ductos gomíferos (derivados dos terpenos) nas células parenquimáticas (células armazenadoras de substâncias

gordurosas, amido, etc.), e no cerne como um todo, onde se encontra os compostos fenólicos responsáveis pela durabilidade desse tecido. Os diversos compostos fenólicos (flavonóides, estilbenzenos, quinonas, etc.) são os que dão a cor característica à madeira (Gomes, 2007).

3.2 Celulose

A celulose é o biopolímero mais abundante do planeta, possuindo característica renovável e com uma produção anual de aproximadamente 15 bilhões de toneladas. Foi descoberta e isolada pela primeira vez por Payen (1838). É um polissacarídeo linear formado por diversas unidades de celobioses. A celobiose, por sua vez, é formada por duas unidades de anidro pirano glicose conectadas por ligações β-(1→4). As cadeias celulósicas são associadas por ligações de hidrogênio formando feixes de fibrilas contendo regiões cristalinas altamente ordenadas e regiões amorfas desordenadas, que por sua vez controla as características físicas da celulose. Possui grau de polimerização de 10.000 a 15.000 (Figura 2) (Bledzki e Gassan, 1999; Ghanshyam et al., 2000; Ahmad et al., 2008; Gómez-Guillén et al., 2009; Valeria et al., 2011).

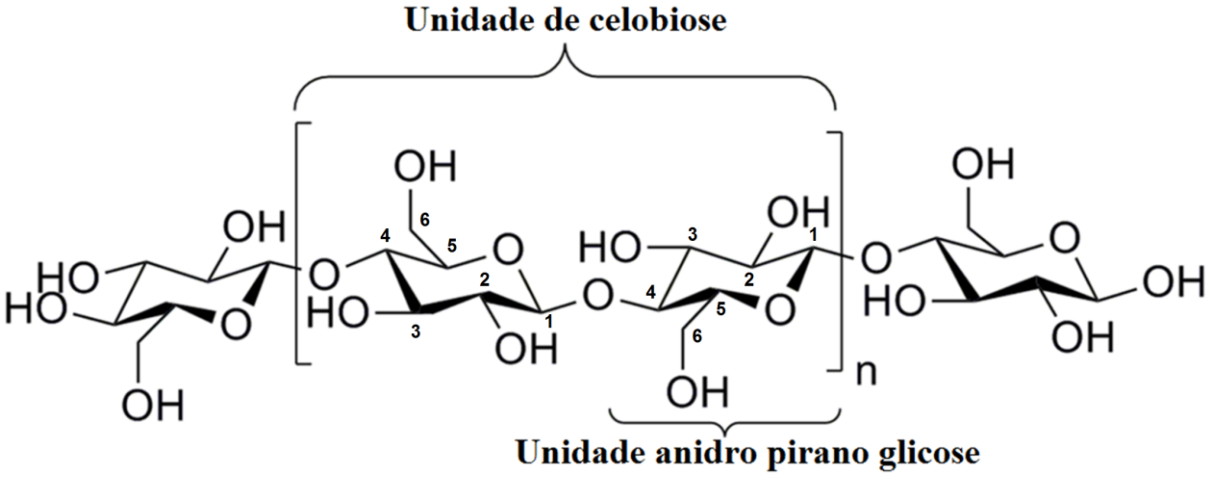

Figura 2. Estrutura molecular básica da celulose. Fonte: Adaptado de Olsson e Westman (2013).

Apesar de possuir simplicidade química em sua estrutura, a celulose possui estrutura física e morfológica complexa e heterogênea. Sua estrutura se torna mais complexa devido à interação direta da celulose com as hemiceluloses, ao fato de estarem associadas com a lignina (Siró e Plackett, 2010).

As hidroxilas presentes na cadeia trazem estabilidade à ligação das cadeias de celulose, sendo que três grupos hidroxilas possuem a capacidade de formação de ligações de

hidrogênio intra e intermoleculares (John e Thomas, 2008). Sabe-se que as hidroxilas presentes no carbono 6 da cadeia celulósica reagem dez vezes mais rápido do que as outras hidroxilas, enquanto que a reatividade do grupo hidroxila da posição de carbono 2 é duas vezes maior que a da posição do carbono 3 (Kevin et al., 2011).

A celulose pode ser produzida em dois tipos de conformação cristalina, nomeadas celulose I e celulose II. A celulose do tipo I é encontrada nos vegetais e é conhecida por ser menos estável, porém, possui melhores propriedades mecânicas. A celulose do tipo II é encontrada naturalmente em algas marinhas e apresenta estrutura mais durável (Ding et al., 2014). Existem ainda outras formas de celulose, a celulose III e a celulose IV. As celuloses do tipo II e do tipo III podem ser produzidas quando a celulose I é submetida a tratamento com hidróxido de sódio em meio aquoso. A celulose IV é formada a partir do tratamento da celulose III. A essa propriedade de se apresentar de diversas formas que a celulose possui, dá-se o nome de polimorfismo (Samir et al., 2005; Lee et al., 2013).

3.3 Nanocelulose

Nanocelulose é um material natural formado por feixes de moléculas de cadeia de celulose longas, flexíveis e emaranhadas, com tamanho variando de 1 a 100 nm (Chakraborty, Sain e Kortschot, 2006). Devido a suas propriedades diferenciadas, as nanoceluloses tem despertado o interesse de pesquisadores e de setores industriais (Moreira, 2010; Souza, 2010; Jonoobi et al., 2015).

A nanocelulose possui características que a diferenciam dos materiais tradicionais. Tais características incluem sua morfologia especial semicristalina, alta superfície específica, alinhamento e orientação, reforço mecânico, propriedades de barreira, reatividade química superficial, biocompatibilidade, biodegradabilidade, entre outros (Sun-Young et al., 2009; Juuso et al., 2011; Hua et al., 2011). É formada por cadeias de celulose, que formam redes de fibrilas, podendo agir como agente de reforço em compósitos (Hubbe et al., 2008). Suas características diferenciadas se devem a sua alta rigidez e resistência, combinadas com baixa densidade, causadas pelo grande número de sítios de ligação de hidrogênio inter e intramoleculares (Juuso et al., 2011).

Comumente, nanoceluloses são subdivididas em três grandes grupos. O primeiro seria o grupo dos hidrogéis de nanocelulose bacteriana e seres tunicados. O segundo grupo seria dos nanocristais de celulose extraídos hidroliticamente, e por último o grupo das nanofibrilas de celulose, geradas mecanicamente (Klemm et al., 2017).

A nanocelulose bacteriana é um material que possui alta pureza, composta quase que exclusivamente de celulose, com uma estrutura de redes de nanofibrilas aderidos a água, formando um hidrogel. Esse hidrogel é mecânica e termicamente estável (Klemm et al., 2017). Um dos primeiros produtos comerciais da nanocelulose bacteriana foi o *Nata de Coco*, uma sobremesa popular em países asiáticos (Lapuz et al., 1967; Phisalaphong e Chiaoprakobkij, 2013). A nanocelulose bacteriana se mostra com potencial como material altamente biocompatível (Lin e Dufresne, 2014), com estudos realizados em camundongos, ratos, coelhos e suínos, sem sinais graves de inflamação, toxicidade no nível genético e celular no prazo de até um ano (Helenius et al., 2006; Jeong et al., 2010; Almeida et al., 2014; Alkhatib et al., 2017).

Como outra divisão de nanocelulose, os nanocristais de celulose têm composição de cristais em formato de bastonete, com larguras variando de 5 a 70 nm. É formado quase que exclusivamente pelas regiões cristalinas da celulose. Seus cristais variam em dimensão e morfologia de acordo com a preparação, fonte, grau de cristalinidade e método de obtenção. Como exemplo, tem-se a formação de nanocristais a partir de madeira e algodão com cristalinidade próxima a 90%, e dimensões de 5 a 10 nm de largura e 100 a 300 nm de comprimento (Moreira, 2010; Klemm et al., 2011).

Por fim, as nanofibrilas de celulose, também chamadas de nanofibras de celulose (Stenstad et al., 2008), celulose nanofibrilar ou celulose microfibrilar (Abe, Iwamoto e Yano, 2007), são componentes da fibra vegetal constituídos pelas regiões cristalinas e amorfas da cadeia celulósica. As nanofibrilas de celulose são geralmente produzidas por processo mecânico de cisalhamento a partir de polpa de madeira (Klemm et al., 2011).

As propriedades das nanofibrilas de celulose variam de acordo com suas dimensões, métodos de obtenção e composição química da matéria-prima (Guimarães Júnior et al., 2015). Apesar de as nanofibrilas de celulose serem produzidas a partir de uma variedade de matérias-primas lignocelulósicas, a polpa Kraft é a mais barata e mais abundante, tendo sido comumente usada como material de partida para a produção de nanocelulose (Saito e Isogai, 2006; Spence et al., 2010; Taipale et al., 2010).

Apesar de ser difícil encontrar valores exatos, estimou-se o módulo e resistência dos cristais de celulose por meio de cálculos teóricos e simulações numéricas. O módulo elástico à tração axial do cristal de celulose foi estimado em valores aproximados de 58-180 GPa, enquanto que a resistência à tração foi estimada em valores na faixa de 0,3-22,0 GPa (Wadood, 2006; Rui et al., 2012). Sun et al. (2018) analisaram as propriedades térmica e mecânica de filmes formados a partir de nanocristais e nanofibrilas de celulose. Os autores

observaram que os filmes permaneceram termicamente estáveis até 340°C contraindo menos que 0,17% entre 20 e 120°C.

3.3.1 Aplicação de nanocelulose

Por ser produzida a partir de fonte renovável com alta disponibilidade e possuir baixa densidade com elevada resistência mecânica, as nanofibrilas de celulose possuem inúmeras aplicações em vários setores. Alguns autores mencionaram as nanoceluloses sendo aplicadas como auxiliadores em armazenamento de energia (Chen et al., 2018), biotintas para bioimpressão tridimensional (Piras et al., 2017), hidrogel e aerogel (De France et al., 2017), sistema de administração de medicamentos (Löbmann e Svagan, 2017) e como agente coagulante no processo de floculação em tratamentos de água (Carpenter et al., 2015).

Devido à alta resistência à tração, baixa expansão térmica, transparência e formação de uma barreira ao oxigênio, os filmes de nanofibrilas de celulose podem ser aplicados em embalagens como revestimento para alimentos e fármacos (Sozer e Kokini, 2009; Villanova et al., 2011; Assis et al., 2012; Mohd Amin et al., 2012; Akhlaghi, Berry e Tam, 2013; Tibolla, Pelissari e Menegalli, 2014).

Segundo Klemm et al. (2011), a nanocelulose bacteriana pode ser utilizada em implantes médicos como reparação de ossos e cartilagem, e também na reconstituição de diferentes tecidos. Têm sido pesquisadas também na construção de dispositivos eletrônicos, energéticos e ambientais. Ainda, as nanofibrilas de celulose atuam no aumento da resistência térmica e aumento na resistência à tração quando combinados com polímeros (Saito et al., 2006; Syverud e Stenius, 2009; Aulin, et al., 2010; Besbes, Vilar e Boufi, 2011; Lavoine et al., 2012; Guimarães Júnior et al., 2015; Mirmehdi et al., 2018a, 2018b).

3.3.2 Rotas para obtenção de nanocelulose

Várias técnicas vêm sendo desenvolvidas para obtenção de nanoceluloses, em que diferentes métodos de extração resultam em diferentes tipos de nanoceluloses, com distintas propriedades (Peng et al., 2011). As técnicas bem-sucedidas avançaram e atualmente, a produção de nanocelulose se expande em escala industrial, se difundindo principalmente no Canadá, Estados Unidos, China, Japão, Irã, Índia, e na Europa. Os principais métodos de obtenção de nanocelulose nas indústrias são métodos convencionais, como a hidrólise ácida

para a produção de nanocristais de celulose (Figura 3a) e o tratamento mecânico para a produção de nanofibrilas de celulose (Figura 3b) (Rajinipriya et al., 2018).

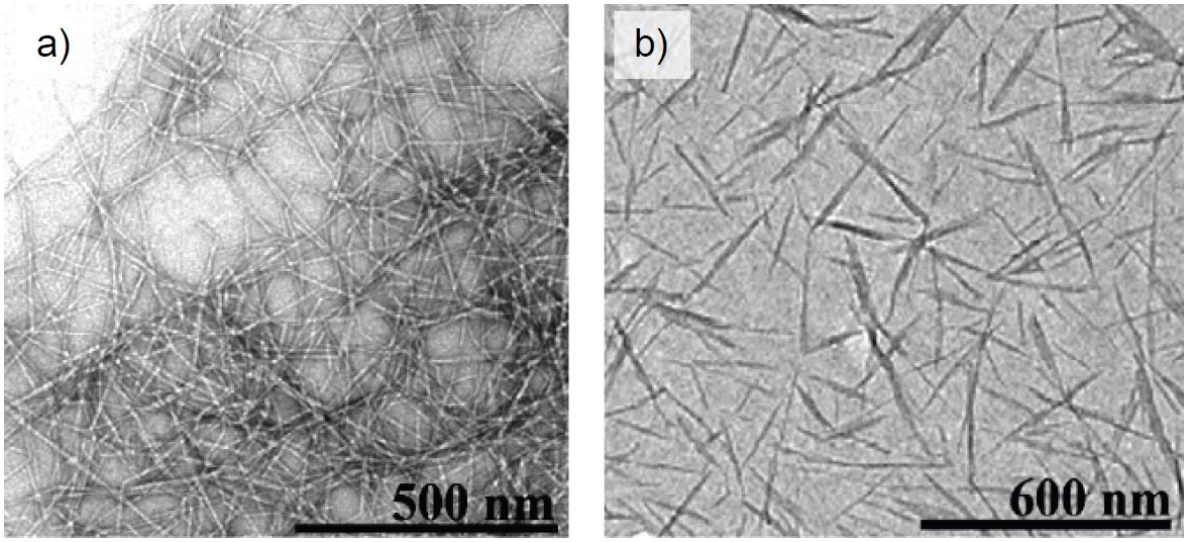

Figura 3. Microscopia eletrônica de transmissão de a) nanofibrilas de celulose e b) nanocristais de celulose. Fonte: Adaptado de Klemm et al. (2011).

A hidrólise ácida para obtenção de nanocristais de celulose é um dos principais processos de obtenção a partir de materiais lignocelulósicos. Esse processo se baseia na retirada das regiões desordenadas das cadeias de celulose, que podem ser facilmente hidrolisadas por ácido. Assim, restam-se as regiões ordenadas das cadeias de celulose (Moon et al., 2011; Lavoine et al., 2012). O ácido sulfúrico é o ácido mais usado na hidrólise ácida (Dong et al.,1998; Bondeson et al., 2006), tornando a nanocelulose um coloide estável. Isso se dá devido à esterificação do grupo hidroxila pelos íons sulfato (Das et al., 2009; Lu e Hsieh, 2010). A hidrólise ácida possui como desvantagem a presença de água ácida residual gerada a partir da lavagem, que neutraliza o pH da suspensão de nanocelulose (Johar et al., 2012). Outros reagentes podem ser utilizados durante a hidrólise ácida.

Existe ainda a possibilidade de produção de nanofibrilas de celulose através de uma rota química por oxidação realizada pelo radical livre 1-oxil-2,2,6,6-tetrametilpiperidina (TEMPO). A oxidação mediada por TEMPO é realizada em água, em que o reagente TEMPO e o sal NaBr são dissolvidos, e a oxidação se inicia com a adição de NaClO. O pH da reação geralmente é básico, mas também podem ser usadas para este processo condições ácido-neutro ou ácido-fraco (Isogai et al., 2011; Nechyporchuk et al., 2016). Uma vantagem da utilização da rota mediada por TEMPO é a uniformidade do tamanho das partículas (3-4 nm) com formação de filmes transparentes e flexíveis (Fukuzumi et al., 2009; Isogai et al., 2011).

Tem-se ainda a possibilidade de se extrair nanofibrilas de celulose a partir de uma rota biologia. A hidrólise enzimática, no qual enzimas são usadas para digerir ou modificar as fibras de celulose, pode auxiliar na desfibrilação, onde condições específicas de pH, temperatura e substrato são necessárias para realizar tal tratamento (Abdul Khalil et al., 2014). O tempo de reação é o principal obstáculo dessa rota de obtenção, e por isso a hidrólise enzimática é sempre incorporada com outras rotas (Abdul Khalil et al., 2014; Moniruzzaman e Ono, 2013).

Uma rota mecânica de extração de nanofibrilas de celulose consiste no isolamento de fibrilas de celulose pela aplicação de alta força de cisalhamento das fibras de celulose no eixo longitudinal (Dufresne, 2012; Abdul Khalil et al., 2012; 2014). Os inventores (Herrick et al., 1983; Turbak et al., 1983) da celulose microfibrilar, como a chamavam, usavam com sucesso homogeneizadores de alta pressão para a desfibrilação mecânica das fibras. Porém, reconheceram que havia alto consumo de energia, o que inviabilizava a produção em larga escala da celulose microfibrilar. Desde então, vários equipamentos têm sido estudados e utilizados, tais como homogeneizadores de alta pressão ou microfluidificadores, refinadores comuns, moagem de bolas, explosão a vapor, ultrassonificação, microfluidizador, moinho desfibrilador *grinder*, *cryocrushing*, *eletrospinning*, misturadores de alta velocidade (Siqueira et al., 2010; Rebouillat e Pla, 2013; Kim et al., 2015; Nechyporchuk et al., 2016).

Um dos processos mecânicos mais estudados atualmente utiliza o desfibrilador. Consiste na passagem da polpa de celulose entre dois discos de pedra, em que um é estacionário e o outro gira com rotações de 1500 rpm, ou mais. Nesse processo são geradas forças de cisalhamento entre as fibras, entre as fibras e a água e entre as fibras e as pedras. O uso do desfibrilador foi relatado pela primeira vez em 1998 por Taniguchi e Okamura, possuindo como vantagem um alto rendimento (Josset et al., 2014). O grau de desfibrilação da polpa aumenta com o aumento do número de passagens pelo desfibrilador. Entretanto, há uma elevação no consumo energético pelo equipamento, podendo ainda ocorrer a degradação da polpa (Taniguchi e Okamura, 1998). Outra desvantagem desse processo é a não uniformidade das partículas formadas (Iwamoto et al., 2007; Karner et al., 2016).

3.4 Consumo energético durante obtenção de nanofibrilas de celulose

Para que a desfibrilação ocorra a nível satisfatório, a polpa celulósica em suspensão deve passar pelo equipamento por mais de uma vez, aumentando a energia para ocorrer o

desprendimento das fibrilas (Henriksson et al., 2007). A quantidade de passagens varia com as condições do equipamento e as características e propriedades da polpa em suspensão.

Buscando a diminuição desse consumo energético, a obtenção das nanofibrilas de celulose pode ocorrer por meio da combinação de vários métodos de extração, em que a polpa celulósica é previamente tratada, e em seguida a suspensão é inserida no processo de obtenção de nanofibrilas. Esses pré-tratamentos podem ainda melhorar as propriedades dos filmes formados a partir das nanofibrilas (Josset et al., 2014; Qing et al., 2013). A combinação pode ocorrer entre os processos químicos e mecânicos, ou biológicos e mecânicos (Chen et al., 2011; Abe, Iwamoto e Yano, 2007; Alemdar e Sain, 2008; Ahuja et al., 2018). O propósito de utilizar pré-tratamentos é tornar as fibras menos rígidas, facilitando a desfibrilação e diminuindo o número de passagens pelo equipamento, e consequentemente, reduzindo o gasto energético (Heriksson et al.,2007).

Siró e Plackett (2010) avaliaram a desfibrilação mecânica, e alcançaram valores no consumo de energia de 20.000-30.000 kW.h/ton de polpa. Esse valor impossibilita a produção em larga escala de nanofibrilas de celulose. Com a utilização de pré-tratamentos químicos, os autores propuseram que o consumo de energia cairia até a 1.000 kW.h/ton de fibra celulósica.

Avaliando o consumo energético, Iwawoto et al. (2008) e Correia (2015) constataram menor consumo na produção de nanofibrilas de celulose a partir de polpa branqueada comparada à polpa não branqueada. Ribes et al. (2018) também avaliaram a produção de nanofibrilas de celulose utilizando o equipamento microprocessador Super Masscolloider Masuko Sangyo MKCA6-2 (*grinder*), e alcançaram uma redução de 45% no consumo energético utilizando pré-tratamento enzimático em polpa Kraft branqueada de *Eucalyptus* sp., e 33% em polpa não branqueada.

He et al. (2018), alcançaram um consumo de 49.000 kW.h/ton de polpa Kraft de *Pinus* sp. não branqueada, com 35 passagens pelo microprocessador. Para polpa quimiotermomecânica, o consumo foi de 15.000 kW.h/ton e para *Eucalyptus* sp., o consumo foi de 34.000 kW.h/ton. Josset et al. (2014), utilizando polpa de *Eucalytpus* sp. branqueada, relataram um consumo de 5.250 kW.h/ton com 10 passagens pelo desfibrilador.

3.5 Pré-tratamento enzimático

As fibras celulares possuem como propriedade a recalcitrância. Essa propriedade confere resistência natural da parede celular de plantas à ação microbiana e enzimática (Himmel et al., 2007). Devido a essa recalcitrância, a extração de nanoceluloses se torna

custosa, tendo como principal barreira, o gasto com reagentes químicos, manutenção de equipamentos, tratamento de água residual, e alto consumo energético (Tonoli et al., 2012; Tuzzin et al., 2016).

Embora existam pré-tratamentos baseados em produtos químicos (TEMPO-oxidação, ácido, alcalino, carboximetilação, sulfonação, etc.) que auxiliem a obtenção de nanofibrilas de celulose, tais processos químicos são relativamente caros e diminuem o rendimento devido a não seletividade de reação, com considerável risco ambiental (Liimatainen et al., 2013; Naderi et al., 2014; Saito et al., 2006). Por outro lado, pré-tratamentos biológicos podem ser mais atraentes devido à alta especificidade de reação, com maior acesso à celulose, além da diminuição de risco ambiental e conservação das características químicas e morfológicas da polpa (Hassan et al., 2010; Wang et al., 2014). Esse acesso ocorre pelo inchamento das fibras lignocelulósicas que influencia na coesão da parede celular (Scallan, 1983; Lindström, 1992). Entre os métodos sucedidos de pré-tratamento biológico para diminuir a coesão da parede celular, está o tratamento enzimático (Henriksson et al., 2007; Pääkkö et al., 2007).

Para ocorrer completa hidrólise de materiais lignocelulósicos, diferentes enzimas agem sobre a biomassa. Isso ocorre devido à presença de diferentes componentes químicos nesses materiais. As principais enzimas envolvidas na hidrólise enzimática em materiais lignocelulósicos são as celulases que hidrolisam a celulose, as xilanases que hidrolisam alguns tipos de hemiceluloses e as peroxidases e as lacases, que hidrolisam a lignina (Hubbe et al., 2008). Como materiais lignocelulósicos possuem maior teor de celulose em sua composição química, as celulases se tornam a principal enzima a agir sobre polpas celulósicas. As enzimas possuem importante papel em aplicações comerciais, como produção de etanol (Castro e Pereira Jr., 2010), modificações de tecidos (Andreaus e Campos, 2000), indústria papeleira (Viikari et al., 2000) e alimentícia (Tenkanen et al., 2003).

As enzimas do tipo celulase atuam principalmente nas regiões amorfas da cadeia celulósica. Isso ocorre por possuírem maior superfície específica, com cadeias de celulose desordenadas (Hubbe et al., 2008). Entretanto, devido a sua complexidade e heterogeneidade, os complexos enzimáticos mostram-se capazes de realizar hidrólise na região cristalina da celulose, reduzindo a cadeia a celobiose e glicose (Pitarelo, 2007). Para clivagem apenas das regiões amorfas, as condições do meio de reação devem ser controladas de acordo com a enzima, pH, temperatura, substrato, etc. (Zhu et al., 2011).

A completa degradação da celulose pela celulase ocorre pela ação sinérgica de três tipos de enzimas. As endoglucanases ou endocelulases hidrolisam ligações glicosídicas do tipo β-(1,4) de forma aleatória nas regiões amorfas da cadeia de celulose, diminuindo seu grau

de polimerização e criando novos terminais na cadeia. As celobiohidrolases ou exocelulases, também conhecidas como exoglucanases, clivam a celulose de cadeia longa produzindo cadeias curtas de celulose. As β-glucosidases ou celobiases, também conhecidas como glucohidrolases de β-glicosídeos, hidrolisam as cadeias curtas de celulose produzindo glicose. Fungos e bactérias excretam extracelularmente as enzimas, sendo os fungos a principal fonte de celulases. Dentre os fungos, pode-se citar *Trichoderma reesei, Trichoderma viride, Volvariella volvacea, Aspergillus niger*, sendo o primeiro o principal produtor de celulases (Ramos, 1992; Bhat e Bhat, 1997).

Long et al. (2017) combinaram o pré-tratamento enzimático com processo ultrassônico de desfibrilação. Analisando a otimização da obtenção de nanofibrilas de celulose utilizando pré-tratamento enzimático com endoglucanase (0,1% m/v) auxiliado por xilanase (0,1% m/v), os autores observaram que houve cooperação sinérgica entre a endoglucanase e a xilanase durante o pré-tratamento enzimático. O pré-tratamento facilitou a desfibrilação de polpa celulósica Kraft branqueada de folhosas pelo acesso à celulose, provocado pela xilanase. Os autores encontraram redução na viscosidade intrínseca da celulose de 1320 para 880 dm^3/kg, aumento no índice de cristalinidade de 54% para 76% e tamanho de cristalitos variando de 2,6 nm a 3,6 nm.

Nie et al. (2018) também realizaram pré-tratamento enzimático para obtenção de nanofibrilas de celulose. A análise foi realizada com enzima xilanase a 0,0, 1,5 e 9,0 μg/g de polpa não branqueada de *Eucalyptus* sp. com consistência de 8% a 50ºC por 2 h. Analisando as propriedades mecânicas de filmes de nanofibrilas de celulose, os autores verificaram melhoria na resistência à tração dos filmes devido ao aumento da ligação de hidrogênio entre os nanofibrilas de celulose, e melhoria na dispersão de nanofibrilas de celulose devido a formação de grupos carboxílicos na superfície das fibras.

Outro trabalho que também avaliou a atividade enzimática como facilitador para extração de nanofibrilas de celulose foi realizado por Silva (2017). O estudo comparou a aplicação de coquetéis enzimáticos endoglucanase monocomponente (100 g/ton de celulose seca ao ar) e endo+exoglucanase (60 g/ton de celulose seca ao ar). Foi avaliado a ação das enzimas sobre cinco polpas comerciais Kraft de *Eucalytpus* sp. e *Pinus* sp. e polpa quimiotermomecânica de *Eucalyptus* sp. O pré-tratamento enzimático ocorreu por 120 min a 50°C. Resultados indicaram economia de energia de até 65% para *Eucalyptus* e até 66% para *Pinus.*

4. CONSIDERAÇÕES FINAIS DA REVISÃO DE LITERATURA

A partir desta revisão bibliográfica, obteve-se entendimento sobre a importância de pré-tratamentos para facilitar a obtenção de nanofibrilas de celulose. O pré-tratamento enzimático, sendo considerado um pré-tratamento que agride menos as fibras quando comparado a pré-tratamentos químicos, se torna um aliado na conservação da polpa e diminuição de água residual ácida, alcalina, ou oxidante. A partir da revisão de literatura também foi possível definir a metodologia aplicada para essa dissertação, vendo a necessidade de se definir melhor as características das nanofibrilas formadas a partir de pré-tratamentos enzimáticos. Com isso, essa pesquisa busca contribuir com conhecimento sobre como um pré-tratamento enzimático age sobre características químicas e morfológicas de fibras, e sobre características físicas e mecânicas de nanofibrilas de celulose após desfibrilação mecânica.

REFERÊNCIAS BIBLIOGRÁGICAS

ABDUL KHALIL, H.P.S.; ABDUL KHALIL, A.H.; BHAT, A.F.; IREANA, Y. Green composites from sustainable cellulose nanofibrils: a review. **Carbohydrate Polymers**, v. 87, p. 963–979, 2012.

ABDUL KHALIL, H. P. S.; DAVOUDPOUR, Y.; NAZRULISLAM, MD.; MUSTAPHA, A.; SUDESH, K.; DUNGANI, R.; JAWAID, M. Production and modification of nanofibrillated cellulose using various mechanical processes: A review. **Carbohydrate Polymers**, v. 99, p. 649–665, 2014.

ABE, K.; IWAMOTO, S.; YANO, H. Obtaining cellulose nanofibrils with a uniform width of 15 nm from wood.**Biomacromolecules**, v. 8, p. 3276-3278, 2007.

AGBOR, V.B.; CICEK, N.; SPARLING, R.; BERLIN, A.; LEVIN, D. B. Biomass pretreatment: fundamentals toward application. **Biotechnology Advances**, v. 29, p. 675–685, 2011.

AHMAD, S.; ABBAS, R.; ZAHRA, B. Sulfonated cellulose and starch: new biodegradable and renewable solid acid catalysts for efficient synthesis of quinolones. **Catalysis Communications,** v. 9, p. 13-16, 2008.

AHUJA, D.; KAUSHIK, A.; SINGH, M. Simultaneous extraction of lignin and cellulose nanofibrils from wastejute bags using one pot pre-treatment. **International Journal of Biological Macromolecules**, v. 107, p. 1294–1301, 2018.

AKHLAGHI, S. P.; BERRY, R. C.; TAM, K. C. Surface modification of cellulose nanocrystal with chitosan oligosaccharide for drug delivery applications. **Cellulose**, v. 20, n. 4, p. 1747–1764, 2013.

ALEMDAR, A.; SAIN, M. Isolation and characterization of nanofibrils from agricultural residues–wheat straw and soy hulls.**Bioresource. Technology**, v. 99, p. 1664–1671, 2008.

ALKHATIB, Y.; DEWALDT, M.; MORITZ, S.; NITZSCHE, R.; KRALISCH, D.; FISCHER, D. Controlled exteded octenidine release from a bacterial nanocellulose/Poloxmer hybrid system. **European Journal of Pharmaceutics and Biopharmaceutics**, v. 112, p 164-176, 2017.

ALMEIDA, F.; PEREIRA, T.; SILVA, N. H. C. S.; GOMES, F. P.; SILVESTRE, A. J. D.; FREIRE, C. S. R.; SOUSA LOBO, J. M.; COSTA, P. C. Bacterial cellulose membranes as drug delivery systems: An *in vivo* skin compatibility study. **European Journal of Pharmaceutics and Biopharmaceutics**, v. 86, p. 332-336, 2014.

ALMEIDA, J. M; SILVA, D. J. Inclusão de um novo e importante parâmetro potencial de seleção de eucalipto para produção de polpa. In: CONFERÊNCIA IUFRO SOBRE SILVICULTAURA E MELHORAMENTO DE EUCALIPTO, 6o Campos do Jordão, SP, 22 a 27 de set. 1990. **Anais**... Sociedade Brasileira de Silvicultura, Campos do Jordão, SP, p. 228-231, 1990.

ALVES, I. C. N. **Potencial da madeira do *Eucalyptus benthamii* Maiden et Cambage visando à produção de celulose Kraft.** Dissertação de Mestrado, Universidade Federal de Viçosa. Viçosa, 2010.

ANDREAUS, J.; CAMPOS, R. Influence of cellulases on indigo backstaining. **Textile Research Journal**, v. 70, n. 7, p. 628-632, 2000.

ASSIS, L. M.; ZAVAREZE, E. R.; PRENTICE-HERNANDEZ, C.; SOUZA-SOARES, L. A. Revisão: características de nanopartículas e potenciais aplicações em alimentos. **Brazilian Journal of Food Technology**, v. 15, n. 2, p. 99–109, 2012.

AULIN, C.; GÄLLSTEDT, M.; LINDSTRÖM, T. Oxygen and oil barrier properties of microfibrillated cellulose films and coatings. **Cellulose**, v. 17, p. 559–574, 2010.

AZADI, P.; INDERWILDI, O. R.; FARNOOD, R.; KING, D. A. Liquid fuels, hydrogen and chemicals from lignin: a critical review. **Renewable and Sustainable Energy Reviews**, v. 21, p. 506–523, 2013.

BARRICHELO, L. E. G; NARIYOSHI, A. B.; BEIG, O. Variação das características da madeira de eucalipto para diferentes espécies, idade e locais. In*:* CONGRESSO ANUAL DE CELULOSE E PAPEL, 17, 1984, São Paulo. **Anais**... São Paulo: ABTCP, v.1, p. 385-399, 1984.

BESBES, I.; VILAR, M. R.; BOUFI, S. Nanofibrillated cellulose from Alfa, Eucalyptus and Pine fibres: Preparation, characteristics and reinforcing potential. **Carbohydrate Polymers**, v. 86, n. 3, p. 1198–1206, 2011.

BHAT, M. K.; BHAT, S. Cellulose degrading enzymes and their potential industrial applications. **Biotechnology advances**, v. 15, n. 3, p. 583-620, 1997.

BLEDZKI, A. K.; GASSAN, J. Composites reinforced with cellulose based fibres. **Progress in polymer Science,** v. 24, n. 2, p. 221-274, 1999.

BONDESON, D.; MATHEW, A.; OKSMAN, K. Optimization of the isolation of nanocrystals from microcrystalline cellulose by acid hydrolysis. **Cellulose**, v. 13, p. 171–180, 2006.

BURGUER, L. M.; RICHTER, H. G. Anatomia da madeira. **Nobel**, São Paulo, 154 p., 1991.

BURHENNE, L.; MESSMER, T.; AICHER, T.; LABORIE, M. The effect of the biomass components lignin, cellulose and hemicellulose on TGA and fixed bed pyrolysis. **Journal of Analytical and Applied Pyrolysis**, v. 101, p. 177-184, 2013.

CARPENTER, A. W.; DE LANNOY, C. F.; WIESNER, M. R. Cellulose Nanomaterials in Water Treatment Technologies. **Environment and Science Technology**, v. 49, p. 5277–5287, 2015.

CASTRO, A. M.; PEREIRA JR.; N. Produção, propriedades e aplicação de celulases na hidrólise de resíduos agroindustriais. **Química Nova,** v. 33, n. 1, p. 181-188, 2010.

CHAKRABORTY, A.; SAIN, M.; KORTSCHOT, M. Reinforcing potential of wood pulp-derived microfibres in a PVA matrix. **Holzforschung**, v. 60, p. 53-58, 2006.

CHEN, W.; YU, H.; LIN, Y.; CHEN, P.; ZHAN, M. Individualization of cellulose nanofibrils from wood using high-intensity ultrasonication combined with chemical pretreatments, **Carbohydrate Polymer**, v. 83, p. 1804-1811, 2011.

CHEN, W.; YU, H.; LEE, S. Y.; WEI, T.; LI, J.; FAN, Z. Nanocellulose: a promising nanomaterial for advanced electrochemical energy storage. **Chemical Society Reviews**, v. 47, p. 2837–2872, 2018.

CORREIA, V. C. **Produção de cellulose nanofibrilada a partir de polpa organossolve de bamboo para nanorreforço de compósitos cimentícios**. Tese de Doutorado. Universidade de São Paulo, Pirassununga, 2015.

D'ALMEIDA, M. L. O. Celulose e papel. Volume I. Tecnologia de fabricação de pasta celulósica. São Paulo: **IPT/SENAI**, 559 p., 1998.

DAS, K.; RAY, D.; BANDYOPADHYAY, N. R.; GHOSH, T.; MOHANTY, A. K.; MISRA, M. A study of the mechanical, thermal and morphological properties of microcrystalline cellulose particles prepared from cotton slivers using different acid concentrations. **Cellulose**, v. 16, p. 783–793, 2009.

DE FRANCE, K. J.; HOARE, T.; CRANSTON, E. D. Review of Hydrogels and Aerogels Containing Nanocellulose. **Chemical of Materials**, v. 29, p. 4609–4631, 2017.

DEMIRBAS, A. Estimating of structural composition of wood and non-wood biomass samples, **Energy Sources**. V. 27, P. 761–767, 2015.

DING, S.Y.; ZHAO, S.; ZENG, Y. Size, shape, and arrangement of native cellulose fibrils in maize cell walls. **Cellulose**, v. 21, p. 863-871, 2014.

DONG, X. M.; REVOL, J. F.; GRAY, D. G. Effect of microcrystallite preparation conditions on the formation of colloid crystals of cellulose. **Cellulose**, v. 5, p. 19–32, 1998.

DUFRESNE, A. Nanocellulose: potential reinforcement in composites. In: JOHN, M. J.; THOMAS, S. Natural Polymers, Volume 2: Nanocomposites. **Green Chemistry Series**, v. 2, p. 1–32, 2012.

FOELKEL, C. E. B., ZVINAKEVICIUS, C., ANDRADE, J. R. Eucaliptos tropicais na produção de celulose Kraft. In*:* CONGRESSO ANUAL DE CELULOSE E PAPEL, 11, 1978, São Paulo. **Anais**... São Paulo: ABTCP, 1978.

FUKUZUMI, H.; SAITO, T.; KUMAMOTO, Y.; IWATA, T.; ISOGAI, A. Transparent and high gas barrier films of cellulose nanofibrils prepared by TEMPO-mediated oxidation.**Biomacromolecules**, v. 10, p. 162–165, 2009.

GHANSHYAM, S. C.; SWATI, M.; LALIT, K. G. Polymers from renewable resources: sorption of Cu^{2+} ions by cellulose graft copolymers. **Desalination**, v. 130, p. 85-88, 2000.

GIRIO, F. M.; FONSECA, C.; CARVALHEIRO, F.; DUARTE, L. C.; MARQUES, S.; BOGEL-LUKASIK, R. Hemicelluloses for fuel ethanol: a review. **Bioresource Technology**, v. 101, p. 4775–4800, 2010.

GOMES, A. F. Avaliação das características da madeira e da polpa de Eucalyptus mediante a aplicação de métodos não destrutivos na madeira viva. Dissertação (Mestrado em Engenharia Florestal) - Universidade Federal de Lavras, Minas Gerais, 124p. 2007.

GÓMEZ-GUILLÉN, M. C.; PÉREZ-MATEOS, M.; GÓMEZ-ESTACA, J.; LÓPEZ-CABALLERO, E.; GIMÉNEZ, B.; MONTERO, P. Fish gelatin: a renewable material for developing active biodegradable films. **Trends in Food Science and Technology**. v. 20, p. 3-16, 2009.

GUIMARÃES JUNIOR, M.; BOTARO, V. R.; NOVACK, K. M.; NETO, W. P. F.; MENDES, L. M.; TONOLI, G. H. D. Preparation of Cellulose Nanofibrils from Bamboo Pulp by Mechanical Defibrillation for Their Applications in Biodegradable Composites. **Nanoscience and Nanotechnology**, v. 15, p. 1–18, 2015.

HASSAN, M.L.; HASSAN, E.A.; OKSMAN, K.N. Effect of pretreatment of bagasse fibers on the properties of chitosan/microfibrillated cellulose nanocomposites. **Journal of Materials Science,** v. 46, p. 1732–1740, 2010.

HE, M.; YANG, G.; CHEN, J.; JI, X.; WANG, Q. Production and characterization of cellulose nanofibrils from different chemical and mechanical pulps. **Journal of Wood Chemistry and Technology**, v. 38, n. 2, p. 149-158, 2018.

HELENIUS, G.; BÄCKDAHL, H.; BODIN, A.; NANNMARK, U.; GATENHOLM, P.; RISBERG, B. *In vivo* biocompatibility of bacterial cellulose. **Journal of Biomedical Materials Research,** v. 76A, p. 431-438, 2006.

HENRIKSSON, M.; HENRIKSSON, G.; BERGLUND, L. A.; LINDSTRÖM, T. An environmentally friendly method for enzyme-assisted preparation of microfibrillated cellulose (MFC) nanofibrils.**European Polymer Journal,** New York, v. 43, n. 8, p. 3434–3441, 2007.

HERRICK, F.W.; CASEBIER, R. L.; HAMILTON, J. K.; SANDBERG, K. R. Microfibrillated cellulose: morphology and accessibility. **Journal of Applied Polymer Science.** V. 37, p. 797–813, 1983.

HIMMEL, M.E.; DING, S.; JOHNSON, D.K.; ADNEY, W.S.; NIMLOS, M.R.; BRADY, J.W.; FOUST, T. D. Biomass recalcitrance: engineering plants and enzymes for biofuels production. **Science,** v. 315, p. 804–807, 2007.

HUA, J.; MARJO, K.; ARI, L.; HANNA, P.; JOUNI, P.; ABRAHAM, M.; OLLI, I.; ROBIN, H. A. R. Superhydrophobic and superoleophobic nanocellulose aerogel membranes as bioinspired cargo carriers on water and oil. **Langmuir,** v. 27, p. 1930-1934, 2011.

HUBBE, M. A.; ROJAS, O. L.; LUCIA, L. A.; SAIN, M. Cellulosic nanocomposites: a review. **Bioresources**, v. 3, n. 3, p. 929-980, 2008.

ISOGAI, A.; SAITO, T.; FUKUZUMI, H. TEMPO-oxidized cellulose nanofibrils. **Nanoscale**, v. 3, p.71–85, 2011.

IWAMOTO, S.; NAKAGAITO, A. N.; YANO, H. Nano-fibrillation of pulp fibers for the processing of transparent nanocomposites. **Applied Physics A: Materials Science and Processing**, Berlin, v. 89, n. 2, p. 461–466, 2007.

IWAMOTO, S.; ABE, K.; YANO, H. The effect of hemicelluloses on wood pulp nanofibrillation and nanofibrils network characteristics. **Biomacromolecules**, v. 9, n. 3, p. 1022–1026, 2008.

JEONG, S.; LEE, S. E.; YANG, H.; JIN, Y.; PARK, C.; PARK, Y. S. Toxicology evaluation of bacterial synthesized cellulose in endothelial cells and animals. **Molecular and Cellular Toxicology**, v. 6, p. 370-377, 2010.

JOHAR, N.; AHMAD, I.; DUFRESNE, A. Extraction, preparation and characterization of cellulose fibres and nanocrystals from rice husk. **Industrial Crops and Products**, v. 37, p. 93–99, 2012.

JOHN, M. J.; THOMAS, S. Biofibres and biocomposites. **Carbohydrate Polymers,** v. 71, n. 8, p. 343-364, 2008.

JONOOBI, M.; OLADI, R.; DAVOUDPOUR, Y.; OKSMAN, K.; DUFRESNE, A.; HAMZEH, Y.; DAVOODI, R. Different preparation methods and properties of nanostructured cellulose from various natural resources and residues: a review. **Cellulose**, Bucharest, v. 22, n. 2, p. 935–969, 2015.

JOSSET, S.; ORSOLINI, P.; SIQUEIRA, G.; TEJADO, A.; TINGAUT, P.; ZIMMERMANN, T. Energy consumption of the nanofibrillation of bleached pulp, wheat straw and recycled newspaper through a grinding process. **Nordic Pulp & Paper Research Journal**, v. 29, n. 1, p. 167-175, 2014.

JUUSO, T. K.; MARJO, K.; ROBIN, H. A. R.; OLLI, I. Hydrophobic nanocellulose aerogels as floating, sustainable, reusable, and recyclable oil absorbents. **ACS Applied Materials and Interfaces,** v. 3, p. 1813-1816, 2011.

KAPU, N. S.; TRAJANO, H. L. Review of hemicellulose hydrolysis in softwoods and bamboo. **Biofuels, Bioproducts and Biorefining**, v. 8, p. 857–870, 2014.

KÄRNER, K.; ELOMAA, M.; KALLAVUS, U. Fibrillation of Aspen by Alkaline Cold Pre-treatment and Vibration Milling. **Materials Science**, v. 22, n. 3, p. 358-363, 2016.

KEVIN, E. S.; WADOOD, Y. H.; MARK, J. M. Chiral nematic mesoporous carbon derived from nanocrystalline cellulose. **Angewandte Chemie International**, v.46, p. 10991-10995, 2011.

KIM, J. ; SHIM, B. S.; KIM, H. S.; LEE, Y. J.; MIN, S.; JANG, D.; ABAS, Z.; KIM, J. Review of nanocellulose for sustainable future materials. **International Journal of Precision Engineering and Manufacturing-Green Technology**, v. 2, p. 197–213, 2015.

KLEMM, D.; KRAMER, F.; MORITZ, S.; LINDSTRÖM, T.; ANKERFORS, M.; GRAY, D.; DORRIS, A. Nanocelluloses: a new family of nature-based materials. **Angewandte Chemie International Edition**, v. 50, p. 5438-5466, 2011.

KLEMM, D.; CRANSTON, E. D.; FISCHER, D.; GAMA, M.; KEDZIOR, S. A.; KRALISCH, D.; KRAMER, F.; KONDO, T.; LINDSTRÖM, T.; NIETZSCHE, S.; PETZOLD-WELCKE, K.; RAUCHFUß, F. Nanocellulose as a natural source for groundbreaking applications in materials science: Today's state. **Materials Today**, 29 p., 2017.

LANGAN, P.; PETRIDIS, L.; O'NEIL, H. M.; PINGALI, S. V.; FOSTON, M.; NISHIYAMA, Y.; SCHULZ, R.; LINDNER, B.; HANSON, B. L.; HARTON, S.; HELLER, W. T.; URBAN, V.; EVAN, B. R.; GNANAKARAN, S.; RAGAUSKAS, A. J.; SMITH, J. C.; DAVISON, B. H. Davison, Common processes drive the thermochemical pretreatment of lignocellulosic biomass, **Green Chemistry**, v. 16, p. 63–68, 2014.

LAPUZ, M. M.; GALLARDO, E. G.; PALO, M. A. The nata organismo cultural requirements characteristics and identity coconut m-acetobacter xylium. **Philippine Journal of Science**, v. 96, p. 91-109, 1967.
LAVOINE, N.; DESLOGES, I.; DUFRESNE, A.; BRAS, J. Microfibrillated cellulose – its barrier properties and applications in cellulosic materials: a review, **Carbohydrate Polymers**, v. 90, p. 735–764, 2012.

LEE, C. M.; MITTAL, A.; BARNETTE, A. L. KAFLE, K.; PARK, Y. B.; SHIN, H.; JOHNSON, D. K.; PARK, S.; KIM, S. H. Cellulose polymorphism study with sum-frequencygeneration (SFG) vibration spectroscopy: identification of exocyclic CH_2OH conformation and chain orientation. **Cellulose,** v. 20, p. 991-1000, 2013.

LI, X.; SUN, C.; ZHOU, B.; HE, Y. Determination of hemicellulose, cellulose and lignin in Moso bamboo by near infrared spectroscopy, **Scientific Reports** v. 5(17210), P. 1–11, 2015.

LIIMATAINEN, H.; VISANKO, M.; SIRVIÖ, J.; HORMI, O.; NIINIMÄKI, J.Sulfonated cellulose nanofibrils obtained from wood pulp through regioselective oxidative bisulfite pre-treatment. **Cellulose**, v. 20, p. 741–749, 2013.

LIN, N.; DUFRESNE, A. Nanocellulose in biomedicine: Current status and future prospect. **European Polymer Journal**, v. 59, p. 302-325, 2014.

LINDSTRÖM, T. Chemical factors affecting the behaviour of fibres during papermaking. **Nordic Pulp and Paper Research Journal**. V. 7, p. 181-192, 1992.

LIU, W.J.; JIAN, H.; YU, H. Q. Thermochemical conversion of lignin to functional materials: a review and future directions. **Green Chemistry,** v. 17, p. 4888–4907, 2015.

LÖBMANN, K.; SVAGAN, A. J.; Cellulose nanofibers as excipient for the delivery of poorly soluble drugs. **International Journal of Pharmaceutics**, v. 533, p. 285–297, 2017.

LONG, L.; TIAN, D.; HU, J.; WANG, F.; SADDLER, J. A xylanase-aided enzymatic pretreatment facilitates cellulose nanofibrillation. **Bioresource Technology**. V. 243, p. 898–904, 2017.

LU, P.; HSIEH, Y. L. Preparation and properties of cellulose nanocrystals: rods, spheres, and network. **Carbohydrate Polymers**, v. 82, p. 329–336, 2010.

MIRMEHDI, S.; DE OLIVEIRA, M. L. C.; HEIN, P. R. G.; DIAS, M. V.; SARANTÓPOULOS, C. I. G. L.; TONOLI, G. H. D. Spraying Cellulose Nanofibrils for Improvement of Tensile and Barrier Properties of Writing & Printing (W&P) Paper. **Journal of Wood Chemistry and Technology**, v. 38, p. 1-13, 2018a.

MIRMEHDI, S.; HEIN, P. R. G.; SARANTÓPOULOS, C. I. G. L.; DIAS, M. V.; TONOLI, G. H. D. Cellulose nanofibrils/nanoclay hybrid composite as a paper coating: Effects of spray time, nanoclay content and corona discharge on barrier and mechanical properties of the coated papers. **Food Packing and Shelf Life**, v. 15, p. 87-94, 2018b.

MOHD AMIN, M. C. I; AHMAD, N.; HALIB, N.; AHMAD, I. Synthesis and characterization of thermo- and pH-responsive bacterial cellulose/acrylic acid hydrogels for drug delivery. **Carbohydrate Polymers**, v. 88, n. 2, p. 465–473, 2012.

MONIRUZZAMAN, M.; ONO, T. Separation and characterization of cellulose fibers from cypress wood treated with ionic liquid prior to laccase treatment. **Bioresource Technology**, V, 127, p. 132–137, 2013.

MOON, R. J.; MARTINI, A.; NAIRN, J.; SIMONSEN, J; YOUNGBLOOD, J. Cellulose nanomaterials review: structure, properties and nanocomposites. **Chemical Society Reviews,** v. 40, p. 3941–3994, 2011.

MOREIRA, F. K. V. **Desenvolvimento de nanocompósitos poliméricos biodegradáveis a partir de pectina, amido e nanofibras de celulose.** 181 p. Dissertação (Mestrado em Engenharia de Materiais) – Universidade Federal de São Carlos (UFSCar), São Carlos, 2010.

NADERI, A.; LINDSTRÖM, T.; SUNDSTRÖM, J. Carboxymethylated nanofibrillated cellulose: rheological studies. **Cellulose**. V. 21, p. 1561–1571, 2014.

NECHYPORCHUK, O.; BELGACEM, M.; BRAS, J. Production of cellulose nanofibrils: a review of recent advances. **Industrial Crops and Products**, v. 93, p. 2–25, 2016.

NIE, S.; ZHANGA, K.; LINA, X.; ZHANGA, C.; YANA, D.; LIANGA, H.; WANGA, S. Enzymatic pretreatment for the improvement of dispersion and film properties of cellulose nanofibrils. **Carbohydrate Polymers**, v.181, p. 1136–1142, 2018.

OLIVEIRA, E. Correlações entre parâmetros de qualidade da madeira e do carvão de Eucalyptus grandis (W.Hill ex-Maiden). **Boletim técnico-SIF**, Viçosa, p. 1-9, 1990.

OLSSON, C.; WESTMAN, G. Direct Dissolution of Cellulose: Background, Means and Applications. In: VEN, T. V.; GODBOUT, L. Cellulose – Fundamental aspects. **Intechopen**, Rijeka, p. 143-178, 2013.

PÄÄKKÖ, M.; ANKERFORS, M.; KOSONEN, H.; NYKÄNEN, A.; AHOLA, S.; ÖSTERBERG, M.; RUOKOLAINEN, J.; LAINE, J.; LARSSON, P. T.; IKKALA, O.; LINDSTRÖM, T.Enzymatic Hydrolysis Combined with Mechanical Shearing and High-Pressure Homogenization for Nanoscale Cellulose Fibrils and Strong Gels. **Biomacromolecules**, v. 8, p. 1934-1941, 2007.

PAYEN, A. Mémoire sur la composition du tissu propre des plantes et du ligneux. **Comptes Rendus,**v. 7, p. 1052–1056, 1838.

PENG B. L.; DHAR, N.; LIU, H. L.; TAM, K. C. Chemistry and applications of nanocrystalline cellulose and its derivatives: a nanotechnology perspective. **The Canadian Journal of Chemical Engineering,** v, 89, p. 1191–1206, 2011.

PHISALAPHONG, M.; CHIAOPRAKOBKIJ, N. Applications and Products - Nata de Coco. IN: GAMA, M.; GATENHOLM, P.; KLEMM, D. Bacterial nanocellulose: a sophisticated multifunctional material. **CRC Press**, p. 143–156, 2013.

PIRAS, C. C.; FERNANDEZ-PRIETO, S.; DE BORGGRAEVE, W. M. Nanocellulosic materials as bioinks for 3D bioprinting. **Biomaterial Science**, v. 5, p. 1988–1992, 2017.

PITARELO, A. P. Avaliação da susceptibilidade do bagaço e da palha da canade-açúcar à bioconversão via pré-tratamento a vapor e hidrólise enzimática. Dissertação (Mestrado em Química) - Universidade Federal do Paraná, Curitiba, 2007.

QING, Y.; SABOB, R.; ZHUB, J. Y.; CAI, Z.; WU, Y. Comparative study of cellulose nanofibrils: disintegrated from different approaches. **Bioresource Technology,** v. 130, p.783–788. 2013.

RAJINIPRIYA, M.; NAGALAKSHMAIAH, M.; ROBERT, M.; ELKOUN, S. Importance of agricultural and industrial waste in the field of nanocellulose and recent industrial developments of wood based nanocellulose: a review. **ACS Sustainable Chemistry and Engineering**, v. 6, p. 2807–2828, 2018.

RAMOS, L. P. **Steam pretreatment and enzymatic hydrolysis of Eucalyptus viminalis chips.** Ph. D. Thesis. Ottawa: University of Ottawa, 1992.

REBOUILLAT, S.; PLA, F. State of the Art Manufacturing and Engineering of Nanocellulose: A Review of Available Data and Industrial Applications. **Journal of Biomaterials and Nanobiotechnology,** v. 4, p. 165–188, 2013.

RIBES, D. D.; ZANATTA, P.; GATTO, D. A.; MAGALÃES, W. L. E.; BELTRAME, R. Produção de suspensão nanofibrilares de celulose vegetal por meio do processo combinado – Avaliação do gasto energético. **Revista Matéria,** v. 23, n. 04, 2018.

ROWELL, R. M. Property enhanced natural fiber composite materials based on chemical modification. IN: KANDIL, S. H.; KAFAFI, Z. H.; MARK, J. E. Science and technology of polymers and advanced materials: emerging technologies and business opportunities. New York: **Plenum**, p. 717-732, 1998.

RUI, X.; XINXING, Z.; DONG, T.; ZEHANG, Z.; CANHUI, L. Comparing microcrystalline with spherical nanocrystalline cellulose from waste cotton fabrics. **Cellulose**, v. 19, p. 1189-1198, 2012.

SAITO, T.; NISHIYAMA, Y.; PUTAUX, J.; VIGNON, M.; ISOGAI, A. Homogeneous Suspensions of individualized microfibrils from TEMPO-catalyzed oxidation of native cellulose. **Biomacromolecules**, v. 7, n. 6, p. 1687–1691, 2006.

SAITO, T.; ISOGAI, A. Introducation of aldehyde groups on surfaces of native cellulose fibers by TEMPO-mediated oxidation. **Biomacromolecules,** v. 289, p. 219–225, 2006.

SAMIR, M. A. S. A.; ALLOIN,J.; DUFRESNE, A. Review of recent research intocellulosic whiskers, their properties and their application in nanocompositefield. **Biomacromolecules**, v. 6, p. 612–626, 2005.

SCALLAN, A.M. The effect of acid groups on the swelling of pulps: A review. **Tappi Journal,** v. 66, p. 73–75, 1983.

SCHELLER, H.V.; ULVSKOV, P. Hemicelluloses, **Annual Review of Plant Biology,** v. 61, p. 263–289, 2010.

SILVA, A. C. Estudo da durabilidade de compósitos reforçados com fibras de celulose. 145 p. Dissertação (Mestrado em Engenharia Civil) - Escola Politécnica da Universidade de São Paulo, São Paulo, 2002.

SILVA, E; MARQUES, M. L; FORNARI JUNIOR, C; VELASCO, F. Análise técnica para o reaproveitamento da fibra de coco na construção civil. **Ambiência Guarapuava,** v.11, n.3 p. 669–683, 2015.

SIQUEIRA, G.; BRAS, J.; DUFRESNE, A. Cellulosic Bionanocomposites: A Review of Preparation, Properties and Applications. **Polymers**, v. 2, n. 4, p. 728-765, 2010.

SIRÓ, I.; PLACKETT, D. Microfibrillated cellulose and new nanocomposite materials: A review. **Cellulose**, Bucharest, v. 17, n. 3, p. 459–494, 2010.

SOUZA, F. S. Obtenção de nanofibras de curauá e aplicação como reforço em compósitos baseados em PVA. 2010. 80 p. Dissertação (Mestrado em Agronomia) – Universidade Estadual Paulista, Botucatu, 2010.

SOZER, N.; KOKINI, J. L. Nanotechnology and its applications in the food sector. **Trends in Biotechnology**, v. 27, n. 2, p. 82–89, 2009.

SPENCE, K.L.; VENDITTI, R.A.; ROJAS, O.J.; HABIBI, Y.; PAWLAK, J.J. The effect of chemical composition on microfibrillat cellulose films from wood pulps: water interactions and physical properties for packaging applications. **Cellulose**, v. 17, p. 835–848, 2010.

STENSTAD, P.; ANDRESEN, M.; TANEM, B. S.; STENIUS, P. Chemical surface modifications of microfibrillated cellulose. **Cellulose**, v. 1, p. 35-45, 2008.

SUN, X.; WU, Q.; ZHANG, X.; REN, S.; LEI, T.; LI, W.; XU, G.; ZHANG, Q. Nanocellulose films with combined cellulose nanofibrils and nanocrystals: tailored thermal, optical and mechanical. **Cellulose**, v. 25, p. 1103–1115, 2018.

SUN-YOUNG, L.; JAGAN, D. M.; IN-AEH, K.; GEUM-HYUN, D.; SOO, L.; SEONG, O. H. Nanocellulose reinforced PVA composite films: effects of acid treatment and filler loading. **Fibers and Polymers,** v. 10(1), p. 77-82, 2009.

SYVERUD, K.; STENIUS, P. Strength and barrier properties of MFC films, **Cellulose**, v. 16, p. 75, 2009.

TAIPALE, T.; ÖSTERBERG, M.; NYKÄNEN, A.; RUOKOLAINEN, J.; LAINE, J. Effect of microfibrillated cellulose and fines on the drainage of Kraft pulp suspension and paper strength. **Cellulose**, v. 17, p. 1005–1020, 2010.

TAIZ, L.; ZEIGER, E. **Plant Physiology**. Third edition, Sinauer Associates in. 2002.

TANIGUCHI, T.; OKAMURA, K. New films produced from microfibrillated natural fibres. **Polymer International**, v. 47, n. 3, p. 291-294, 1998

TENKANEN, M. et al. Cellulases in food processing. **Journal Food Science Engineering,** v. 122, p. 771–789, 2003.
TIBOLLA, H.; PELISSARI, F. M.; MENEGALLI, F. C. Cellulose nanofibrils produced from banana peel by chemical and enzymatic treatment.**LWT - Food Science and Technology**, v. 59, n. 2P2, p. 1311–1318, 2014.

TIENNE, D. L. C.; OLIVEIRA, J. N.; PAERMO, G. O. M.; SOUSA, J. S.; LATORRACA, J. V. F. Influência do espaçamento no ângulo das microfibrilas e comprimento de fibras de clone de eucalipto. **Revista Forestal Latinoamericana,** Mérida, v. 24, n.1, p. 67-83, 2009.

TONOLI, G. H. D.; TEIXEIRA, E. M.; CORREA, A. C.; MARCONCINI, J. M.; CAIXETA, L. A.; PEREIRA DA SILVA, M. A.; MATTOSO, L. H. C. Cellulose micro/nanofibres from *Eucalyptus* Kraft pulp: Preparation and properties. **Carbohydrate Polymers**, v. 89, p. 80-88, 2012.

TURBAK, A. F.; SNYDER, F. W.; SANDERB, K. R. Microfibrillated cellulose, a new product: properties, uses, and commercial potential. **Journal ofApplied Polymer Science**, v. 37, p. 815–827, 1983.

TUZZIN, G.; GODINHO, M.; DETTMER, A.; ZATTERA, A.J. Nanofibrillated cellulose from tobacco industry wastes. **Carbohydrate Polymer**. V. 148, p. 69–77, 2016.

VALERIA, F.; MANUELA, M.; LINDA, F.; MASSIMO, Z.; ILSE, M.; WERNER, O.; GIULIANO, G.; MARCO, F.; GUIDO, G.; NADIA, C. Poly(lactic acid) as a transparent matrix for luminescent solar concentrators: a renewable material for a renewable energy technology. **Energy and Environmental Science**, v. 4, p. 2849-2853, 2011.

VIIKARI, L.; OKSANEN, T.; SUURNAKKI, A.; BUCHERT, J.; PCRE, J. Cellulases in pulp and paper processing. **VTT Biotechnology and Food Research,** p. 69-80, 2000.

VILLANOVA, J. C. O.; AYRES, E.; CARVALHO, S. M.; PATRICIO, P. S.; PEREIRA, F. V.; OREFICE, R. L. Pharmaceutical acrylic beads obtained by suspension polymerization containing cellulose nanowhiskers as excipient for drug delivery. **European Journal of Pharmaceutical Sciences**, v. 42, n. 4, p. 406–415, 2011.

WADOOD, H. On the development and applications of cellulosic nanofibrillar and nanocrystalline materials. **The Canadian Journal of Chemical Engineering**, v. 84(5), p. 513-519, 2006.

WANG, Y.; WEI, X.; LI, J.; WANG, F.; WANG, Q.; KONG, L. Homogeneous isolation of nanocellulose from cotton cellulose by high pressure homogenization. **Journal of Materials Science and Chemical Engineering**, v. 1, p. 49–52, 2013.

WANG, H.; LI, D.; YANO, H.; ABE, K. Preparation of tough cellulose II nanofibrils with high thermal stability from wood.**Cellulose**, v. 21, n. 3, p. 1505–1515, 2014.

ZHU, J. Y.; SABO, R.; LUO, X. Integrated production of nano-fibrillated cellulose and cellulosic biofuel (ethanol) by enzymatic fractionation of wood fibers. **Green Chemistry**, London, v. 13, n. 5, p. 1339, 2011.

SEGUNDA PARTE

ARTIGO: Bleached cellulosic nanofibrils extraction: Energy consumption decrease by endoglucanase-mediated pretreatment

Allan de Amorim dos Santos[a], Maryella Júnnia Ferreira e Silva[a], Luiz Eduardo Silva[a], Alisson Farley Soares Durães[a], Matheus Cordazzo Dias[a], Renato Augusto Pereira Damásio[b], Gustavo Henrique Denzin Tonoli[a]*.

a Forest Science department, University of Lavras, University Campus, P.O. Box 3037, 37200-000, Lavras, Minas Gerais, Brazil.

b Industrial RDI – Technology Center Fazenda Monte Alegre, St Harmonia, 03 Postal code 84275-000 – Telêmaco Borba PR, Brazil.

**Corresponding author: gustavotonoli@yahoo.com.br, +553538291426.*

ABSTRACT

Enzymatic hydrolysis has been used as pretreatment for mechanical extraction of cellulose nanofibrils. Pretreatment using cellulases assists in fiber swelling and generates dislocations, thereby the energy consumption for fibrillation of cellulosic pulps drops significantly. This work aimed to evaluate the influence of enzymatic pretreatment on mechanical nanofibril obtention. It was analyzed the chemical and anatomical characteristics of fibers, morphological and structural characteristics of suspended nanofibrils and films, comparing to the extraction of nanofibrils pretreated with 2,2,6,6-tetramethylpiperidine 1-oxyl (TEMPO) oxidation. Bleached pulps of *Eucalyptus* sp. and *Pinus* sp. were pretreated with two different endoglucanase-like enzymes (A and B), and without the addition of enzyme as a control. The mechanical fibrillation process was performed in 5 cycles through the fibrillator with 2% w/w suspension. It was recorded the cycle in which a gel appearance of the suspension was observed. Suspension samples were collected at each cycle. Results showed that pretreatment did not significantly modify the contents of the chemical components of both pulps, as well as their anatomical characteristics. The energy consumption of pretreated pulps was lower than that shown by pulp pretreated with TEMPO. Compared with control (untreated), enzymatic pretreatement reached up to 58% of energy savings. Nanofibrils pretreated with enzyme A and B presented smaller median diameter, close to that found for TEMPO-mediated nanofibrils. Furthermore, enzyme A showed efficient stabilization of the nanofibrils suspension, with higher supernatant turbidity and higher zeta potential value in relation to untreated (control) pulps. The films generated from TEMPO-treated nanofibrils had a lower

tensile strength than those found for the enzymatic treatment. Therefore, the enzymatic pretreatment mediated by endoglucanase produces high quality nanofibrils.

Keywords: Endoglucanase. Enzymatic hydrolysis. Green extraction. Microfibrillated cellulose. TEMPO-mediated oxidation.

1 INTRODUCTION

Cellulose nanofibrils (CNFs) were first developed in the late 1970's in the United States. But it was not until the early twenty-first century that its study became attractive. Research has focused on cellulose nanofibrils for their production, modification, characterization and properties, looking for a better use of their potential (Herrick et al., 1983). They are mostly structural components of the primary and secondary cell walls of lignocellulosic plants. However, they are also found in marine tunicates, algae, fungi and bacteria (Gharehkhani et al., 2015, Habibi et al., 2010).

To be characterized as a nanostructure, the nanofibrils must have one of their dimensions in a nanometric scale of 10 to 100 nm, usually the diameter. They are distinguished by their high aspect ratio, high strength and stiffness, lightness, and high specific strength (Herrick et al., 1983, Bledzki & Gassan, 1999; Ishii et al., 2011). Its current production is based on commercial cellulosic pulp. In addition to being the most abundant polymer found in the environment, cellulose presents biodegradable, renewable and non-toxic characteristics.

Nanofibrils can be applied as reinforcement in packaging and paper (Matos et al., 2019; Mirmehdi et al., 2018; Abdul Khalil et al., 2014), rheological modifier in foods (Resende et al., 2018; Shi et al., 2013), in the automotive sector (Kalia et al., 2014), batteries and panels (Cunha Arantes et al., 2018; Huang et al., 2013), biomedics (Ling et al., 2018), nanotechnological sensors (Huang et al., 2013; Wu et al., 2015), reinforcement in composites (Fonseca et al., 2019a; Guimarães Júnior et al., 2018; Lopes et al., 2018), among others. Cellulose nanofibrils production consists of their construction, molecule by molecule, via bottom-up methods such as electrospinning and bacterial nanocellulose formation. On the other hand, top-down methods include the deconstruction of lignocellulosic materials. It can be mentioned the mechanical processes (Wang et al., 2012), enzyme hydrolysis (Siró and Plackett, 2010) and chemical processes (Abraham et al., 2011; Tonoli et al., 2016).

A disadvantage regarding the use of the mechanical process in cellulosic pulps is the high energy consumption necessary to break down numerous hydrogen bonds between the

hydroxyl groups in nanofibrils surface (Chinga-Carrasco, 2011). Siró and Plackett (2010), evaluating mechanical fibrillation, achieved an energy consumption of about 20,000-30,000 kW.h/ton of pulp. A number of authors studied energy savings during nanofibrils extraction (Fonseca et al., 2019b; Bauli et al., 2019; Ribes et al., 2018; Long et al., 2017; Qing et al., 2013; Henriksson et al. al., 2007; Pääkkö et al., 2007). These authors suggested the combination of different production methods as pretreatments in order to reduce such consumption as well as modify characteristics of the pulp, adapting to its application purpose.

A chemical pretreatment that has stood out in recent studies is the pretreatment involving the oxidation of 2,2,6,6-tetramethylpiperidine 1-oxyl, known as the TEMPO-oxidation method (Wu et al., 2019; Gamelas et al., 2015). It generates nanofibrils with smaller and more uniform diameters, with more stable suspension and it makes the films more transparent (Isogai et al., 2011). However, in addition to being an expensive reagent, TEMPO produces films of nanofibrils with low thermal stability due to carboxylation of carbon 6 caused in the cellulosic chain (Saito et al., 2009).

The enzymatic pretreatment has been studied in the last years with the purpose of reducing the energy consumption during the mechanical extraction of cellulose nanofibrils. Furthermore, enzymatic pretreatment do not cause significant modifications in the chemical and morphological composition of the fibers. This modification could contribute to the alteration of the properties of nanofibrils (Sacui et al., 2014; Zhu et al., 2011). Enzymes may cause detachment of fibrils from the cell wall. Moreover, they can cause ruptures, known as dislocations, which may cause a reduction in the mechanical properties of fibers facilitating the disintegration of fibers in nanoscale structures (Durães, 2018; Ander et al., 2008). Its action is specific to a fiber component. As most of the fiber is composed of cellulose (Burguer and Ritcher, 1991), cellulases become important in this process. During enzymatic hydrolysis, cellulases can act with endoglucanase activity, generating oligosaccharides from the random cleavage of cellulose chains (Kim et al., 2017).

Even with numerous studies related to the mechanical production of nanofibrils on reduction of energy consumption and on the enzymatic activity in cellulosic pulp, it is still necessary to study the quality of nanofibrils formed. Therefore, this study aimed to evaluate the modification in energy consumption during extraction of pretreated cellulose pulps with cellulase enzymes. Also, the morphological characterization of suspended fibers and nanofibrils was carried out as well as the mechanical resistance of the films generated from the nanofibrils. A comparison of these characteristics was performed between enzymatic

pretreatments and control treatment (untreated) and nanofibrils extracted with TEMPO-mediated oxidation pretreatment.

2 EXPERIMENTAL

2.1 Materials

Bleached *Eucalyptus* sp. (B-Euc) and *Pinus* sp. (B-Pin) Kraft pulps were provided by Klabin S.A. (Paraná/Brazil). The oxidant 2,2,6,6-tetramethylpiperidine 1-oxyl (TEMPO; T) was provided by Sigma-Aldrich. Two endoglucanase enzymes, A and B, were used in this work and their application conditions are specified in Table 1.

Table 1. Enzymes specifications.

	Enzyme A	**Enzyme B**
Product	NS51137 / CGK20092	NS51179 / CVN04076
Activity	Endoglucanase	Endoglucanase
pH	7.0 – 7.5	6.0 – 6.5
Temperature (°C)	45 – 55	45 – 65
Dosage (g/ton)	50 – 150	50 – 150

2.2 Pretreatments and mechanical fibrillation

This study was conducted by the application of enzymatic hydrolysis with two enzymes (A and B), and compared with the TEMPO oxidation (T) as pretreatments, as well as a treatment control without the addition of enzyme (WE). The analysis was conducted on B-Euc and B-Pin pulps. Figure 1 depicts the pretreatments and analysis realized in this work.

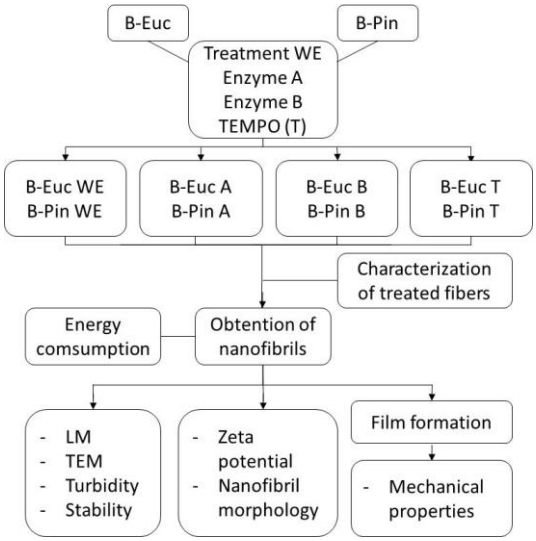

Figure 1. Flowchart containing the pretreatments and others stages of the present work. LM: Light microscopy. TEM: Transmission electron microscopy.

2.2.1 Enzymatic pretreatment

For enzymatic pretreatments, 60 g of each pulp were immersed in 2 L of deionized water for 24 h in order to disintegrate pulp aggregates and make the cellulose more accessible to the enzymatic hydrolysis, as Silva (2018) suggested. Temperature was kept at 50±2°C and pH was adjusted during hydrolysis with NaOH 5% w/w or H_2SO_4 5% w/w, following conditions presented in Table 1. Then, it was added 100 g/ton of endoglucanase enzyme to the suspension. Enzymatic hydrolysis was carried for 120 min under 750 rpm. After enzymatic pretreatment, pulps were washed at 90±2ºC until pH is neutral in order to stop enzyme activity. For each pulp, one sample was designated as control treatment, and the other two were pretreated with cellulase at same conditions. Washed suspensions were oven-dried, used for analysis and subsequently submitted to mechanical fibrillation.

2.2.2 TEMPO-mediated oxidation pretreatment

This pretreatment was included to compare with the final characteristics of the nanofibrils submitted to enzymatic pretreatment. The oxidation pretreatment mediated by TEMPO followed indications suggested by Saito et al. (2007). It was used 60 g of cellulose at 2% w/w, containing TEMPO (0.96 g) and NaBr (6 g). TEMPO-mediated oxidation occurred with the addition of 10% NaClO (3.1 g, 5.0 mmol) at room temperature under agitation of 750 rpm. The pH was maintained at 10 by adding 0.5 mol/L NaOH solution. When pH stabilized, the reaction occurred for 3 h. Then, the pH was adjusted to 7 by adding 0.5 mol/L HCl solution and the suspension was thoroughly washed with deionized water. Pulps were oven dried for further analysis.

2.2.3 Mechanical fibrillation

Cellulose nanofibrils were obtained by the mechanical process based on Bufalino et al. (2014) and Guimarães Júnior et al. (2015). 60 g of oven-dried pretreated pulp were previously hydrated in 3 L of deionized water for 72 h. The suspension was agitated at 750 rpm for 30 min (NT134 high torque mechanical) in order to individualize cellulosic fibers. Pulp was taken to the Super Masscolloider Masuko Sangyo MKCA6-2 (grinder fibrillator) microprocessor for 5 cycles. The cycle at which the suspension had gel-like appearance was used for energy consumption calculation. The procedure to adjust zero movement position of the fibrillator followed the study of Wang et al. (2012). Samples of each cycle were refrigerated at 5±1°C to avoid any degradation by microorganisms.

During mechanical fibrillation, the energy consumption of the grinder was calculated using Equation (1), following the work of Dias (2017).

$$\mathbf{EC} = \frac{\mathbf{p\ x\ h}}{\mathbf{m}} \quad (1)$$

EC is energy consumption (kW.h/ton), p is power in kW (voltage x current), h is time for passing through the fibrillator in hours and m is mass of dried pulp in tons. Energy index was also calculated in order to compare pretreatments according to its energy consumption. It was estimated by the Equation (2):

$$\mathbf{EI} = \left(\frac{\mathbf{ECtreat - ECref}}{\mathbf{ECtreat}}\right)\mathbf{x\ 100} \quad (2)$$

EI is energy index in %, ECtreat is energy consumption of the enzymatic treatment, and ECref is the energy consumption of the control treatment.

2.3 Analytic methods

2.3.1 Chemical and anatomic characterization of pretreated pulps

In order to verify the effect of enzymatic pretreatment on the cellulosic fibers, pulps were chemically and anatomically characterized before and after pretreatments. Chemically, monosaccharides were quantified as indicated by Wallis, Wearne and Wright (1996) using Dionex ICS 5000 ion chromatography system. Ash content and lignin content were disregarded.

Fiber anatomic characterization was performed with the Valmet FS5 (Finland) fiber image analyzer. It was analyzed weighted average fiber length, witdh, cell wall thickness, fines and cell wall fibrillation. Cell wall fibrillation is an important characterization because it represents the delamination of the surface layers of fibers (Fardim and Durán, 2003). Fines are particles with diameter under 75 μm or fibrils that can pass through a 200-mesh fiber classifier (TAPPI, 1995).

2.3.2 Light microscopy

In order to evaluate pulp fibrillation of each cycle through the grinder, nanofibril suspensions (0.75% w/w) with 1.0% v/v ethanol-safranin were analyzed by light optical microscope Olympus BX51, comparing control and enzymatic pretreatments.

2.3.3 Transmission electron microscopy

Morphological analysis by transmission electron microscopy of cellulose nanofibrils from the gel formation cycle after mechanical fibrillation were performed by Tecnai G2-12, accelerated voltage of 80 kV, following recommendations described by Tonoli et al. (2016). Control, enzymatic and TEMPO nanofibrils diameter analysis were performed on 200 fibril structures by ImageJ software (Schindelin et al., 2012) .

2.3.4 Turbidity

Visual aspect of nanofibrils suspensions followed suggestion of Winter et al. (2010). Samples were diluted to 0.1% w/w and held in test tubes for 1.5 h to decant. Following, supernatant was analyzed in triplicate by a Turbidimeter Plus Alfakit apparatus. Turbidity checks how clear or how turbid a suspension is. Such turbidity increases with increasing number of individual particles in the suspension, and it is measured using the Nephelometric Turbidity Units (NTU) unit.

2.3.5 Stability of cellulose nanofibril suspensions

Stability of nanofibrils in water was investigated following suggestions of Guimarães Júnior et al. (2015). Samples were diluted at 0.25% w/w and 30 mL of suspension kept in test tubes for 48 h decantation. Stability of cellulose nanofibrils of each cycle through grinder were measured by ImageJ software (Schindelin et al., 2012) .

2.3.6 Zeta potential

Cellulose nanofibrils suspension (0.05% w/w) in pure water were sonified for 5 min and prepared to determine potential charges on nanofibrils surface by a Malvern 30000 zetasizer, and the control and enzymatic treated suspensions were analyzed.

2.3.7 Film mechanical properties

Films of gel formation cycle and 5 cycles were formed according to Guimarães Júnior et al. (2015), in which 40 mL suspension (1.0 % w/w) samples were poured onto 15 cm

diameter acrylic petri dishes. Suspensions were dried in a circulation oven at 45 ºC for 48 h to form the films.

The tensile strength of the films was evaluated following the ASTM D828-16 (ASTM, 2016) standard. Test specimens of 10 cm long and 1 cm width were carried out in the texture analyzer equipment (Stable Microsystems, TATX2i model, England), with a distance between jaws of 50±2 mm and a speed of 1 mm/min. Five specimens were analyzed and the tensile strength was calculated following Equation (2).

$$\sigma_{max} = \frac{F}{A_0} \quad (3)$$

Whereas: σmax is the maximum tensile stress (MPa); F is the maximum force applied on the test piece (N); A_0 is the cross-sectional area of the specimen (mm^2).

It was also observed the strain at rupture and the Young's modulus of the films. The tangent of the linear region of the stress-strain curves, considered the elastic region, provides the Young's modulus or modulus of elasticity (Santos and Yoshida, 2011).

3 RESULTS AND DISCUSSION

3.1 Effect of enzymatic pretreatment on chemical and anatomical characteristics

Enzymatic pretreatment is known to have specific reaction, in the case of cellulase its specificity is with the cutting of the cellulose chains, thus not degrading other components of the cellulosic fibers. This reaction occurs mainly on amorphous region of cellulose, in which cellulose is more accessible (Henriksson et al., 1999). During the enzymatic hydrolysis there is extraction of sugars from the cellulosic pulp, including glucose. The more cellulose reacts, more losses are observed for the cellulose content (Rabelo, 2007).

As shown in Figure 2, the contents of cellulose and hemicelluloses kept similar to all pretreatments. B-Euc cellulose pulp content surrounded 86%. B-Pin also presented similar cellulose content with 83%. The hydrolysis of cellulose into sugars is only beneficial when it is considered a co-product, as shown by Zhu et al. (2011). As this work looks for a higher production yield with lower energy cost, the degradation of cellulose is undesirable.

Hemicelluloses content surrounds 14% for B-Euc and 17% for B-Pin. Hemicelluloses degradation may occur due to stirring in water and temperature (Brito et al., 2008), even under milder conditions (Dahlman et al., 2003). As cellulose content decreased,

hemicelluloses content increased. Similar results were found by Silva (2018). Liu et al. (2019) also noted that the loss of cellulose into sugars was quite limited after enzymatic pretreatment.

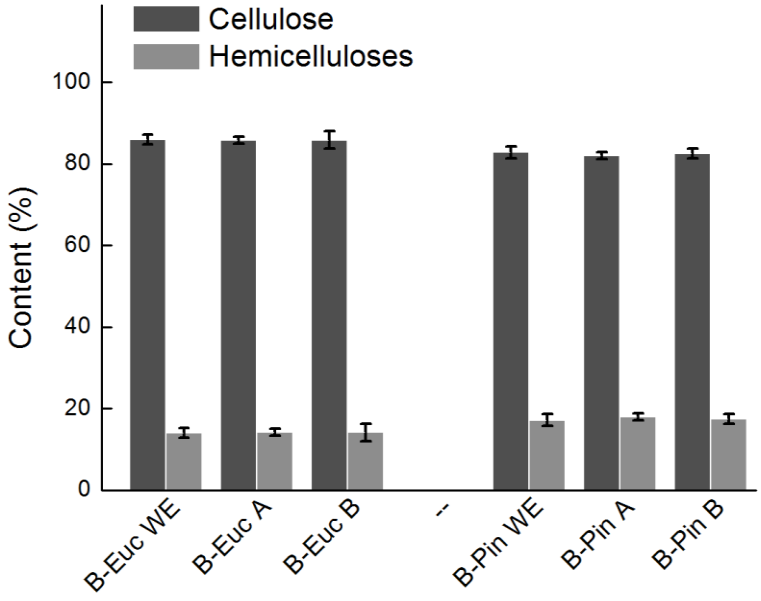

Figure 2. Chemical composition (cellulose and hemicelluloses) of bleached pulps.

While enzymatic pretreatment did not affect chemical fiber composition, chemical pretreatments significantly modify them. The content of cellulose and hemicelluloses differ greatly from control as observed by Dias (2017) and Mendonça (2018). Alkaline treatments are also efficient to remove xylan from commercial pulps (Bufalino et al., 2015).

Table 2 shows the average and standard deviations of fibers anatomical characteristics after pretreatments. The fiber length of B-Euc did not change after enzymatic pretreatments, with 0.71 ± 0.01 mm for control and also for pretreatment A and B. For B-Euc T, the average was higher probably due to cell wall swelling promoted by the TEMPO oxidation. For B-Pin, it was observed a decrease in average length from 1.81 ± 0.05 mm to 1.64 ± 0.04 mm in the pretreatment with enzyme A, and to 1.76 ± 0.01 mm for enzyme B. As enzymes act mainly on the amorphous region of the cellulosic chains, the decrease of the average length of the fiber should be related to this enzymatic action, breaking fibers during pretreatment. Length decreasing can be also related to a curl fiber index (Blomstedt et al., 2017) or the fact that pulps were dried after the pretreatment, causing hornification and loss of fiber volume (Ballesteros et al., 2017).

A slight decrease was observed on width for all pretreated fibers compared to control pulps, but values were similar, according to Tukey's test. B-Euc width surrounds 15.8 ± 0.1 µm for WE, A and B pretreatment. B-Pin presented slight changing from 26.1 ± 0.2 µm for

WE to 24.9 ± 0.2 µm for A and B pretreatment. This decrease can be related to enzymatic action in amorphous regions with consequent decrease in width. Again, as reported above, oven-drying after pretreatment may have caused lumen collapse due to hornification (Ballesteros et al., 2017).

Table 2. Average and standard deviation values of the fiber morphology obtained with the Valmet FS5 fiber image analyzer.*

	Length (mm)	Width (µm)	CWT (µm)	Fines (%)	CWF (%)
B-Euc WE	0.71 ± 0.01 ^{f}	15.8 ± 0.1 ^{d}	3.2 ± 0.1 ^{b}	14.9 ± 0.1 ^{c}	1.05 ± 0.01 ^{b}
B-Euc A	0.71 ± 0.01 ^{f}	15.8 ± 0.1 ^{d}	3.9 ± 0.1 ^{a}	15.5 ± 0.1 ^{b}	1.07 ± 0.01 ^{a,b}
B-Euc B	0.71 ± 0.01 ^{f}	15.6 ± 0.1 ^{d}	3.5 ± 0.1 ^{b}	15.8 ± 0.1 ^{b}	1.07 ± 0.01 ^{a,b}
B-Euc T	0.78 ± 0.01 ^{e}	16.4 ± 0.1 ^{c}	4.1 ± 0.2 ^{a}	7.6 ± 0.1 ^{e}	1.08 ± 0.01 ^{a}
B-Pin WE	1.81 ± 0.05 ^{b}	26.1 ± 0.2 ^{a}	ND	13.2 ± 0.8 ^{d}	0.82 ± 0.01 ^{d}
B-Pin A	1.64 ± 0.04 ^{d}	24.9 ± 0.1 ^{b}	ND	17.2 ± 0.3 ^{a}	0.94 ± 0.01 ^{c}
B-Pin B	1.76 ± 0.01 ^{c}	24.9 ± 0.1 ^{b}	ND	15.7 ± 0.2 ^{b}	0.93 ± 0.01 ^{c}
B-Pin T	1.97 ± 0.02 ^{a}	26.2 ± 0.2 ^{a}	ND	5.3 ± 0.2 ^{f}	0.92 ± 0.01 ^{c}

* Same letters in the columns do not differ according to Tukey's statistic test at 5%. CWT: Cell wall thickness. Fines are particles particles with diameter under 75 µm or fibrils that can pass through a 200-mesh fiber classifier (TAPPI, 1995). CWF: Cell wall fibrillation. ND: Not detected.

Cell wall thickness of B-Euc had different values for pretreated pulp and untreated with enzymes. The cell wall increased from 3.2 ± 0.1 µm to 3.9 ± 0.1 µm for enzyme A and 3.5 ± 0.1 µm for enzyme B. With increasing binding of water to fibrils, there is a decrease in fiber recalcitrance, and the yield of enzymatic hydrolysis process becomes greater (Weiss et al., 2017). The variety of fibers found in softwood growth rings, earlywood and latewood, may have made it difficult to analyze the cell wall thickness for *Pinus* samples.

Pretreatments A and B presented higher values of fines and cell wall fibrillation than control (untreated). The highest increase in fines was observed for B-Euc A and B-Pin B. Previous work has shown that enzymatic hydrolysis affect cellulosic fibers by breaking and cutting actions (Clarke et al., 2011; Li et al., 2012; Arantes et al., 2014). For cell wall fibrillation, B-Euc A presented 0.94 ± 0.01% value compared to WE treatment with 0.82 ± 0.01%. This can indicate higher enzyme activity for enzyme A. For B-Pin, both enzymes increased fibrillation from 1.05 ± 0.01 to 1.07 ± 0.01 %. This can be explained by the fact that pre-treatments reach fibers more superficially and on amorphous regions, generating fines and causing fibrillation of the fiber surface (Dahlman et al., 2003). The increase in fibrillation after enzyme pretreatments may indicate an enzymatic action on fiber surface, which may facilitate the detachment of nanofibrils. For both *Eucalyptus* sp. and *Pinus* sp. pulps, it was

observed that cell wall fibrillation was lower than enzymatic pretreatments, this may have caused by fibrils detachment from the cell wall by oxidative reaction.

Taking into account the non-alteration in the anatomical structure of the fibers, it can be said that enzymatic pretreatment does not cause significant damages to the cellulosic pulp.

3.2 Energy consumption during fibrillation

According to Pérez and Samain (2010), in aqueous suspensions, nanofibrils become a viscous material that tends to have a gel appearance. This phenomenon occurs due to the ability of the cellulose fibrils isolated to group large amounts of water on their surface through the hydrogen bonds (Ioelovich and Figovsky, 2008). Thus, gel appearance indicates nanofibril formation, and additional cycles through the defibrillator grinder may indicate unnecessary energy expenditure.

Figure 3 presents the energy consumption accumulated in each cycle during fibrillation (Figures 3a,b) as well as corresponding energy index (Figure 3c).

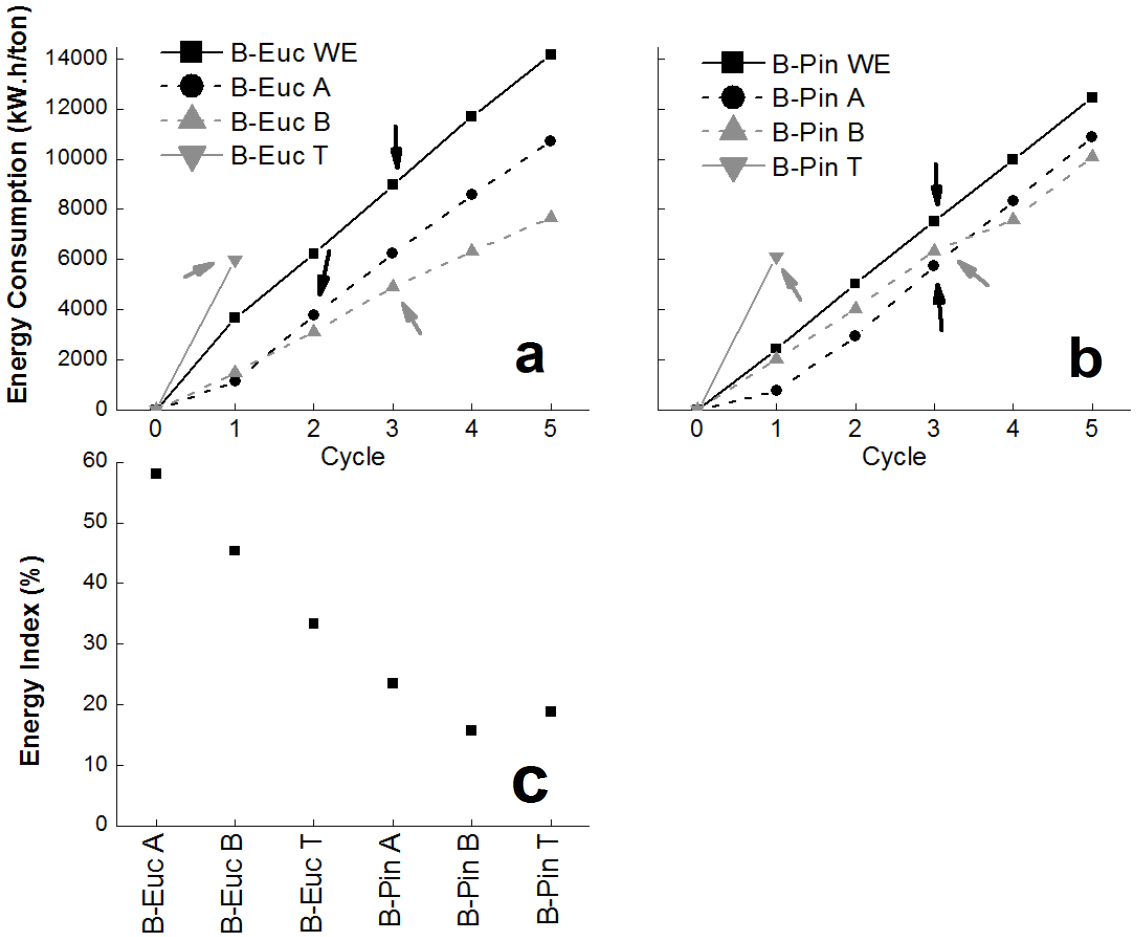

Figure 3. Energy consumption of bleached (a) *Eucalyptus* sp. fibers, (b) *Pinus* sp. tracheids during fibrillation and (c) Energy index. Arrows indicate gel formation.

It is observed in Figure 3 that the fibrillation was facilitated for pulps pretreated with enzymes. The activity of endoglucanase, in which there is random cleavage of the cellulosic chain, may favor modifications in structural arrangement of the cellulose fibril to fibril bonds, facilitating the separation of nanofibrils. In general, B-Euc fibers were easier to fibrillate than B-Pin because *Pinus* sp. fibers are longer and thicker than *Eucalyptus* sp. fibers. Also, softwood fibers are more difficult to disperse in water, leading to fiber accumulation at the base of the grinder (Gunawardhana et al., 2017).

For B-Euc (Figure 3a), gel formation was observed in the 3rd cycle for control (untreated), 2nd cycles for enzyme A and 3rd cycle for enzyme B. The lowest energy consumption for B-Euc was obtained for enzyme A with ~3,700 kW.h/ton, indicating 58% savings in energy consumption when compared to control (Figure 3c). B-Euc B presented a consumption of ~4,900 kW.h/ton of energy, indicating 45% savings in energy.

As the enzyme A pretreated pulp showed higher cell wall fibrillation than the enzyme B, it was expected that B-Euc A fibrillation would be easier than B-Euc B. For bleached Kraft pulp from *Eucalyptus* sp., Ribes et al. (2018) reduced 45% of energy consumption by using cellulase-mediated enzyme pretreatment and Josset et al. (2014) reported a consumption of 5,250 kW.h/ton with 10 cycles through the grinder.

The gel formation cycle for B-Pin (Figure 3b) was observed at the 3rd cycles for all pretreated pulps, but the energy consumption was different for each pretreatment. The lowest energy consumption was also for enzyme A with ~5,800 kW.h/ton, implying around 24% energy savings compared to control pulp. Enzyme B treatment for B-Pin showed 16% energy savings (Figure 3 c). Liu et al. (2019) applying xylanase enzyme pretreatment in bleached softwood pulp reached fibrillation with energy savings up to 55%. Due to the pretreatment, they also produced smaller diameters and more uniform nanofibrils, which generated high transparent films.

TEMPO-mediated oxidation pretreated nanofibrils was compared to enzyme and control treatments about energy consumption. TEMPO is well known for producing nanofibrils with high quality. Both suspensions of B-Euc T and B-Pin T nanofibrils formed a gelatinous appearance in the first cycle through grinder, exhibiting extremely high viscosity. As a result, the high viscosity suspension does not pass through the microfibrillator making it impossible to continue the mechanical extraction process. Then, only one cycle of passage through the grinder was carried out for the samples pretreated with TEMPO. Even though TEMPO pretreated pulp did not present the lowest energy consumption; it was possible to

observe the gel-like appearance of the suspension with just one cycle and resulting in a gel with high transparency.

A significant increase in energy consumption during the extraction of nanofibrils was observed for all pretreatments as the number of cycles through the grinder increase. Comparing the gel formation cycle (3 cycles for WE and B, and 2 cycles for A) and the 5th cycle, B-Euc WE showed 57% increase of energy consumption; B-Euc A and B-Euc B presented increase in energy consumption higher than 100%. Suspensions pretreated with enzymes demonstrated an increase in viscosity, making it difficult to pass through the grinder and consequently increasing energy consumption. The same behavior was observed for B-Pin samples, which was observed a gel formation with 3 cycles for all pretreatments. WE pretreatment presented an increase of 65% in energy consumption during nanofibril extraction, whereas enzymes A and B pretreatment presented 270% and 150%, respectively, as the number of cycles increased. Excessive increase in energy consumption may be caused by the difficulty of dispersing *Pinus* sp. in water.

3.3 Nanofibrils microscopic aspects

Light microscopy (ML) images assist in checking the efficiency of fibrillation by monitoring nanofibrils extraction after passing pulps through the grinder. Figures 4 and 5 are presenting the light microscopy images of suspension for each cycle and also the transmission electron images (TEM) of nanofibrils at the gel formation cycle for *Eucalyptus* sp.. According to Figure 4 for the control treatment without enzymes, it is possible to visualize that as the number of cycles through the fibrillator grinder increases (Figures 4a-f), the number of whole fibers decreases and fiber fragments increases due to mechanical shear over the fibers.

It is observed individualized fibrils were obtained at 3 cycles through the grinder for B-Euc treated without enzymes (Figure 4d), but it was still possible to see intact fibers in the suspension. At this cycle, the suspension had a gel appearance. Whereas, for enzyme A (Figure 5c), the gel appearance happened with 2 cycles, which intact fibers were also viewed but in lower frequency than B-Euc WE (Figure 4d). The decreasing of the number of cycles for B-Euc A may have occurred due to endoglucanase activity on the fibers, assuming that cell wall fibrillation percentage was higher for pulp treated with enzyme A as mentioned in early section. For enzyme B (B-Euc B), fibrillation showed no decreasing of the number of cycles, however, as discussed in section 3.2, there was some decrease in energy consumption.

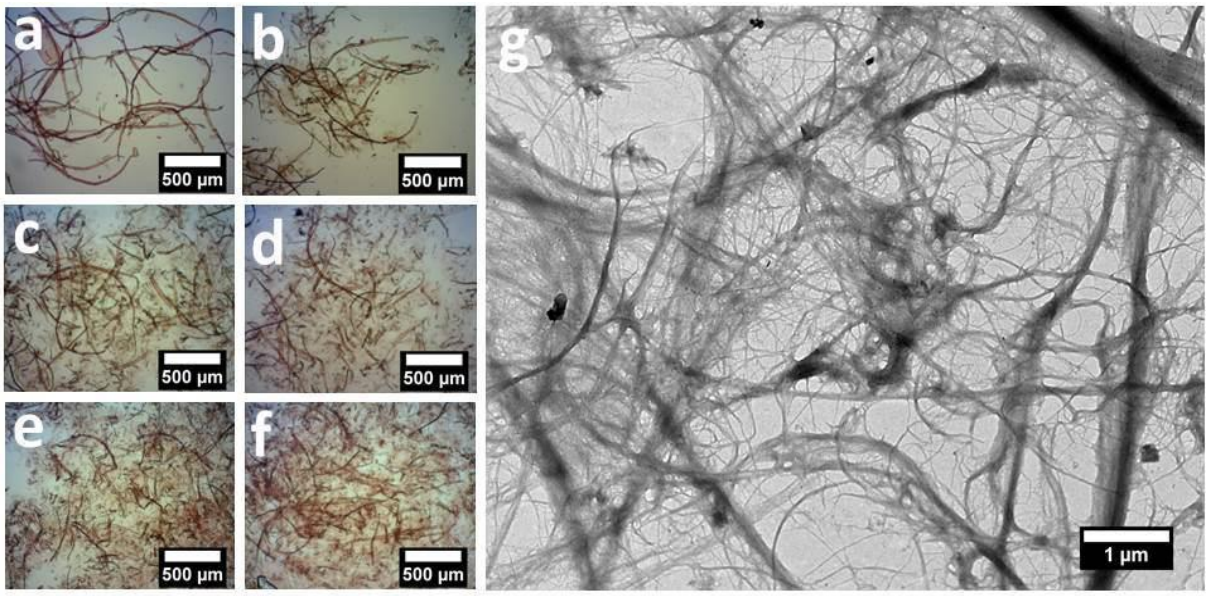

Figure 4. Typical light microscopic (LM) and transmission electron microscopic (TEM) images of B-Euc WE during mechanical fibrillation: a) LM at no cycle; b) LM at 1 cycle; c) LM at 2 cycles. d) LM at 3 cycles. e) LM at 4 cycles; f) LM at 5 cycles; g) TEM of "net" nanofibrils (Wang et al., 2012) produced with 3 cycles (gel formation cycle).

Figure 5h presents TEM images of TEMPO-mediated oxidation suspension of *Eucalyptus*, in which isolated nanofibrils are more evident than enzyme A nanofibrils (Figure 5g). Pretreated TEMPO suspension formed a network of nanofibrils well individualized. It is known that cellulose nanofibrils obtained by TEMPO-mediated oxidation are well dispersed in water and have its diameters distributed with more uniformity (Habibi et al., 2006). Tang et al. (2017) treated NaOH/urea cellulose suspensions with TEMPO oxidation and noticed that microparticles formed agglomerates, which it was not observed in this work.

Following Wang et al. (2012) morphology study, B-Euc WE presented mainly a "net" structure (Figure 4g), which is composed of cross over backbone fibrils of different scales and completely twisted and curled nanofibrils that entangled the backbone fibrils. B-Euc A nanofibrils presented a "blooming tree" structure (Figure 5g); the left side of the TEM image would be the "branch of the tree" in which "highly curled and twisted" nanofibrils appear, similar to the ones found by Wang et al. (2012). B-Euc T presented "kinked but untwisted and not entangled" nanofibrils (Figure 5h). These structures are formed due to the difference in the ratio of cellulose amorphous and crystalline regions presented in P, S1 and S2 cell wall layers (Wang et al., 2012). Fibrils presented in P and S1 layers are usually more amorphous than those presented in the S2 layer (Panshin and de Zeeuw, 1980).

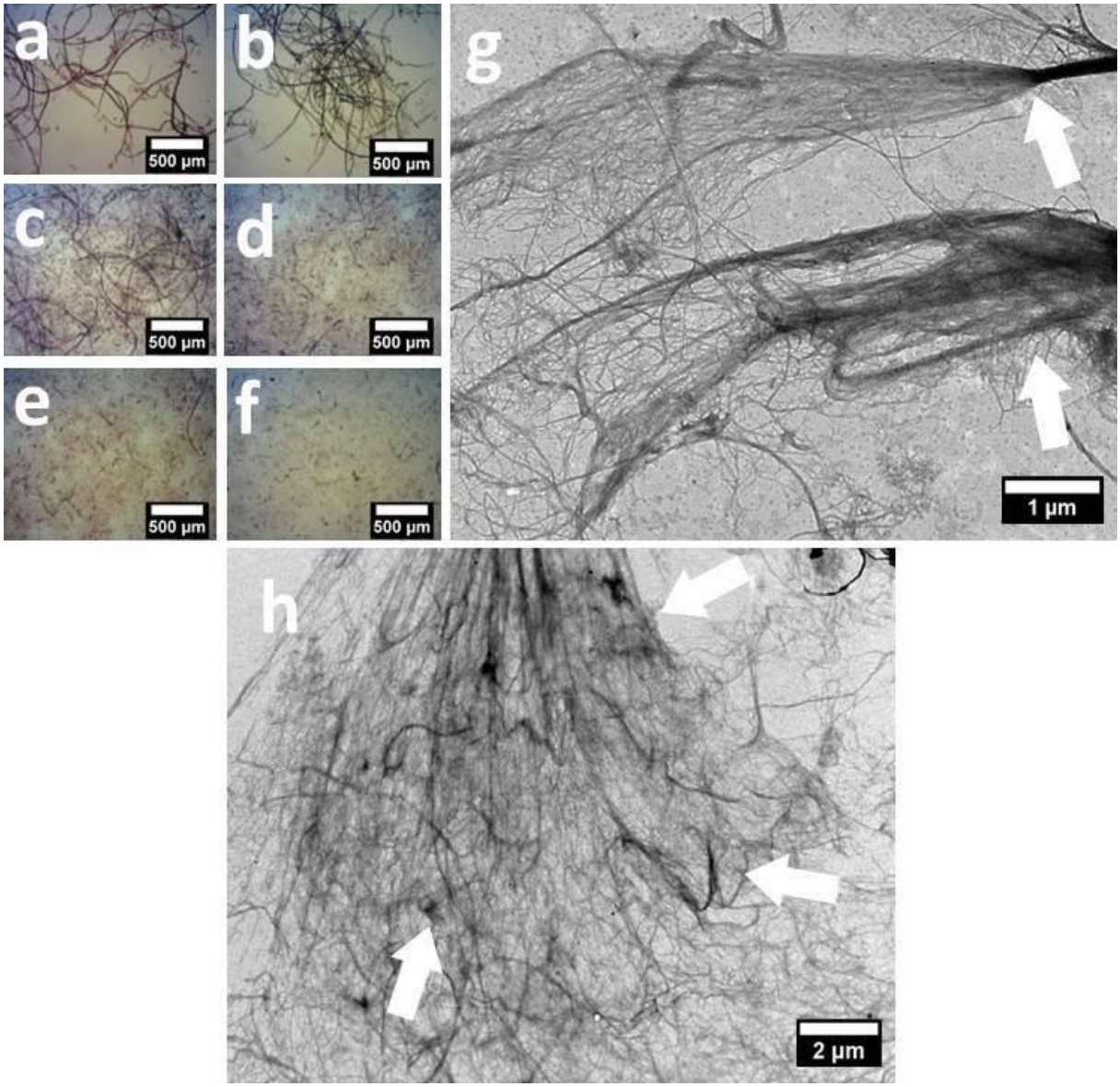

Figure 5. Typical light microscopic (LM) and transmission electron microscopic (TEM) images of B-Euc A during mechanical fibrillation: a) LM at no cycle; b) LM at 1 cycle; c) LM at 2 cycles; d) LM at 3 cycles; e) LM at 4 cycles; f) LM at 5 cycles; g) TEM at 2 cycles (gel formation cycle), arrows show the "blooming tree" structure (Wang et al., 2012); h) TEM of "kinked but untwisted and not entangled" nanofibrils (Wang et al., 2012) produced with 1 cycle for TEMPO-mediated oxidation treatment.

The ML images of all 5 cycles through fibrillator for *Pinus* sp. suspensions for WE and enzyme A pretreatment are presented in Figures 6 and 7, respectively. They present TEM images of gel formation cycle for WE, A and TEMPO treatments. These images are helpful for checking the performance of pretreated pulps during cellulose nanofibrils extraction. Gel formation for the WE, A and B *Pinus* sp. pretreatments were observed in the 3rd cycle. Figures 6d and 7d present *Pinus* sp. suspensions in gel formation cycle without large fiber fragments. Yet, Figure 6g evidences large nanofibril structures in contrast to B-Pin A nanofibrils (Figure

7g) and B-Pin TEMPO nanofibrils (Figure 7h). B-Pin WE nanofibrils presented a “net-like” structure (Wang et al., 2012) (Figure 6g). B-Pin A showed “entangled and twisted” nanofibrils (Figure 7g) whereas B-Pin TEMPO pretreatment resulted in nanofibrils well isolated (Figure 7h), similar to Wang et al. (2012) findings.

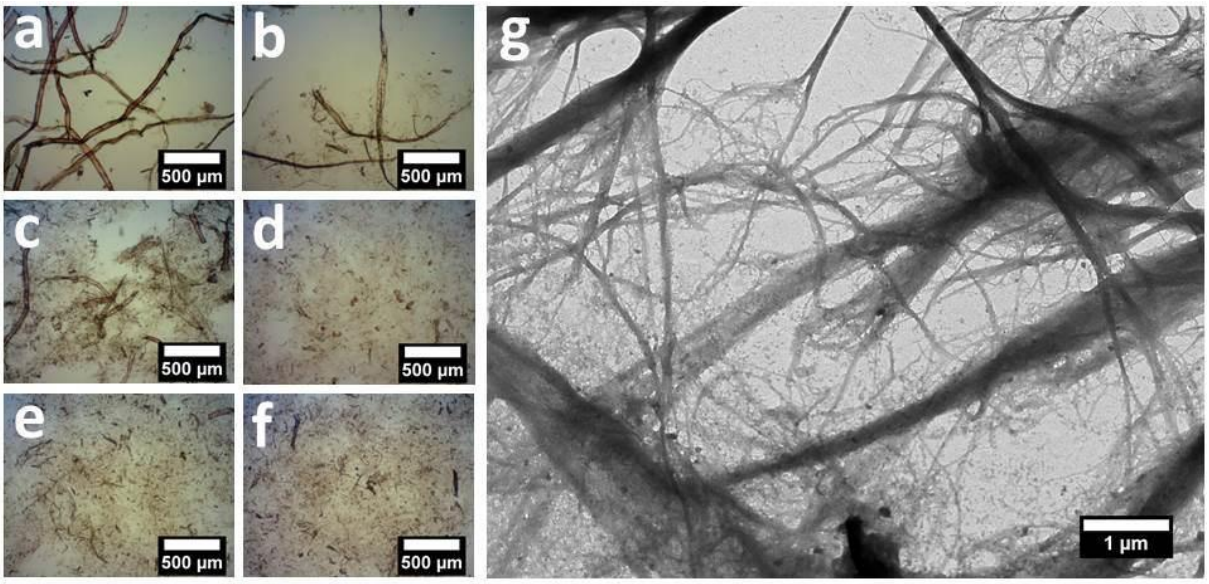

Figure 6. Typical light microscopic (LM) and transmission electron microscopic (TEM) images of B-Pin WE (with no enzymes) during fibrillation: a) LM at no cycle; b) LM at 1 cycle; c) LM at 2 cycles; d) LM at 3 cycles; e) LM at 4 cycles; f) LM at 5 cycles; and g) TEM of “net-like” nanofibrils (Wang et al., 2012) produced with 3 cycles (gel formation cycle).

Similar to *Eucalyptus* sp. suspensions, the fibrillation of *Pinus* sp. pulp was facilitated by endoglucanase activity and TEMPO-mediated oxidation, resulting well-isolated nanofibril structures. As observed in Figure 6F, even after 5 cycles of fibrillation, B-Pin WE still presented large fiber particles when compared to B-Pin A pretreatment (Figure 7f). As nanofibrils were isolated with 3 cycles, subsequent cycles may be considered unnecessary.

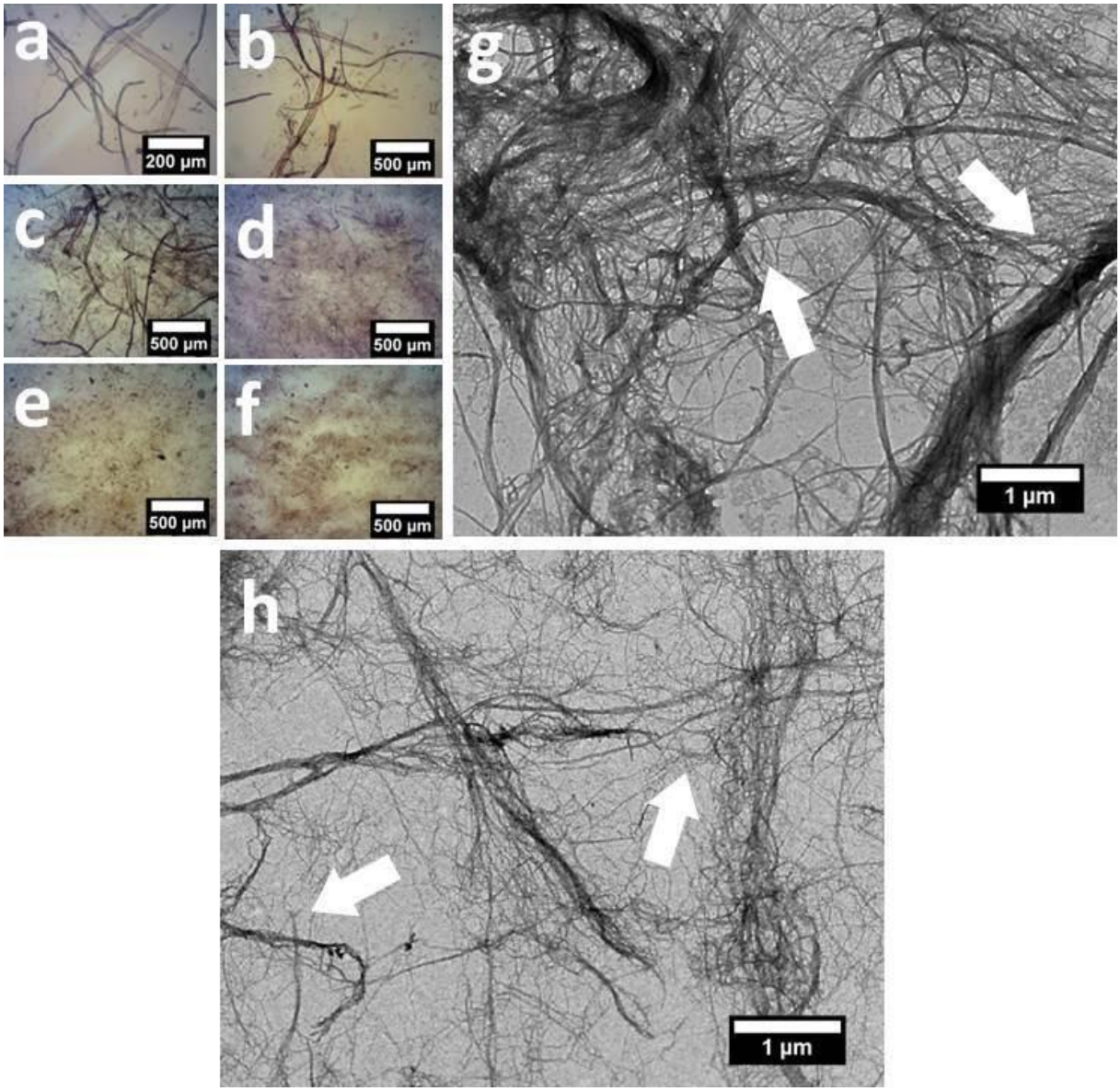

Figure 7. Typical light microscopic (LM) and transmission electron microscopic (TEM) images of B-Pin A during fibrillation: a) LM at no cycle; b) LM at 1 cycle; c) LM at 2 cycles; d) LM at 3 cycles; e) LM at 4 cycles; f) LM at 5 cycles; g) TEM at 3 cycles (gel formation cycle) of "entangled and twisted" nanofibrils (Wang et al., 2012); and h) TEM of well isolated nanofibrils with 1 cycle for TEMPO-mediated oxidation treatment.

From the transmission electron microscopy (TEM) images, it was possible to measure the diameter of the nanofibrils in suspension. Figure 8 presents the diameter distribution of cellulose nanofibrils at gel formation cycle. It is observed that the content of nanofibrils has similar patterns for all treatments. TEMPO treatments showed higher content of nanofibrils smaller than 15 nm, while control (untreated) pulp presented the lower content in that range.

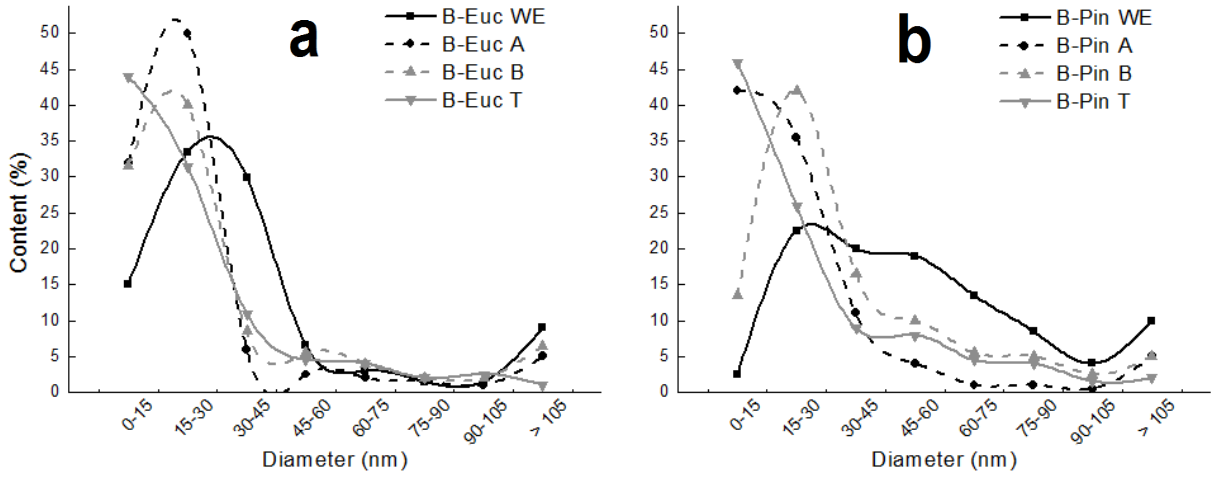

Figure 8. Diameter distribution of the cellulose nanofibrils obtained with the different pretreatments for: (a) B-Euc; and (b) B-Pin. Diameters were measured form the TEM images.

According to Tonoli et al. (2016), nanofibrils with diameter lower than 30 nm have a great reinforcement potential for composites. B-Euc A presented the highest content of nanofibrils for *Eucalyptus* sp. suspensions with mean diameter lower than 30 nm with 82%, followed by B-Euc B with 78%. On the other hand, B-Pin A presented only 56% of nanofibrils under 30 nm. The highest content for B-Pin was observed for TEMPO-mediated oxidation pretreated nanofibrils, with 72%. *Eucalyptus* sp. control and pretreated with enzyme B suspensions showed around 9% and 7% of less fibrillated (with diameters higher than 105 nm) nanofibrils, respectively. For *Pinus* sp. samples, it was observed 10% for control and 5% for enzyme B of fibrils higher than 105 nm.

Nanofibrils obtained from B-Euc and B-Pin pretreated with no enzyme showed average diameter of 24 nm (12-79 nm) and 51 nm (20-152 nm), respectively. The enzymatic pretreatment that presented the lowest mean diameter for both pulps were observed with the enzyme A pretreatment. B-Euc A showed 19 nm (9-67 nm) while B-Pin A showed 18 nm (7-68 nm). TEMPO nanofibrils presented average diameter of 17 nm (8-68 nm) and 24 nm (12-65 nm) for B-Euc and B-Pin, respectively. In addition to producing nanofibrils of smaller diameters, TEMPO-mediated oxidation generated well individualized nanofibrils.

Dias (2017) reported an average diameter of 42 ± 16 nm for untreated *Eucalyptus* sp. nanofibrils and 36 ± 14 nm for nanofibrils from untreated *Pinus* sp. In his work, Dias (2017) observed that the content of nanofibrils with an average diameter lower than 30 nm was around 23% and 36% for B-Euc WE and B-Pin WE, respectively; around 72% and 76% for B-Euc and B-Pin pulps treated with NaOH 5% for 2 h, respectively.

3.4 Suspension characterization

During decantation of cellulose suspension, larger particles and agglomerates of nanofibrils are deposited in the bottom of the flask. The isolated nanofibrils, being lighter, become dispersed in the supernatant (McKee et al., 2014). With this, it is expected that with the increase of the number of fibrillation cycles, there will also be an increase of the turbidity of the supernatant. Thus, the more turbid the supernatant, the more isolated nanofibrils are dispersed therein.

The supernatant turbidity evolution of bleached nanofibrils at each cycle is presented in Figure 9. Enzymatic pretreatment increased the turbidity values of the suspension supernatant. With the evolution of the cycles through the fibrillator, a gradual increase in the turbidity of the pretreatments for both cellulosic pulps was observed. However, for the pretreatment with enzyme A, turbidity presented a reduction after the third cycle. B-Euc and B-Pin presented higher values of turbidity for treatment with enzyme A, with values of 303 NTU and 380 NTU, respectively. As fibrillation using enzyme A was more facilitated by decreasing energy consumption and its nanofibrils obtained smaller average diameters, it was expected that the turbidity of these samples would show higher turbidity values. Following same thought, treatments without the addition of enzyme showed lower turbidity values in the supernatant in gel formation cycle.

Xiao et al. (2001) showed alterations in the turbidity of the cellulose suspension due to the use of pretreatments that modify the fibers cellular wall, dissolving hemicelluloses and lignin. However, as shown in section 3.1, there was no significant change in the chemical composition of the pulps after enzymatic pretreatment. The larger average diameter of individualized nanofibrils observed by B-Pin may explain the higher turbidity in the supernatant of that suspension compared to B-Euc.

TEMPO-mediated oxidation pretreatments did not follow the same pattern as enzyme pretreatments and control. TEMPO showed small values of turbidity, with 10.6 NTU and 105.7 NTU for B-Euc and B-Pin, respectively. It can be explained by the fact that even though there were higher nanofibrils contents in the supernatant, mean diameter for TEMPO treatments were smaller and presented lower turbidity (high transparency).

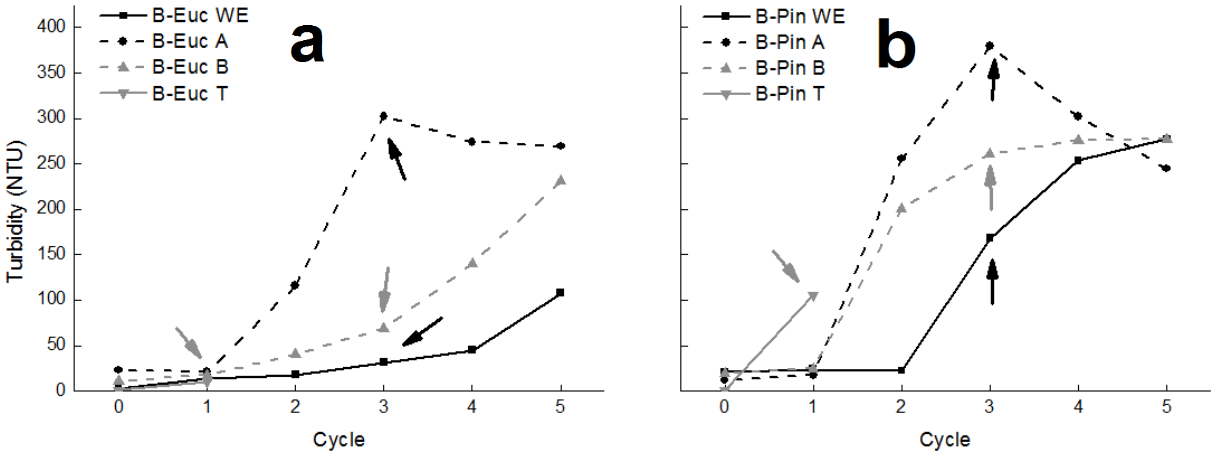

Figure 9. Evolution of the turbidity of nanofibrils suspension supernatant after 1.5 h decantation in different cycles for (a) B-Euc and (b) B-Pin. Arrows indicate gel formation.

The suspension stability analysis of nanofibrils in water was quantitatively assessed at 0.25% w/w concentration, and the suspension level measured by ImageJ software (Schindelin et al., 2012) after 48 h decantation (Figure 10). It is expected that the higher the degree of fibrillation, the more stable is the suspension (Guimarçães Júnior et al., 2015). It is also expected that when there is a gel formation of nanofibrils the suspensions become more stable causing less decantation.

Complete stability in water was observed for B-Euc for enzyme A after 2 cycles of fibrillation in the grinder and for TEMPO treatment at 1 cycle (Figure 10a). For treatment WE, it was not possible to see complete stability, but at gel appearance cycle, suspension presented maximum stability with 85%. Lower stability in early cycle could happen due to larger particles in the suspensions, as it is shown in section 3.3. Enzyme A improved nanofibrils suspension stability from 85% to 97% at gel cycle formation, and kept stability at 100% for cycles 3, 4 and 5. Enzyme B increased stability for each cycle and had its maximum stability only in the 4th cycle, with 90% stability.

It is known that TEMPO treatment particularly oxidizes hydroxyl groups present in carbon 6 position in the cellulose chain and transforming them into carboxylate groups (Habibi, 2014). Carboxylate groups facilitate the dispersion and stability of nanofibrils in aqueous suspension (Dong et al., 1998; Huq et al., 2012).

For B-Pin (Figure 10b), all treatments presented complete stability in water when gel appearance was observed. B-Pin WE fibers and B-Pin T presented low stability, with 40% and 25%, respectively. Nanofibrils are more dispersed in the supernatant because they are lighter, and non-nanoscale material is decanted (McKee et al., 2014). Control treatment

decreased its suspension stability after gel formation cycle. This may have happened due to nanofibrils flocculation in the suspension.

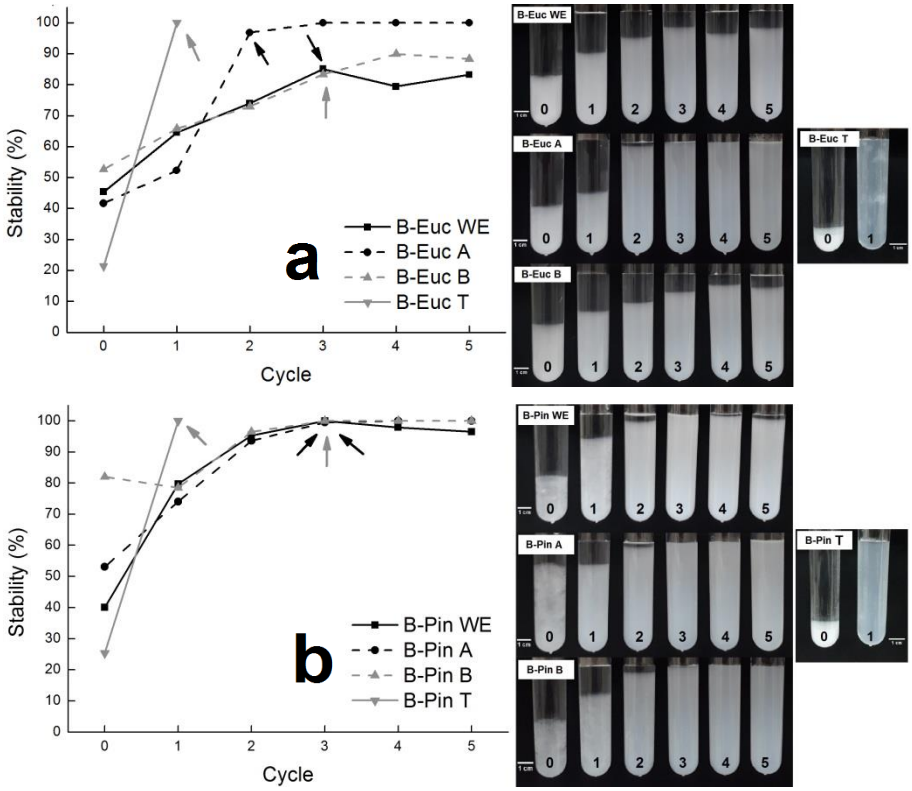

Figure 10. Stability of cellulose nanofibrils suspensions in water after 48 h decantation at concentration of 0.25% (w/w), for (a) B-Euc and (b) B-Pin. Arrows indicate gel formation.

3.5 Zeta potential

The potential charges on nanofibrils surface for enzyme treated nanofibrils and control nanofibrils are presented in Table 3. Higher zeta potential values, in module, suggest higher dispersion in water as well as low values suggest low dispersion in water (Tonoli et al., 2012; Lu et al., 2014). Nanocellulose suspensions with values higher than -25 mV is considered stable (Mirhosseini et al., 2008).

Zeta potential values presented for B-Euc nanofibrils was higher than B-Pin. Zeta potential can be influenced by ionic strength caused by hydroxyl groups and hemicelluloses (Klemm et al., 2011). The presence of COO- derived from COOH groups present in uronic and hexenuronic acids from hardwood Kraft pulps can contribute to higher zeta potential values for B-Euc nanofibrils (Winuprasith and Suphantharika, 2013).

For pretreatment A, gel formation cycle showed a zeta value of -47.7 ± 2.4mV and -33.4 ± 0.4mV, for B-Euc and B-Pin respectively. For pretreatment B, B-Euc showed a -40.2 ±

1.7 mV value and B-Pin a -31.1 ± 0.7mV value. These values are similar to the ones found by Demuner (2017) of -45.0 mV for *Eucalyptus* and -31.8 mV for *Pinus*. Similar results were also observed by Gamelas et al. (2015) with -41 mV for *Eucalyptus* samples; and by Lengowski (2016) for *Pinus* samples with -26.9 mV.

Table 3. Zeta potential results for cellulose nanofibrils.

Cycle		B-Euc	B-Pin
WE	**Gel formation**	-42.7 ± 1.7 ^{b,c}	-11.5 ± 0.7 ^{f}
	5	-16.8 ± 1.6 ^{f}	-10.8 ± 5.1 ^{f}
A	**Gel formation**	-47.7 ± 1.7 ^{a,b}	-33.4 ± 1.0 ^{d,e}
	5	-35.2 ± 0.6 ^{d}	-11.6 ± 1.8 ^{f}
B	**Gel formation**	-40.2 ± 2.4 ^{c,d}	-31.1 ± 0.4 ^{e}
	5	-16.4 ± 2.5 ^{b}	-12.4 ± 1.9 ^{f}
T	**Gel formation**	-52.9 ± 2.4 ^{a}	-31.9 ± 4.4 ^{e}

Same letters do not differ according to Tukey's statistic test at 5%.

With the increase of fibrillation cycles, zeta potential decreased for all treatments. According to Siqueira et al. (2009), one factor that can lead to changes in the reading of zeta potential is the entanglement of nanocelluloses caused by difference in the structure sizes. Dufresne et al. (1997) and Tonoli et al. (2012) also attributed residual hemicelluloses agglutination capacity on zeta potential value changing.

3.6 Film tensile properties

Stress-strain curves of the tensile test of nanofibril films are presented in Figure 11 and results are presented in Table 4.

Tensile strength of B-Euc WE and A increased with the increase of grinding cycles due probably to the improvement of fibrillation with the shear applied. B-Euc B presented tensile strength at 2 cycles similar to films formed at gel formation cycle at 5 cycles. In general, enzyme A promoted higher tensile strength. As the average diameter of the nanofibrils pretreated with enzyme A were smaller compared to the control treatment, and then there was greater interaction between the nanofibrils and increased hydrogen bonding between nanofibrils.

Enzymatic pretreatment did not affect drastically the Young's modulus for *Pinus* sp. samples. Same pattern was observed for strain at rupture. Liu et al. (2019) concluded in their work that mechanical strength was not significantly affected by enzymatic pretreatment. But in their work, pretreatment was mediated by xylanase.

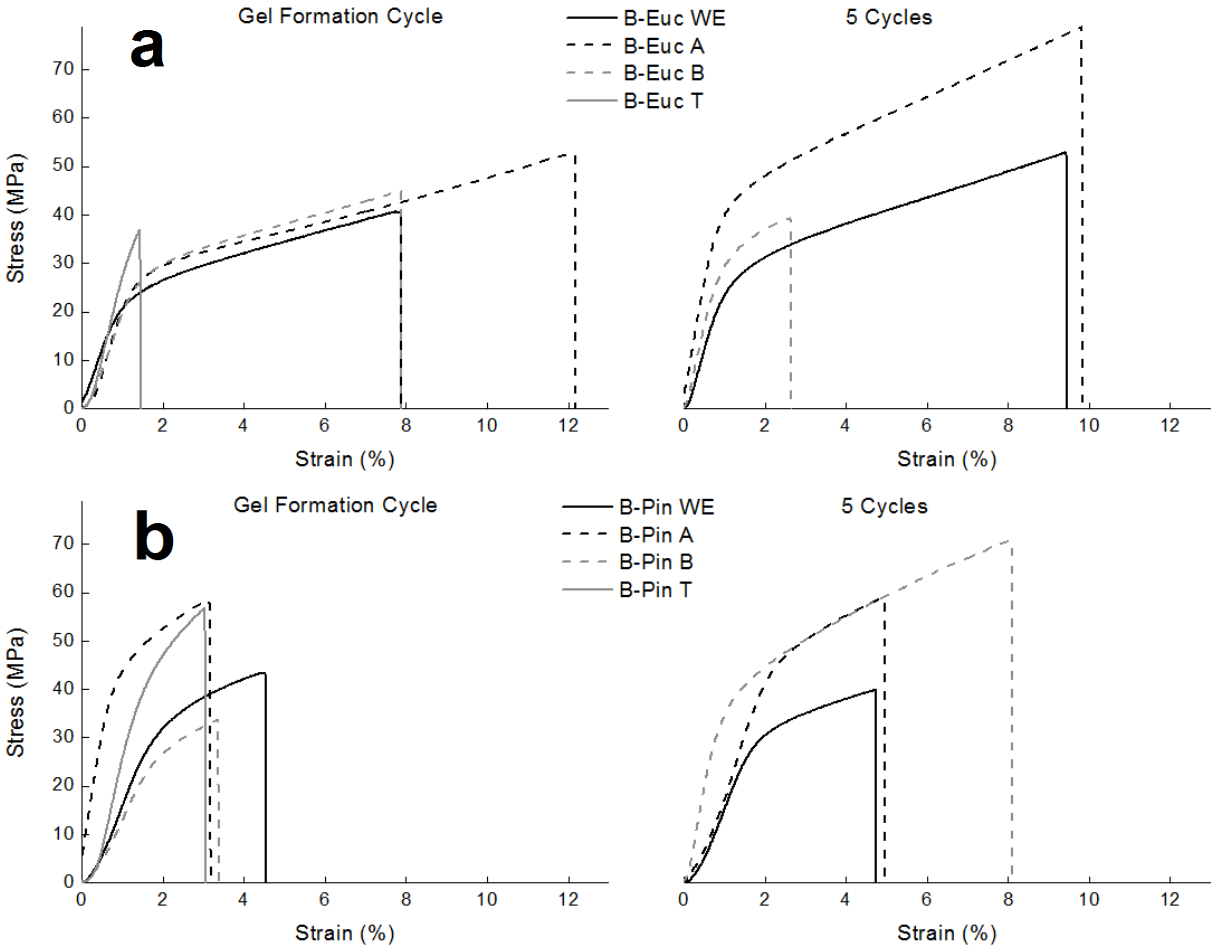

Figure 11. Typical stress-strain curves of cellulose nanofibril films in different cycles (gel-like formation and 5 cycles) for: (a) B-Euc; and (b) B-Pin.

B-Euc TEMPO-oxidation mediated films presented a reduction on tensile strength as well as Yong's modulus and strain at break. This reduction on tensile strength is due to the formation of carboxylate in hydroxyl groups from carbon 6 of nanofibrils surfaces during oxidation (Fukuzumi et al., 2010; Saito et al., 2009).

With the increase of the number of cycles between the gel formation and the 5th cycle, it was observed an increase of 57%, 184% and 145% of energy consumption for WE, A and B pretreatments, respectively, as mentioned in early sections. These increases in energy promoted only 30% of increase in tensile strengths for B-Euc WE and A and B-Pin B.

Table 4. Average and standard deviation values of tensile strength, Young's modulus and strain of the films obtained with the different nanofibrils.[1]

	Cycle	Tensile strength (MPa)	Young's modulus (GPa)	Strain (%)
B-Euc WE	**3***	30.5 ± 5.7 ^{c,d}	2.0 ± 0.2 ^{c}	4.8 ± 2.0 ^{a,b,c}
	5	46.3 ± 6.2 ^{a,b,c}	2.3 ± 0.4 ^{c}	7.8 ± 1.1 ^{a}
B-Euc A	**2***	44.5 ± 3.6 ^{a,b,c,d}	2.2 ± 0.4 ^{c}	7.8 ± 2.1 ^{a}
	5	60.3 ± 8.3 ^{a}	3.9 ± 0.4 ^{a}	6.8 ± 2.3 ^{a,b}
B-Euc B	**3***	39.2 ± 3.5 ^{b,c,d}	2.8 ± 0.3 ^{a,b,c}	5.1 ± 1.4 ^{a,b,c}
	5	35.4 ± 2.7 ^{b,c,d}	2.8 ± 0.6 ^{a,b,c}	4.6 ± 1.8 ^{a,b,c}
B-Euc T	**1***	28.8 ± 10.2 ^{d}	2.1 ± 1.0 ^{c}	2.2 ± 1.2 ^{c}
B-Pin WE	**3***	49.4 ± 4.2 ^{a,b}	2.8 ± 0.5 ^{a,b,c}	6.5 ± 2.5 ^{a,b}
	5	34.0 ± 5.5 ^{b,c,d}	2.5 ± 0.7 ^{b,c}	3.6 ± 1.6 ^{b,c}
B-Pin A	**3***	45.1 ± 14.1 ^{a,b,c}	3.6 ± 0.8 ^{a,b}	3.8 ± 2.4 ^{b,c}
	5	48.3 ± 13.8 ^{a,b}	2.5 ± 1.1 ^{b,c}	4.6 ± 1.1 ^{a,b,c}
B-Pin B	**3***	40.6 ± 7.4 ^{b,c,d}	2.9 ± 0.6 ^{a,b,c}	4.7 ± 2.1 ^{a,b,c}
	5	48.6 ± 14.4 ^{a,b}	3.1 ± 0.7 ^{a,b,c}	5.0 ± 2.7 ^{a,b,c}
B-Pin T	**1***	41.7 ± 18.2 ^{b,c,d}	1.9 ± 1.0 ^{c}	2.7 ± 1.5 ^{c}

[1] Same letters in the columns do not differ according to Tukey's statistic test at 5%.*: Gel formation cycle.

4 CONCLUSIONS

Both endoglucanase used in this work promoted limited damage to the pulp fibers. In addition, enzymatic pretreatment did not induce large hydrolyzes of cellulose into sugars. Enzymatic pretreatment promoted energy savings on mechanical fibrillation, reaching up to 58%. It may be considered that there was an excess of energy consumption with an increase in the number of cycles above the gel-like formation cycle. TEMPO-mediated oxidation pretreatment presented more individualized nanofibrils with smaller average diameter. Nanofibrils produced by enzymatic pretreatment showed nanofibrils with average diameter as small as TEMPO-oxidation pretreatment and improved suspensions dispersion characteristics. The enzymatic pretreatment seems to have affected the *Eucalyptus* sp. pulp more efficiently, since there was a higher energy index for both enzymes in this pulp. Among the enzymes A and B, A enzyme mainly affected the *Eucalyptus* pulp while both enzymes showed similar values of energy consumption for the *Pinus* sp. pulps. Mechanical properties slightly increased due to hydrogen bonding between nanofibrils over endoglucanase activity. Thereby, cellulase pretreatment smoothed mechanical grinding and it generated nanofibrils with smaller diameters, similar to TEMPO-mediated oxidation nanofibrils.

ACKNOWLEDGMENTS

This study was financed in part by the Coordenação de Aperfeiçoamento de Pessoal de Nível Superior – Brasil (CAPES) – Finance Code 001. Authors also appreciate the support of Conselho Nacional de Desenvolvimento Científico e Tecnológico (CNPq), Fundação de Amparo à Pesquisa do Estado de Minas Gerais (FAPEMIG), and to the Wood Science and Technology graduation program from Federal University of Lavras (UFLA), Brazil. Likewise, Klabin S.A. for commercial pulps supplying and some of the pulp characterizations. To the Center of Microscopy at Federal University of Minas Gerais (http://www.microscopia.ufmg.br) for providing technical support and the equipment for experiments involving transmission electron microscopy.

REFERENCES

ABDUL KHALIL, H. P. S.; NAZRULISLAM, MD.; MUSTAPHA, A.; SUDESH, K.; DUNGANI, R.; JAWAID, M. Production and modification of nanofibrillated cellulose using various mechanical processes: A review. **Carbohydrate Polymers**, v. 99, p. 649–665, 2014.

ABRAHAM, E.; DEEPA, B.; POTHAN L. A.; JACOB, M.; THOMAS, S.; CVELBAR, U.; ANANDJIWALA, R. Extraction of nanocellulose fibrils from lignocellulosic fibres: A novel approach. **Carbohydrate Polymers**, v. 86, n. 4, p. 1468–1475, 2011.

ANDER, P.; HILDÉN, L.; DANIEL, G. Cleavage of softwood Kraft pulp fibres by HCl and cellulases. **BioResources**, v. 3, p. 477-490, 2008.

ARANTES, V.; GOURLAY, K.; SADDLER, J. N. The enzymatic hydrolysis of pretreated pulp fibers predominantly involves "peeling/erosion" modes of action. **Biotechnology for Biofuels**, v. 7, p. 87, 2014.

ASTM. American Society For Testing And Materials. **ASTM D828-16**: Standard Test Method for Tensile Properties of Paper and Paperboard Using Constant Rate of Elongation Apparatus. Philadelphia, 2016.

BALLESTEROS, J. E. M.; SANTOS, V.; MARMOL, G.; FRIAS, M.; FIORELLI, J. Potential of the hornification treatment on *Eucalyptus* and pine fibers for fiber-cement applications. **Cellulose**, v. 24, n. 5, p. 2275-2286, 2017.

BAULI, C. R.; ROCHA, D. B.; OLIVEIRA, S. A.; ROSA, D. S. Cellulose nanostructures from wood waste with low input consumption. **Journal of Cleaner Production**, v. 211, p. 408-416, 2019.

BLEDZKI, A. K.; GASSAN, J. Composites reinforced with cellulose based fibres. **Progress in Polymer Science**, v. 24, n.2, p. 221-274, 1999.

BLOMSTEDT, M. Modification of cellulosic fibers by carboxymethyl cellulose: effects on fiber and sheet properties. **Minna Blomstedt**: Helsinki University of Technology, 2007.

BRITO, J. O.; SILVA, F. G.; LEAO, M.M.; ALMEIDA, G. Chemical composition changes in *Eucalyptus* and PIN woods submitted to heat treatment. **Bioresource technology**, v. 99, n. 18, p. 8545-8548, 2008.

BUFALINO, L.; NETO, A. R. S.; TONOLI, G. H. D.; FONSECA, A . S.; COSTA, T. G.; MARCONCINI, J. M.; COLODETTE, J. L.; LABORY, C. R. G.; MENDES, L. M. How the chemical nature of Brazilian hardwoods affects nano-fibrillation of cellulose fiber and film optical quality. **Cellulose**, v. 22, p. 3657-3672, 2015.

BUFALINO, L.; MENDES, L. M.; TONOLI, G. H. D.; RODRIGUES, A.; FONSECA, A.; CUNHA, P. I.; MARCONCINI, J. M. New products made with lignocellulosic nanofibers from Brazilian amazon forest. In: IOP CONFERENCE SERIES: MATERIALS SCIENCE AND ENGINEERING, **Anuais…** v. 64, n. August, p. 1–5, 2014.

BURGUER, L. M.; RICHTER, H. G. Anatomia da madeira. **Nobel**, São Paulo, 154 p., 1991.

CHINGA-CARRASCO, G. Cellulose fibres, nanofibrils and microfibrils: The morphological sequence of MFC components from a plant physiology and fibre technology point of view. **Nanoscale Research Letters**, New York, v. 6, n. 1, p. 417, 2011.

CLARKE, K.; LI, X.; LI, K. The mechanism of fiber cutting during enzymatic hydrolysis of wood biomass. **Biomass & Bioenergy**, v. 35, p. 3943–3950, 2011.

CUNHA ARANTES, A. C.; SILVA, L. E.; WOOD, D. F.; DAS GRAÇAS ALMEIDA, C.; TONOLI, G. H. D.; DE OLIVEIRA, J. E.; DA SILVA, J. P.; WILLIAMS, T. G.; ORTS, W. J.; BIANCHI, M. L. Bio-based thin films of cellulose nanofibrils and magnetite for potential application in green electronics. **Carbohydrate Polymers** , v. 207, p. 100-107, 2018.

DAHLMAN, O.; JACOBS, A.; SJÖBERG, J. Molecular properties of hemicelluloses located in the surface and inner layers of hardwood and softwood pulps. **Cellulose,** v. 10, p. 325–334, 2003.

DEMUNER, I. F. Produção e caracterização de lignocelulose nanofibrilada (LCNF) e celulose nanofibrilada (CNF) e aplicação de LCNF na manufatura de papéis de embalagem nanoestruturados. 2017. 98 p. Dissertação (Mestrado em Ciência Florestal) - Universidade Federal de Viçosa, Viçosa, 2017.

DIAS, M. C. Alkaline pre-treatments and different parameters as facilitators for obtaining cellulose nanofibrils. 2017. 62 p. Dissertação (Mestrado em Ciência do Solo)-Universidade Federal de Lavras, Lavras, 2017.

DONG, X. M.; REVOL, J. F.; GRAY, D. G. Effect of microcrystallite preparation conditions on the formation of colloid crystals of cellulose. **Cellulose**, v. 5, p. 19–32, 1998.

DUFRESNE, A.; CAVAILLE, J.; VIGNON, M.R. Mechanical behavior of sheets prepared form sugar beet cellulose microfibrils. **Journal of Applied Polymer Science**, v. 64, n. 6, p. 1185-1194, 1997.

DURÃES, A. F. S. Evaluation of dislocations in cellulose pulps submitted to pre-treatments. 2018. 63 p. Dissertação (Mestrado em Ciência e Tecnologia da Madeira)–Universidade Federal de Lavras, Lavras, 2018.

FARDIM, P.; DURÁN, N. Modification of fibre surfaces during pulping and refining as analysed by SEM, XPS, and ToF-SIMS. **Colloids and Surfaces A**, v. 223, p. 263-276, 2003.

FONSECA, A. S. ; PANTHAPULAKKAL, S.; KONAR, S. K.; SAIN, M.; BUFALINO, L.; RAABE, J.; MIRANDA, I. P. A.; MARTINS, M. A.; TONOLI, G. H. D. Improving cellulose nanofibrillation of non-wood fiber using alkaline and bleaching pre-treatments. **Industrial Crops and Products**, v. 131, p. 203-212, 2019b.

FONSECA, C. S.; SILVA, M. F.; MENDES, R. F.; HEIN, P. R. G.; ZANGIACOMO, A. L.; SAVASTANO, H.; TONOLI, G. H. D. Jute fibers and micro/nanofibrils as reinforcement in extruded fiber-cement composites. **Construction and Building Materials**, v. 211, p. 517-527, 2019a.

FUKUZUMI, H.; SAITO, T.; OKITA, Y.; ISOGAI, A. Thermal stabilization of TEMPO-oxidized cellulose. **Polymer Degradation and Stability**, v. 95, n. 9, p. 1502-1508, 2010.

GAMELAS, J. A. F.; PEDROSA, J.; LOURENÇO, A. F.; MUTJE, P.; GONZALEZ, I.; CHINGA-CARRASCO, G.; SINGH, G.; FERREIRA, P. On the morphology ´ of cellulose nanofibrils obtained by TEMPO-mediated oxidation and mechanical treatment. **Micron**, v. 72, p. 28-33, 2015.

GHAREHKHANI, S.; SADEGHINEZHAD, E.; KAZI, S. N.; YARMAND, H., AHMAD, BADARUDIN, A.; SAFAEI, M. R.; ZUBIR, M. N. M. Basic effects of pulp refining on fiber properties - A review. **Carbohydrate Polymers**, v. 115, p. 785-803, 2015.

GUIMARÃES JUNIOR, M.; BOTARO, V. R.; NOVACK, K. M.; NETO, W. P. F.; MENDES, L. M.; TONOLI, G. H. D. Preparation of Cellulose Nanofibrils from Bamboo Pulp by Mechanical Fibrillation for Their Applications in Biodegradable Composites. **Nanoscience and Nanotechnology**, v. 15, p. 1–18, 2015.

GUIMARÃES JUNIOR, M.; TEIXEIRA, F. G.; TONOLI, G. H. D. Effect of the nano-fibrillation of bamboo pulp on the thermal, structural, mechanical and physical properties of nanocomposites based on starch/poly(vinyl alcohol) blend. **Cellulose** , v. 25, p. 1-27, 2018.

GUNAWARDHANA, T.; BANHAM, P.; RICHARDSON, D. E.; PATTI, A. BATCHELOR, W. Upgrading waste whitewater fines from a *Pinus* radiata thermomechanical pulping mill. **Nordic Pulp & Paper Research Journal**, v. 32, n. 4, p. 656-665, 2017.

HABIBI, Y. Key advances in the chemical modification of nanocelluloses. **Chemichal Society Reviews**, v. 43, p. 1519–1542, 2014.

HABIBI, Y.; CHANZY, H.; VIGNON, M. R. TEMPO-mediated surface oxidation of cellulose whiskers. **Cellulose**, v. 13, p. 679–687, 2006.

HABIBI, Y.; LUCIA, L. A.; ROJAS, O. J. Cellulose nanocrystals: chemistry, self-assembly, and applications. **Chemical Reviews**, v. 110, p. 3479–3500, 2010.

HENRIKSSON, M.; HENRIKSSON, G.; BERGLUND, L. A.; LINDSTRÖM, T. An environmentally friendly method for enzyme-assisted preparation of microfibrillated cellulose (MFC) nanofibrils.**European Polymer Journal,** New York, v. 43, n. 8, p. 3434–3441, 2007.

HENRIKSSON, G.; NUTT, A.; HENRIKSSON, H.; PETTERSSON, B.; STAHLBERGH, J.; JOHANSSON, G.; PETTERSSON, G. Endoglucanase 28 (cel12A), a new Phanerochaete chrysosporium cellulase. **European Journal of Biochememistry**, v. 259, p. 88–95, 1999.

HERRICK, F. W.; CASEBIER, R. L.; HAMILTON, J. K.; SANDBERG, K. R. Microfibrillated cellulose: Morphology and accessibility. Shelton, WA: ITT Rayonier Inc., 1983.

HUANG, J.; ZHU, H. L.; CHEN, Y. C.; PRESTON, C.; ROHRBACH, K.; CUMINGS, J. Highly transparent and flexible nanopaper transistors. **ACS Nano**, v. 7, p. 2106–2113, 2013.

HUQ, T.; SALMIERI, S.; KHAN, A.; KHAN, R. A.; LE TIEN, C.; RIEDL, B.; FRASCHINI, C.; BOUCHARD, J.; URIBE-CALDERON, J.; KAMAL, M. R.; LACROIX, M. Nanocrystalline cellulose (NCC) reinforced alginate based biodegradable nanocomposite film. **Carbohydrate Polymers**, v. 90, n.4, p. 1757-1763, 2012.

IOELOVICH, M.; FIGOVSKY, O. Nano-cellulose as promising biocarrier. In: Advanced Materia ln Research. **Trans Tech Publications**. p. 1286-1289, 2008.

ISHII, D.; SAITO, T.; ISOGAI, A. Viscoelastic Evaluation of Average Length of Cellulose Nanofibers Prepared by TEMPO-Mediated Oxidation. **Biomacromolecules**, v. 12, n.3, p. 548-550, 2011.

ISOGAI, A.; SAITO, T.; FUKUZUMI, H. TEMPO-oxidized cellulose nanofibrils. **Nanoscale**, v. 3, p.71–85, 2011.

JOSSET, S.; SIQUEIRA, G.; ORSOLINII, P.; TEJADO, A. Energy consumption of the nanofibrillation of bleached pulp, wheat straw andre cycled news paper through a grinding process. **Nordic Pulp and Paper Research Journal**, v. 29, n. 1, p. 167-175, 2014.

KALIA, S.; BOUFI, S.; CELLI,A.; KANGO, S. Nanofibrillatedcellulose: surface e modification and potential applications. **Colloid and Polymer Science**, v. 292, n. 1, p. 5-31, 2014.

KIM, K-J. et al. Effect of enzyme beating on grinding method for microfibrillated cellulose preparation as a paper strength enhancer. **Cellulose,** v. 24, n. 8, p. 3503-3511, 2017.

KLEMM, D.; KRAMER, F.; MORITZ, S.; LINDSTRÖM, T.; ANKERFORS, M.; GRAY, D.; DORRIS, A. Reviews: Nanocelluloses: A New Family of Nature-Based Materials. **Angewandte Chemie International Edition**, v.50, p.5438 – 5466, 2011.

LENGOWSKI, E. Bioembalagens produzidas com nanocelulose microfibrilada. Tese (Doutorado em Engenharia Florestal). UFPR, Curitiba, 234p., 2016.

LI, X.; CLARKE, K.; LI, K.; CHEN, A. The pattern of cell wall deterioration in lignocellulose fibers throughout enzymatic cellulose hydrolysis. **Biotechnology Progress**, v. 28, n.6, p. 1389–1399, 2012.

LING, S.; CHEN, W.; FAN, Y.;ZHENG, K.; JIN, K.; YU, H.; MARKUS, J. B. ; KAPLAN, D. L. Biopolymer nanofibrils: structure, modeling, preparation, and applications. **Progress in Polymer Science**, 2018.

LIU, X.; JIANGA, Y.; SONG, X.; QIN, C.; WANG, S., LI, K. A bio-mechanical process for cellulose nanofiber production – Towards a greener and energy conservation solution. **Carbohydrate Polymers,** v. 208, p. 191–199, 2019.

LONG, L.; TIAN, D.; HU, J.; WANG, F.; SADDLER, J. A xylanase-aided enzymatic pretreatment facilitates cellulose nanofibrillation. **Bioresource Technology**. V. 243, p. 898–904, 2017.

LOPES, T.A.; BUFALINO, L.; JÚNIOR, M.G.; TONOLI, G. H. D.; MENDES, L. M. Eucalyptus wood nanofibrils as reinforcement of carrageenan and starch biopolymers for improvement of physical properties. **Journal of Tropical Forest Science**, v. 30, p. 292-303, 2018.

LU, Q.; TANG, L.; WANG, S.; HUANG, B.; CHEN, Y.; CHEN, X. An investigation on the characteristics of celulose nanocrystals from Pennisetum sínese. **Biomass and Bioenergy**, v. 70, p. 267-272, 2014.

MATOS, L. C.; ROMPA, V. D.; DAMÁSIO, R. A. P.; MARCONCINI, J. M. TONOLI, G. H. D. Incorporação de Nanomateriais e emulsão de ceras no desenvolvimento de papéis multicamadas. **Scientia Forestales**, Piracicaba, v. 47, n. 122, p. 1-15, 2019

MCKEE, J.; HIETALAT, S.; SEITSONEN, J.; LAINE, J.; KONTTURI, E.; IKKALA, O. Thermoresponsive nanocellulose hydrogels with tunable mechanical properties. **ACS Macro Letters**, v. 3, n. 3, p. 266-270, 2014.

MENDONÇA, M. C. Pré-tratamentos alcalinos como facilitadores da obtenção de nanofibrilas de polpas celulósicas não branqueadas. 2018. 66 p. Dissertação (Mestrado em Engenharia de Biomateriais)-Universidade Federal de Lavras, Lavras, 2018.

MIRHOSSEINI, H.; TAN, C.P.; HAMID, N.S.A.; YUSOF, S. Effect of Arabic gum, xanthan gum and orange oil contents on ζ-potential, conductivity, stability, size index and pH of orange beverage emulsion. **Colloids and Surfaces A: Physicochem. Eng. Aspects**, v.315, p.47–56, 2008.

MIRMEHDI, S.; DE OLIVEIRA, M. L. C.; HEIN, P. R. G.; DIAS, M. V.; SARANTÓPOULOS, C. I. G. L.; TONOLI, G. H. D. Spraying Cellulose Nanofibrils for Improvement of Tensile and Barrier Properties of Writing & Printing (W&P) Paper. **Journal of Wood Chemistry and Technology** , v. 38, p. 1-13, 2018.

PÄÄKKÖ, M.; ANKERFORS, M.; KOSONEN, H.; NYKÄNEN, A.; AHOLA, S.; ÖSTERBERG, M.; RUOKOLAINEN, J.; LAINE, J.; LARSSON, P. T.; IKKALA, O.; LINDSTRÖM, T.Enzymatic Hydrolysis Combined with Mechanical Shearing and High-Pressure Homogenization for Nanoscale Cellulose Fibrils and Strong Gels. **Biomacromolecules**, v. 8, p. 1934-1941, 2007.

PANSHIN, A. J.; DE ZEEUW, C. Textbook of wood technology. **McGraw-Hill Book Company**, New York, 1990.

PÉREZ, S., SAMAIN, D. Structure and Engineering of Celluloses. **Advances in Carbohydrate Chemistry and Biochemistry.** p. 25 – 116, 2010.

QING, Y.; SABO, R.; ZHU, J. Y.; AGARWAL, U.; CAI, Z.; WU, Y. A comparative study of celulose nanofibrils disintegrated via multiple processing approaches. **Carbohydrate Polymers**, v. 91, n. 1, p. 226-234, 2013.

RABELO S. C. Avaliação do desempenho do pré-tratamento com peroxide de hidrogênio alcalino para a hidrólise enzimática do bagaço de cana-de-açúcar. 2007. Dissertação de mestrado. Universidade Estadual de Campinas (Unicamp) Campinas, 2007.

RESENDE, N. S.; GONÇALVES, G. A. S.; REIS, K. C.; TONOLI, G. H. D.; BOAS, E. V. B. V. Chitosan/Cellulose Nanofibril Nanocomposite and Its Effect on Quality of Coated Strawberries. **Journal of Food Quality**, v. 2018, p. 1-13, 2018.

RIBES, D. D.; ZANATTA, P.; GATTO, D. A.; MAGALÃES, W. L. E.; BELTRAME, R. Produção de suspensão nanofibrilares de celulose vegetal por meio do processo combinado – Avaliação do gasto energético. **Revista Matéria,** v. 23, n. 04, 2018.

SACUI, I. A.; NIEUWENDAAL, R. C.; BURNETT, D. J.; STRANICK, S. J.; JORFI, M.; WEDER, C. Comparison of the properties of cellulose nanocrystals and cellulose nanofibrils isolated from bacteria, tunicate, and wood processed using acid, enzymatic, mechanical, and oxidative methods. **ACS Applied Materials & Interfaces**, v. 6, n. 9, p. 6127–6138, 2014.

SAITO, T.; HIROTA, M.; TAMURA, N.; KIMURA, S.; FUKUZUMI ,H.; HEUX, L.; ISOGAI, A. Individualization of nano-sized plant cellulose fibrils by direct surface carboxylation using TEMPO catalyst under neutral conditions. **Biomacromolecules**, v. 10, n. 7, p. 1992-1996, 2009.

SAITO, T.; KIMURA, S.; NISHIYMA, Y.; ISOGAI, A. Cellulose nanofibers prepared by TEMPO-mediated oxidation of native cellulose. **Biomacromolecules**, v. 8, p. 2485-2491, 2007.

SANTOS, A. M. P.; YOSHIDA, M. P. Embalagens. Recife: **Edufre,** 152p. ISBN 978-85-7946-090-6, 2011.

SCHINDELIN, J.; ARGANDA-CARRERAS, I.; FRISE, E.; KAYNIG, V.; LONGAIR, M.; PIETZSCH, T.; PREIBISCH, S.; RUEDEN, C.; SAALFELD, S.; SCHMID, B.; TINEYEZ, J. Y.; WHITE, D. J.; HARTENSTEIN, V.; ELICEIRI, K.; TOMANCAK, P.; CARDONA, A. Fiji: an open-source platform for biológica-imagem analysis. **Nature methods**, v. 9, n. 7, p. 676:682.

SHI, Z.; PHILLIPS, G. O.; ZHANG, Y.; YANG, G. Utilization of bacterial cellulose in food. **Food Hydrocolloids**, v. 35, p. 539-545, 2013.

SILVA, M. J. F. Avaliação de pré-tratamentos enzimáticos na obtenção de nanofibrilas celulósicas de *Eucalyptus* sp. e *Pinus* sp. 2018. 127 p. Dissertação (Mestrado em Ciência da Madeira) - Universidade Federal de Lavras, Lavras, 2018.

SIQUEIRA, G.; BRAS, J.; DUFRESNE, A. Cellulose whiskers versus microfibrils: Influence of the nature of the nanoparticle and its surface functionalization on the thermal and mechanical properties of nanocomposites. **Biomacromolecules**, v. 10, p. 425–432, 2009.

SIRÓ, I.; PLACKETT, D. Microfibrillated cellulose and new nanocomposite materials: A review. **Cellulose**, Bucharest, v. 17, n. 3, p. 459–494, 2010.

TANG, Z.; LI, W.; LIN, X.; XIAO, H.; MIAO, Q.; HUANG, L.; CHEN, L.; WU, H. TEMPO-Oxidized Cellulose with High Degree of Oxidation. **Polymers**, v. 9, p 421, 2017.

TAPPI. Technical Association of The Pulp And Paper Industry. Test Method T 233 cm-95. Fiber length of pulp by classification. Atlanta, 1995.

TONOLI, G. H. D.; HOLTMAN, K. M.; GLENN, G.; FONSECA, A. S.; WOOD, D.; WILLIANS, T.; SA, V. A.; TORRES, L.; KLAMCZYNSKI, A.; ORTS, W. J. Properties of cellulose micro/nanofibers obtained from *Eucalyptus* pulp fiber treated with anaerobic digestate and high shear mixing. **Cellulose**, v. 23, n. 2, p. 1239–1256, 2016.

TONOLI, G. H. D.; TEIXEIRA, E. M.; CORREA, A. C.; MARCONCINI, J. M.; CAIXETA, L. A.; PEREIRA DA SILVA, M. A.; MATTOSO, L. H. C. Cellulose micro/nanofibres from *Eucalyptus* Kraft pulp: Preparation and properties. **Carbohydrate Polymers**, v. 89, p. 80-88, 2012.

WALLIS, A. F. A.; WEARNE, R. H.; WRIGHT, P. J. Chemical analysis of polysaccharides in plantation eucalypt woods and pulps. **Appita Journal**, v. 49, n. 4, p. 258-262, 1996.

WANG, Q. Q.; ZHU, J. Y.; GLEISNER, R.; KUSTER, T. A.; BAXA, U.; MCNEIL, S. E.. Morphological development of cellulose fibrils of a bleached *Eucalyptus* pulp by mechanical fibrillation. **Cellulose**, v. 19, n. 5, p. 1631-1643, 2012.

WEISS, N. D.; THYGESEN, L. G.; FELBY, C.; ROSLANDER, C.; GOURLAV. K. Biomass-Water Interactions Correlate to Recalcitrance and Are Intensified by Pretreatment: An Investigation of Water Constraint and Retention in Pretreated Spruce Using Low Field NMR and Water Retention Value Techniques. **Biotechnology Progress**, v. 33, n. 1, p. 146-153, 2017.

WINTER, H. T.; CERCLIER, C.; DELORME, N.; BIZOT, H.; QUEMENER, B.; CATHALA, B. Improved colloidal stability of bacterial cellulose nanocrystal suspensions for the elaboration of spin-coated cellulose-based model surfaces. **Biomacromolecules**, v. 11, n. 11, p. 3144-3151, 2010.

WINUPRASITH, T.; SUPHANTHARIKA, M. Microfibrillated cellulose from mangosteen (Garcinia mangostana L.) rind: Preparation, characterization, and evaluation as an emulsion stabilizer. **Food Hydrocolloids**, v.32, p.383-394, 2013.

WU, W.; TASSI, N. G.; ZHU, H.; FANG, Z.; HU, L. Nanocellulose-based translucent diffuser for optoelectronic device applications with dramatic improvemente of light coupling. **ACS Applied Materials and Interfaces**, v. 7, n. 48, p 26860–26864, 2015.

WU, T.; CAI, B.; WANG, J.; ZHANG, C.; SHI, Z.; YANG, Q.; HU, G.; XIONG, C. TEMPO-oxidized cellulse nanofibril/layered double hydroxide nanocomposite films with improved hydrophobicity, flame retardancy and mechanical properties. **Composites Science and Technology**, v. 171, p. 111-117, 2019.

XIAO, B.; SUN, X. F.; SUN, R. C. Chemical, structural, and thermal characterizations of alkali-solublelignins and hemicelluloses, and cellulose from maizestems, ryestraw, and rice straw. **Polymer degradation and stability**, v. 74, n. 2, p. 307-319, 2001.

ZHU, J. Y.; SABO, R.; LUO, X. Integrated production of nano-fibrillated cellulose and cellulosic biofuel (ethanol) by enzymatic fractionation of wood fibers. **Green Chemistry**, London, v. 13, n. 5, p. 1339, 2011.

TERCEIRA PARTE

ARTIGO: Evaluation of the mechanical extraction of unbleached cellulose nanofibrils with application of enzymatic pretreatment

Allan de Amorim dos Santos[a], Maryella Júnnia Ferreira e Silva[a], Luiz Eduardo Silva[a], Maressa Carvalho Mendonça[a], Renato Augusto Pereira Damásio[b], Gustavo Henrique Denzin Tonoli[a]*.

a Forest Science department, University of Lavras, University Campus, P.O. Box 3037, 37200-000, Lavras, Minas Gerais, Brazil.

b Industrial RDI – Technology Center Fazenda Monte Alegre, St Harmonia, 03 Postal code 84275-000 – Telêmaco Borba PR, Brazil.

**Corresponding author: gustavotonoli@yahoo.com.br, +553538291426.*

ABSTRACT

Cellulose nanofibrils have been gaining prominence due to their structure composed of crystalline and amorphous regions. Different extraction approaches can be used to generate nanofibrils. The objective of this work was to evaluate the application of endoglucanase in different types of unbleached cellulosic pulps as pretreatment for reduction of energy consumption of mechanical extraction of cellulose nanofibrils. Chemical, morphological and mechanical characteristics of the pretreated fibers/nanofibrils with and without enzyme were also evaluated. Unbleached *Eucalyptus* sp. Kraft pulp, *Pinus* sp. Kraft pulp and chemithermomechanical (CTMP) pulp were pretreated at 50°C, under 750 rpm, adequate pH and 100 g/ton of enzyme A, enzyme B and without enzyme (as control). Mechanical grinding process was performed in 5 cycles by the grinder microprocessor at 2% w/w suspension. Results indicated that chemical and anatomical characteristics of all pulps were not affected by the enzymatic pretreatment. All Kraft pulps pretreated with enzyme A and B presented a decrease in energy consumption, but the same was not obtained for CTMP, which did not result on a gelatinous suspension. It was possible to reach 52% of energy savings for pulps pretreated with enzyme A. By applying enzymes, it was possible to see an increase in water stability of the suspensions as well as the decrease of average diameter of the nanofibrils extracted. Tensile strength of films also increased with the increase of cycles through the grinder. So, enzymatic pretreatment proved to be a sustainable alternative as pretreatment for extraction of nanofibrils, generating well fibrillated cellulose nanofibrils at low energy consumption.

Keywords: Endoglucanase. Cellulase. Enzymatic hydrolysis. Grinding. Kraft pulp. Chemithermomechanical pulp.

1 INTRODUCTION

The increase of consumption of non-renewable source materials has caused concern. The replacement of such materials and their deposition in nature is not feasible in long terms. Thus, the search for renewable and biodegradable materials has grown in recent years (Bian et al., 2017; Abitbol et al., 2016). Cellulose is the most abundant polymer in nature. It has renewable and biodegradable characteristics, high availability, and it is found in different types of biomass, such as wood, cotton, bagasse, leaves and fruits, among others (Nie et al., 2016). In addition, cellulose is composed of a crystalline region that gives it high mechanical properties, being possible to use in bioengineering, in flexible electronics, batteries, etc. (Resende et al., 2018; Cunha Arantes et al., 2018; Scatolino et al., 2018; Zhu et al., 2016).

Among the biodegradable materials currently studied, cellulose nanofibrils (CNF) have been gaining prominence due to their structure composed of crystalline and amorphous regions. They can confer increased strength in composites or modify the gas, water or oil barrier properties, improving packaging (Matos et al., 2019; Claro et al., 2019; Lopes et al., 2018; Mirmehdi et al., 2018; Moon et al. 2011, Habibi et al., 2010). It is extracted from lignocellulosic materials by different routes, such as mechanical, chemical or biological, or even by a process composed of more than one route (Fonseca et al., 2019; Kanmani et al., 2017, Lu et al., 2013).

The mechanical process known as a microfibrillator, or grinder, is one of the main methods of extracting nanofibrils and it uses the principles of refiners already established by the paper industry. However, the energy consumption during the process is a barrier to the mass production of CNF's (Spence et al., 2011). The extraction with the use of enzymatic cocktails is an eco-friendly technique with the obstacle of requiring a greater amount of time for complete extraction of nanofibrils, in addition to loss of yield within time (Henriksson et al., 2007). In this way, the union of both techniques has been outstanding to overcome the challenges of each method, facilitating the extraction of CNF's and generating nanofibrils with high quality (Tian et al., 2017; Zhu et al., 2011; Filson et al., 2009).

The enzymes are classified according to their specificity. Cellulases, for example, are the enzymes that cause degradation in cellulose. The endoglucanases, a classification of cellulases, are responsible for cleaving the cellulosic chain randomly in the amorphous regions (Gupta and Lee, 2009; Pääkkö et al., 2007).

Despite studies already performed with enzymatic pretreatment, it is still necessary to study its effect on the energy consumption of the fibrillator and its impact on the quality of the CNF's generated. Notwithstanding, the objective of this work was to evaluate the application of endoglucanase in different types of unbleached cellulose pulp as a pretreatment in the energy consumption of the mechanical extraction of cellulose nanofibrils. Chemical, morphological and mechanical characteristics of the pretreated fibers/nanofibrils with and without enzyme were also evaluated.

2 EXPERIMENTAL

2.1 Materials

Klabin S.A. (Paraná/Brazil) provided unbleached *Eucalyptus* sp. (UB-Euc), unbleached *Pinus* sp. Kraft pulp (UB-Pin) and chemithermomechanical (CTMP) pulp for this work. It was also provided two types of endoglucanase enzymes, A and B. Table 1 has the specifications and conditions of use for the enzymes.

Table 1. Endoglucanase enzymes specifications.

	Enzyme A	**Enzyme B**
Product	CGK20092 / NS51137	CVN04076 / NS51179
Activity	Endoglucanase	Endoglucanase
pH	7.0 – 7.5	6.0 – 6.5
Temperature (°C)	45 – 55	45 – 65
Dosage (g/ton)	50 – 150	50 – 150

2.2 Cellulosic nanofibril extraction

UB-Euc, UB-Pin and CTMP were submitted to pretreatments with the enzymes described in Table 1 and without enzymes (WE). The process and characterization are depicted in Figure 1. The fibers were analyzed prior and after fibrillation in order to compare the pretreatment efficiency.

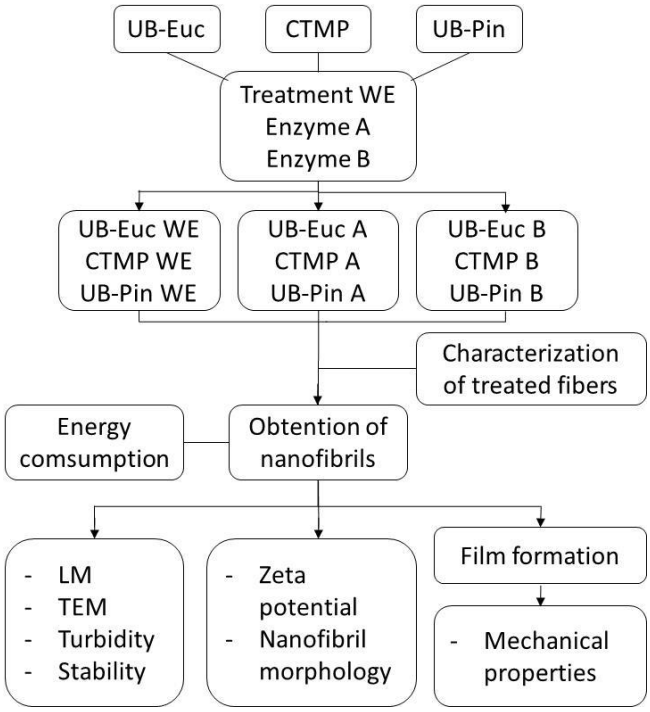

Figure 1. Schematic representation of the pretreatments and characterization. LM: Light microscopy. TEM: Transmission electron microscopy.

2.2.1 Enzymatic hydrolysis

Enzymatic pretreatments followed Silva (2018) recommendations. Pulps were previously diluted to 3% w/w with deionized water for 24 h. Temperature and pH range were set according to conditions in Table 1, followed by addition of 100 g/ton of endoglucanase enzyme. The fibers were then kept under agitation for 2 h at 750 rpm. After the treatment, the pulps were washed with 90±2°C deionized water to stop enzyme activity. To prepare the WE treatment, the pulps followed all the same steps without the addition of endoglucanase enzymes. Thereafter, pretreated pulps were oven-dried to further be analyzed and fibrillated.

2.2.2 Pulp fibrillation

Mechanical fibrillation was carried out on a grinder (Super Masscolloider Masuko Sangyo MKCA6-2). Each oven-dried pretreated pulp was hydrated (2% w/w) for 72 h. Afterwards, the suspension was dispersed in a NT134 High Torque Mechanical instrument at 750 rpm for 30 min. Suspension with individualized fibers was passed 5 times (cycles) through the grinder and the cycle which the suspension had a gel-like consistency was noted for further energy saving discussion. The procedure followed Bufalino et al. (2014) and Guimarães Júnior et al. (2015), and the equipment zero movement position point followed

Wang et al. (2012). Nanofibrils were kept under refrigeration to avoid degradation by microorganisms.

Following Dias (2017) recommendations, energy consumption during fibrillation was calculated according to Equation (1):

$$\mathbf{EC} = \frac{\mathbf{p\ x\ h}}{\mathbf{m}} \quad (1)$$

EC is energy consumption in kW.h/ton, p is power in kW (voltage x current), h is time in hours and m is mass of pulp in tons. Energy index was also calculated in order to compare pretreatments according to its energy consumption. It was estimated by the Equation (2):

$$\mathbf{EI} = \left(\frac{\mathbf{ECtreat - ECref}}{\mathbf{ECtreat}}\right)\mathbf{x\ 100} \quad (2)$$

EI is energy index in %, ECtreat is energy consumption of the enzymatic treatment, and ECref is the energy consumption of the control treatment (untreated).

2.3 Characterization of fibers/nanofibrils

2.3.1 Chemical and anatomical analysis

Chemical and anatomical characteristics of all pretreated pulps were executed to evaluate the effect of enzymatic pretreatments. Monosaccharides contents measurement followed indication of Wallis, Wearne and Wright (1996), using Dionex ICS 5000 ion chromatography system. Soluble lignin content measurement followed indication of Goldschimid (1971) and insoluble lignin content, the modified Klason method followed according procedures proposed by Gomide and Demuner (1986) and TAPPI T 222 om-02 (TAPPI, 2006). Ash content was disregarded.

The anatomical characteristics of fibers were estimated by Valmet FS5 (Finland) fiber analyzer. Fiber length, width, cell wall thickness, fines and cell wall fibrillation were assessed. Fines represent particles with diameter smaller than 75 µm or that passes through a 200-mesh sieve classifier (TAPPI, 1995). Cell wall fibrillation in morphological analysis represents the delamination of fibrils from the surface of fibers (Fardim and Durán, 2003) and is depicted as a parameter that explains possible degradation or enzyme action onto the cell walls.

2.3.2 Light microscopy (LM)

Light optical microscope Olympus BX51 was used to compare fibrillation, indicating nanofibril formation, on each cycle during mechanical extraction. Suspension was diluted to 0.75% w/w, and an ethanol-safranin solution (1.0% v/v) used to highlight fiber features.

2.3.3 Transmission electron microscopy (TEM)

The morphological analysis of cellulose nanofibrils was performed in a transmission electron microscope (TEM, Tecnai G2-12 instrument) with accelerating voltage of 80 kV (Tonoli et al., 2016). Nanofibril diameters were measured on 200 structures by ImageJ software (Schindelin et al., 2012) for diameter distribution analysis.

2.3.4 Turbidity

Turbidity of supernatant suspensions may correlate to the presence of nanofibrils. With the increase of particles size in suspension, the turbidity increases. It is measured by the Nephelometric Turbidity Units (NTU) unit. The measurement followed suggestions of Winter et al. (2010), with diluted samples (0.1% w/w) kept in test tubes for 1.5 h for decantation prior to the analysis. Then, supernatant was measured in triplicate by Turbidimeter Plus Alfakit equipment.

2.3.5 Stability of cellulose nanofibrils suspensions in water

Stability of cellulose nanofibrils in deionized water was performed according to Guimarães Júnior et al. (2015). Pictures of 30 mL diluted suspensions (0.25% w/w) kept in test tubes were taken hourly for the first 8 h, then daily for 2 days, completing 48 h. The sedimentation of cellulose nanofibrils was measured in the ImageJ software (Schindelin et al., 2012).

2.3.6 Zeta potential

Cellulose nanofibrils suspension were diluted to 0.05% w/w in deionized water, and prepared to determine zeta potential on the surface of nanofibrils in a Malvern 30000 zetasizer, following Tonoli et al. (2012) indications.

2.3.7 Mechanical properties

Tensile tests were performed in samples of nanofibrils that achieved a gel-like consistency and those after 5 grinding cycles, according to Guimarães Júnior et al. (2015).

The films were formed by 40 mL 1.0% w/w suspension casted onto a 15 cm diameter acrylic Petri dish and oven dried under circulation at 45ºC for 2 days.

The tensile test was performed in the texture analyzer equipment (Stable Microsystems, TATX2i model, England), following ASTM D828-16 (ASTM, 2016). Specimens of 10 cm long and 1 cm high were tested. The distance between clamps was 50±2 mm and test speed was 1 mm/min. Ten samples per treatment were analyzed. Tensile strength was calculated following Equation (3):

$$\sigma_{max} = \frac{F}{A_0} \quad (3)$$

σ_{max} is the maximum tensile stress (MPa); F is the maximum load applied on the specimen (N); A_0 is the cross-sectional area of the specimen (mm^2). The strain at rupture and the Young's modulus were also determined. Young's modulus or modulus of elasticity is the tangent line in the linear portion of the elastic region of a stress-strain curve and represents the stiffness of the material (Santos and Yoshida, 2011).

3 RESULTS AND DISCUSSION

3.1 Chemical and morphological characterization of the pulps

During the enzymatic hydrolysis of cellulose, cellulase enzymes cleave the cellulosic chain and extract sugars, such as glucose, from commercial fibers (Rabelo, 2007). Figure 2 presents the cellulose, hemicelluloses and total lignin (Figure 2A), soluble and insoluble lignin contents (Figure 2B) for unbleached Kraft *Eucalyptus* (UB-Euc) pulp, unbleached Kraft *Pinus* (UB-Pin) pulp and chemithermomechanical (CTMP) pulp. The ash content was not considered.

Cellulose content was similar when comparing treatments for UB-Euc with values around 65%. Hemicelulloses content was similar between the treatments as well, and values surrounding 12%. Due to the specificity of the enzymes to cellulosic chains it was expected no difference in lignin content as it shows in Figure 2. Lignin content is close to 23% for all UB-Euc treatments.

For CTMP pulp, cellulose content ranges from 49% to 52% without any difference between enzymes and WE treatments. Chemical results are relative to the total mass of the sample. This way, cellulose content was smaller than UB-Euc probably due to higher lignin content in CTMP pulp. Lignin from CTMP pulp is more difficult to extract than Kraft pulp,

which is mainly represented by the insoluble lignin content (Figure 2B). Moreover, higher quantities of insoluble lignin may indicate greater recalcitrance of the cellulosic pulp. Hemicelluloses contents were around 14% for all CTMP treatments.

UB-Pin presents cellulose and hemicelluloses content higher than UB-Euc. Cellulose content is between 68% and 71% whereas hemicelluloses content are between 11% and 13%. The main content of hemicelluloses of hardwoods is related to xylan, while softwoods have higher glucomannan content (Colodette and Gomes, 2015). Xylans are hemicelluloses that undergo more easily autohydrolysis, even in mild temperature conditions. This is due to its acidic character and its chemical properties (Ramos, 2003). Lignin confers limitation on the performance of cellulases on cellulosic pulps, in which even in smaller amounts, it can cause a decrease or retardation in the enzymatic activity (Castro and Pereira Jr., 2010). Lower contents of soluble Klason lignin are observed for UB-Pin (Figure 2B).

Even though it was observed small variations, Tukey's test confirmed that there was no statistic difference among chemical analysis. Therefore, enzymatic pretreatment did no cause significant changes to cellulosic pulp.

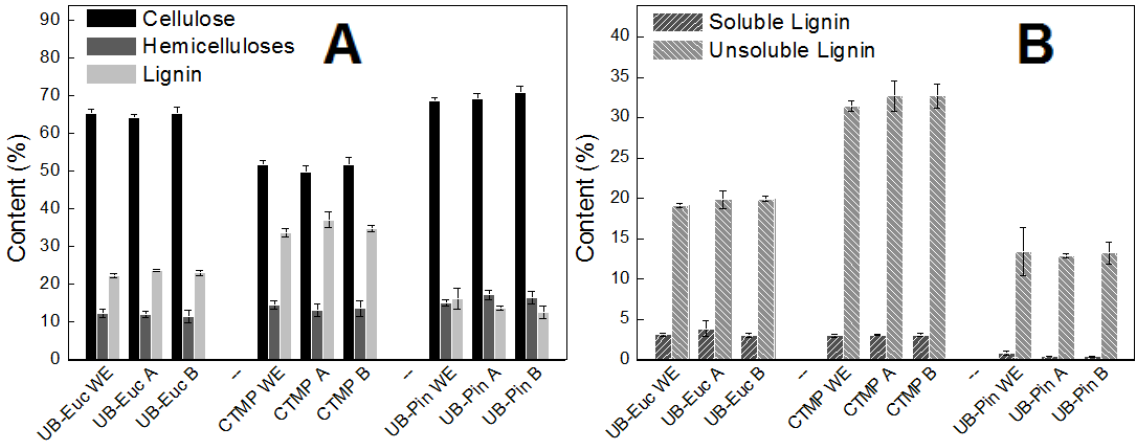

Figure 2. Chemical composition for UB-Euc, UB-Pin and CTMP treated with enzymes A and B compared with pulp without enzymes (WE). (A) Cellulose, hemicelluloses and lignin content and (B) soluble and insoluble lignin content.

Table 2 presents the fiber morphology parameters for pulps after enzymatic pretreatment. UB-Euc and CTMP have similar results of fiber length between control and enzyme treatments due to the fact that they are both from *Eucalyptus* with different pulping processes. Because CTMP includes a mechanical step in its pulping process, it was expected that its length would be smaller. For UB-Pin, length of control treatment and enzyme A pretreatment had similar results close to 1.84 mm. UB-Pin B presented higher length (1.93 ±

0.01 mm) that may be caused by pulp washing after enzymatic pretreatment. Very small particles were probably washed out, increasing weighted average fiber length of fibers.

Table 2. Average values and standard deviation of fiber morphology parameters for UB-Euc, UB-Pin, CTMP pretreated with A and B enzymes and without enzymes.

	Length (mm)	Width (µm)	CWT (µm)	Fines (%)	CWF (%)
UB-Euc WE	0.81 ± 0.00 ^{c}	19.61 ± 0.01 ^{c,d}	7.36 ± 0.20 ^{c}	16.82 ± 0.11 ^{d}	1.01 ± 0.01 ^{c}
UB-Euc A	0.81 ± 0.00 ^{c}	19.66 ± 0.08 ^{c,d}	7.40 ± 0.13 ^{c}	16.99 ± 0.24 ^{d}	0.99 ± 0.00 ^{c}
UB-Euc B	0.80 ± 0.00 ^{c}	19.50 ± 0.08 ^{c,d}	6.53 ± 0.01 ^{c}	18.59 ± 0.16 ^{c}	1.01 ± 0.01 ^{c}
CTMP WE	0.61 ± 0.00 ^{d}	19.37 ± 0.04 ^{d}	4.01 ± 0.01 ^{d}	38.60 ± 0.03 ^{a}	1.70 ± 0.01 ^{b}
CTMP A	0.61 ± 0.00 ^{d}	19.64 ± 0.04 ^{c,d}	4.49 ± 0.04 ^{d}	38.08 ± 0.14 ^{a,b}	1.74 ± 0.01 ^{a}
CTMP B	0.62 ± 0.00 ^{d}	19.71 ± 0.04 ^{c}	4.45 ± 0.05 ^{d}	37.20 ± 0.33 ^{b}	1.70 ± 0.00 ^{b}
UB-Pin WE	1.83 ± 0.04 ^{b}	27.57 ± 0.08 ^{b}	10.10 ± 0.69 ^{a}	16.22 ± 0.78 ^{d}	0.86 ± 0.01 ^{d}
UB-Pin A	1.86 ± 0.01 ^{b}	27.68 ± 0.14 ^{a,b}	10.48 ± 0.29 ^{a}	14.40 ± 0.21 ^{e}	0.83 ± 0.00 ^{e}
UB-Pin B	1.93 ± 0.01 ^{a}	27.95 ± 0.15 ^{a}	8.51 ± 0.18 ^{b}	13.67 ± 0.01 ^{e}	0.87 ± 0.00 ^{d}

CWT: Cell wall thickness. Fines represent particles with diameter smaller than 75 µm or that passes through a 200-mesh sieve classifier (TAPPI, 1995). CWF: Cell wall fibrillation. Same letters in the columns do not differ according to Tukey's statistic test at 5%.

The width of UB-Euc and CTMP kept similar to all treatments with values close to 19.6 µm. For UB-Pin, the average width of 27.6 µm was observed, which is expected since *Pinus* tracheids are larger than *Eucalyptus* fibers.

The cell wall thickness was almost the double for UB-Euc in comparison to CTMP. High contents of lignin in the cell wall may have blocked CTMP fiber from swelling, keeping the wall thinner than UB-Euc. However, enzyme A and B pretreatments demonstrated the increasing of the cell wall thickness. Both treatments for CTMP resulted in average cell wall thickness of 4.5 µm, indicating enzymatic activity on amorphous regions of the cell wall promoting its swelling. UB-Pin WE and UB-Pin A treatments presented similar cell wall thickness, but it was observed a decrease for UB-Pin B. As fibers were dried after enzymatic pretreatment, cell wall thickness may lose volume due to hornification, that promotes a reduction in fiber swelling, making mechanical fibrillation difficult (Ballesteros et al., 2017).

An increase in fines contents from UB-Euc WE to B may indicate an enzymatic activity on the fiber cell wall (Clarke et al., 2011; Li et al., 2012; Arantes et al., 2014). Although, cell wall fibrillation was affected by enzyme A in CTMP, the fact that both fines and cell wall fibrillation characteristics were not strongly affected by enzyme hydrolysis is probably because the large presence of lignin in all analyzed pulps.

As fiber morphology of all pretreated pulps did not present significant alterations, it can be suggested that cellulose hydrolysis used in this work did not impair fiber quality.

3.2 Energy consumption during fibrillation

Figure 3 shows the overall energy consumption of all pretreated pulps and energy index. It was not observed a gel-like consistency for CTMP, so the energy index was compared at 5 cycles. Authors have difficulty in the formation of nanofibrils from chemithermomechanical pulp, because they did not exhibit a strong gel formation during fibrillation (Osong et al., 2016; Silva, 2018; Mendonça, 2018). When nanofibrils are formed, a gel appearance is visualized in aqueous suspension (Pérez e Samain, 2010). Therefore, excessive grinding cycles after gel formation implies unnecessary energy expense (Henniges et al., 2014).

It is observed in Figure 3A the decrease in gel formation cycle for UB-Euc from 3 cycles to 2 cycles for both enzymes A and B pretreatments. This decrease indicates energy savings of about 44% with enzyme A pretreatment, and 35% with enzyme B pretreatment (Figure 3D). Endoglucanase enzyme acts in amorphous regions of the cellulose chain by breaking the glycosidic bond β(1→4). In addition enzyme pretreatment decreases the degree of polymerization of cellulose, which also assists in fiber swelling, facilitating fibrillation.

Energy consumption for both UB-Euc A (~3,900 kW.h/ton) and UB-Euc B (4,600 kW.h/ton) were lower than the control UB-Euc WE (~7,000 kW.h/ton). The most significant decrease in energy consumption for enzyme A may indicate more affinity with unbleached *Eucalyptus* Kraft pulp, easing the extraction of nanofibrils. Ribes et al. (2018) using cellulase hydrolysis as pretreatment for grinding extraction of unbleached *Eucalyptus* nanofibrils, reached around 41% of energy savings.

Cellulase hydrolysis did not significantly affect CTMP extraction of nanofibrils, thus not forming the gel-like appearance in the suspension (Figure 3B). Energy consumption in 5 cycles through grinder did not follow the same pattern as for UB-Euc; energy consumption of CTMP A (~8,500 kW.h/ton) was higher than CTMP WE (~7,100 kW.h/ton). Even though CTMP B showed lower energy consumption (~6,200 kW.h/ton) its suspension did not indicate a gel appearance as well. He et al. (2018) reached 15,000 kW.h/ton of energy consumption for CTMP nanofibril extraction with 35 cycles.

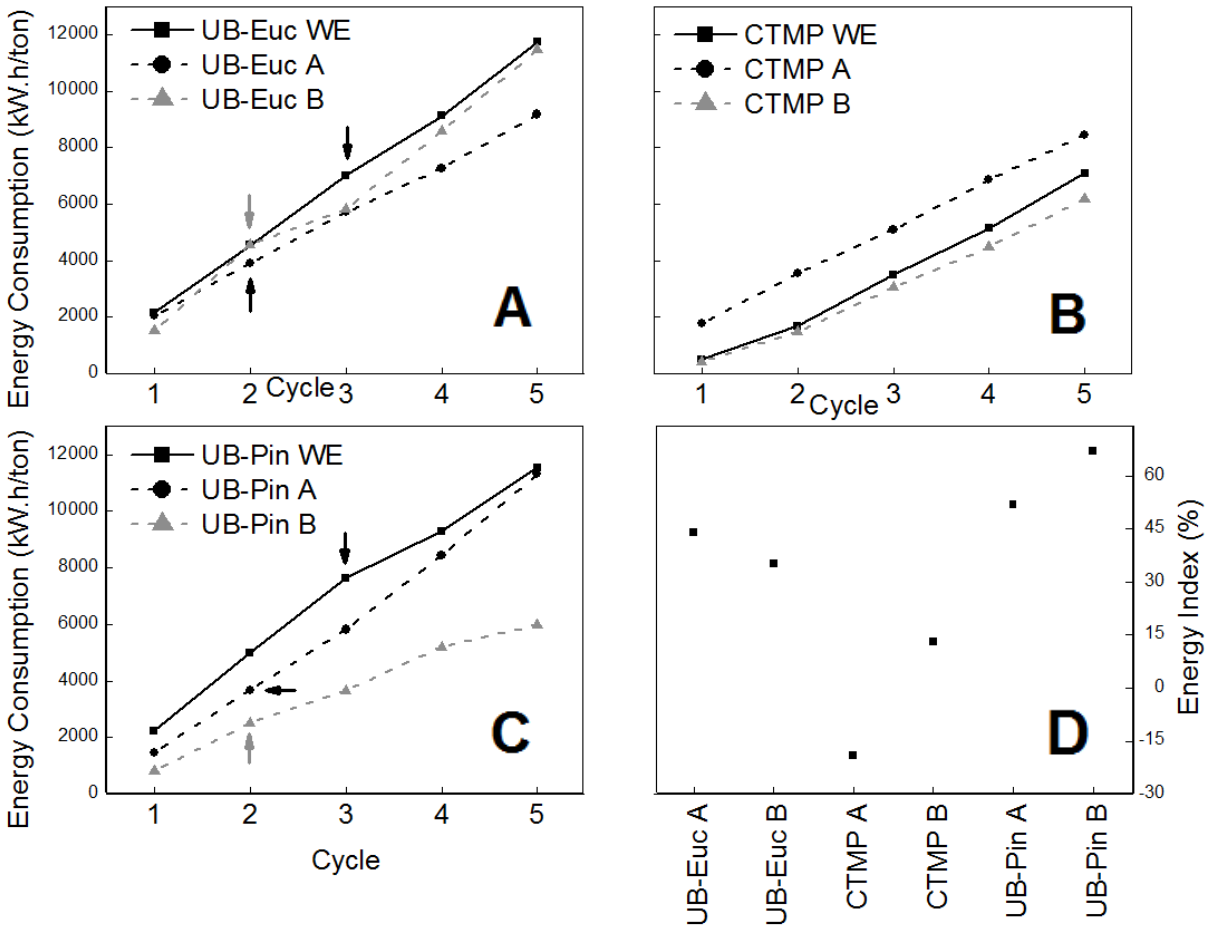

Figure 3. Evolution of energy consumption during fibrillation of: *Eucalyptus* sp. (UB-Euc) Kraft pulp (A); chemithermomechanical pulp (CTMP) (B); *Pinus* sp. (UB-Pin) Kraft pulp (C); and energy index (D). Arrows show gel formation for each suspension.

The extraction of nanofibers from UB-Pin WE (~7,600 kW.h/ton) consumed higher energy than UB-Euc WE (~7,000 kW.h/ton). *Pinus* tracheids are thicker and longer than *Eucalyptus* fibers (Burguer and Richter, 1991), promoting decantation during the fibrillation process, making difficult its passage through the equipment (Gunawardhana et al., 2017).

UB-Pin fibers treated with enzymes showed the same tendency as UB-Euc, whose gel formation occurred in less passes through grinder than untreated fibers. UB-Pin A demanded around 3,700 kW.h/ton at 2 cycles through the grinder. This indicates an energy saving of 52%. UB-Pin B had even lower energy consumption (2,500 kWh/ton) with 67% of energy savings. An energy consumption of 34,000 kW.h/ton with 35 cycles has been reported for softwood nanofibril extraction (He et al., 2018) showing that the fibrillation process is being optimized with the use of enzymes.

With the increase of cycles, the energy consumption increased for all pretreatments. UB-Euc WE, for instance, used 76% more energy to reach the 5th cycle when comparing with gel formation cycle. For UB-Euc A and B, it was observed an increase of 135% and 96%,

respectively. The fibrillation of UB-Pin also presented high energy consumption with 51%, 95% and 63% more energy used for UB-Pin WE, A and B, respectively, to reach five cycles. This increase in energy consumption is related to the viscosity change on the suspension, making it more difficult to fibrillate when compared to untreated fibers.

3.3 Nanofibrils morphology

Transmission electron microscopy (TEM) images of gel formation cycle were analyzed to understand how the pretreatments affected cellulose nanofibrils morphology. Typical light microscopy (LM) images of all 5 cycles, including prior to the process, were also analyzed to monitor fibers fibrillation.

It is observed in Figure 4A, a typical TEM image of UB-Euc WE nanofibrils. It is noticed that cellulose nanofibrils are well individualized, but with apparent differences in the diameter distribution. Wang et al., (2012), analyzing the morphology of nanofibrils, called this pattern "network" nanofibrils. It is observed in LM typical images (Figure 4 B-G) that as the number of cycles increases, the number of whole fibers decreases with the increase of fragmented fibers. Gel-like formation cycle for WE was noted in the 3rd cycle (Figure 4E). Even so, on the gel formation cycle and following cycles, it was observed high content of intact fibers in the suspension, showing that fibrillation was less effective.

In Figure 5A, UB-Euc A nanofibrils presented "untwisted backbone fibrils entangles by twisted nanofibrils" as Wang et al. (2012) proposed in their work. The difference in structures comes from the proportion of amorphous and crystalline cellulose regions (Wang et al., 2012). For UB-Euc A ML images (Figure 5 B-G), which showed 44% energy savings when compared to WE, it was still possible to see intact fibers in the gel formation cycle, but with the increase of cycles, the number of whole fibers declined drastically. This decrease was more evident when compared to the control treatment. Gel formation cycle decreased from 3 to 2 cycles probably due to an enzymatic activity over the fibers.

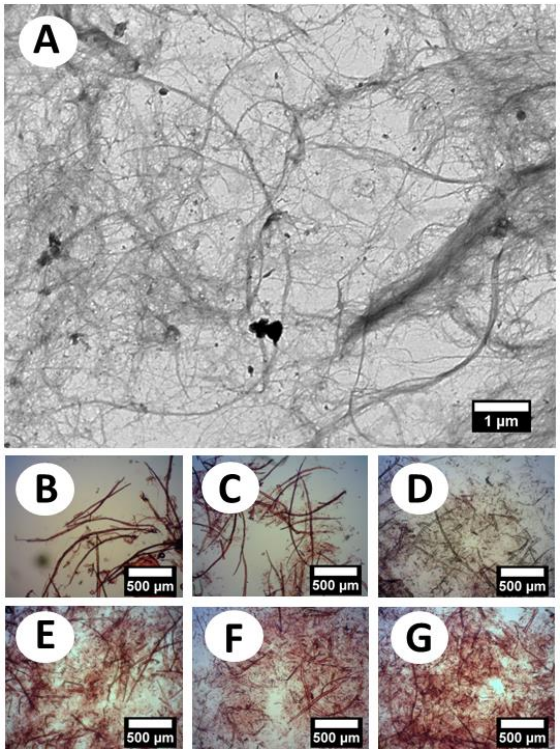

Figure 4. Typical transmission electron microscopic (TEM) and light microscopic (LM) images of UB-Euc WE. A) TEM in gel formation cycle (3 cycles) of "network" nanofibrils (Wang et al., 2012). B) LM prior to fibrillation. C) LM in 1 cycle. D) LM in 2 cycles. E) LM in 3 cycles. F) LM in 4 cycles. G) LM in 5 cycles.

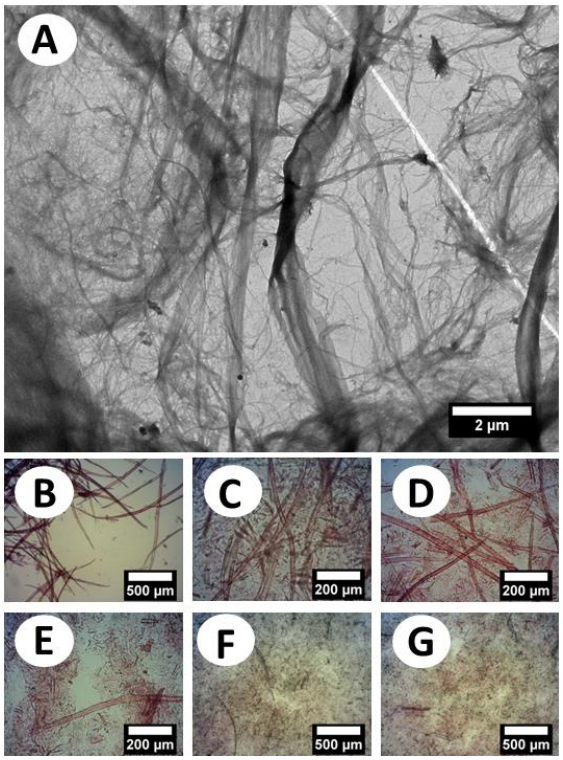

Figure 5. Typical transmission electron microscopic (TEM) and light microscopic (LM) images of UB-Euc A: A) TEM in gel formation cycle (2 cycles) of "untwisted backbone fibrils entangles by twisted nanofibrils" (Wang et al., 2012; B) LM in prior to fibrillation; C) LM in 1 cycle; D) LM in 2 cycles; E) LM in 3 cycles; F) LM in 4 cycles; G) LM in 5 cycles.

Although not achieving a gel-like consistency, CTMP suspension formed nanofibrils. However, less nanofibrils and bigger particles in the suspension were observed when compared with control and enzymatic treatments of UB-Euc (Figure 4A and 5A). Typical TEM image of CTMP pretreated with enzyme B (Figure 6A) showed bigger fibrils particles, indicating that enzymatic pretreatment was not efficient. For CTMP pulp, the process severed fibers rather than fibrillating them. With the increase of cycles (Figure 6 B-G), ML images showed the decrease of fibers length, but particles in microscale formed aggregates and films after drying for TEM preparation, differently of what was observed for preparation of the nanofibrils from Kraft pulps.

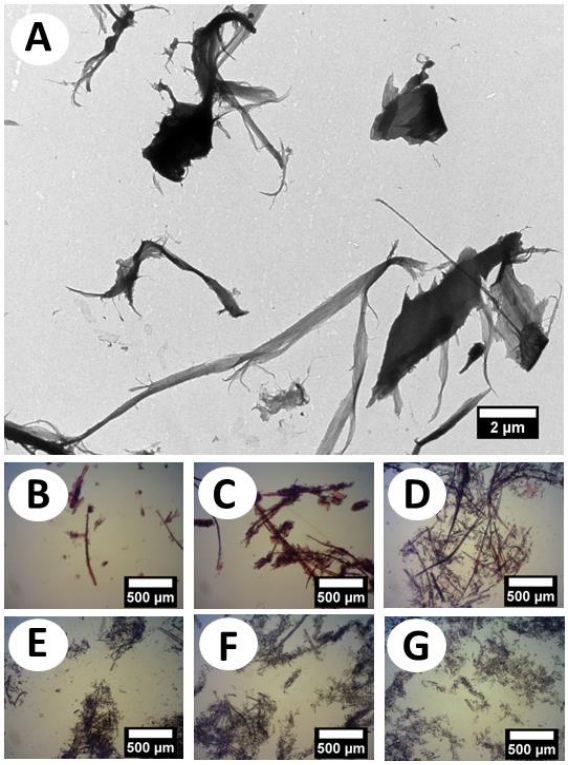

Figure 6. Typical transmission electron microscopic (TEM) and light microscopic (LM) images of CTMP B. A) TEM in 5 cycles; B) LM in no cycles; C) LM in 1 cycle; D) LM in 2 cycles; E) LM in 3 cycles; F) LM in 4 cycles; G) LM in 5 cycles.

Figure 7 shows the TEM and ML images of UB-Pin WE fibers/nanofibrils. Gel-like formation was observed at the 3rd cycle. It is observed in Figure 7A that the extraction of nanofibrils in gel formation cycle presented nanofibrils with different diameters in a “net” structure, as suggested by Wang et al. (2012). Comparing with UB-Euc WE (untreated), the UB-Pin nanofibrils presented less intact fibers with the increase of cycles through grinder (Figure 7 B-G). This can indicate that the fibrillation of UB-Pin pulp is easier than UB-Euc.

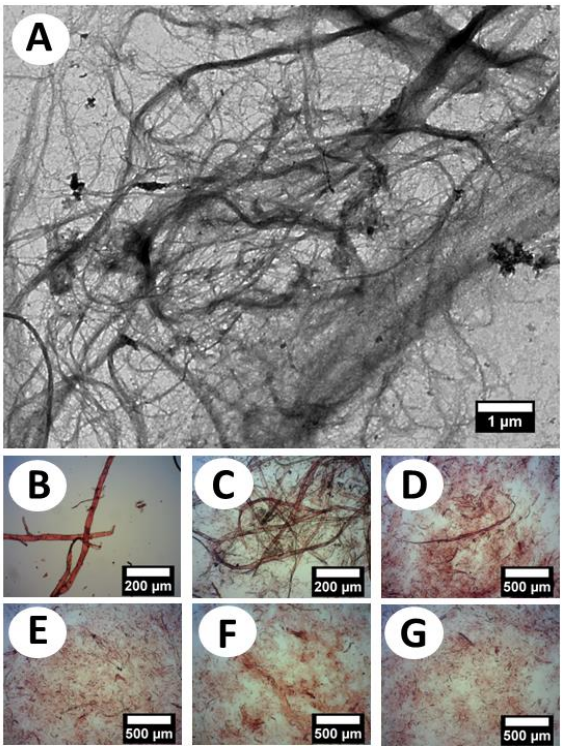

Figure 7. Typical transmission electron microscopic (TEM) and light microscopic (LM) images of UB-Pin WE. A) TEM of "net" nanofibrils (Wang et al., 2012) in gel formation cycle (3 cycles); B) LM in no cycles; C) LM in 1 cycle; D) LM in 2 cycles; E) LM in 3 cycles; F) LM in 4 cycles; G) LM in 5 cycles.

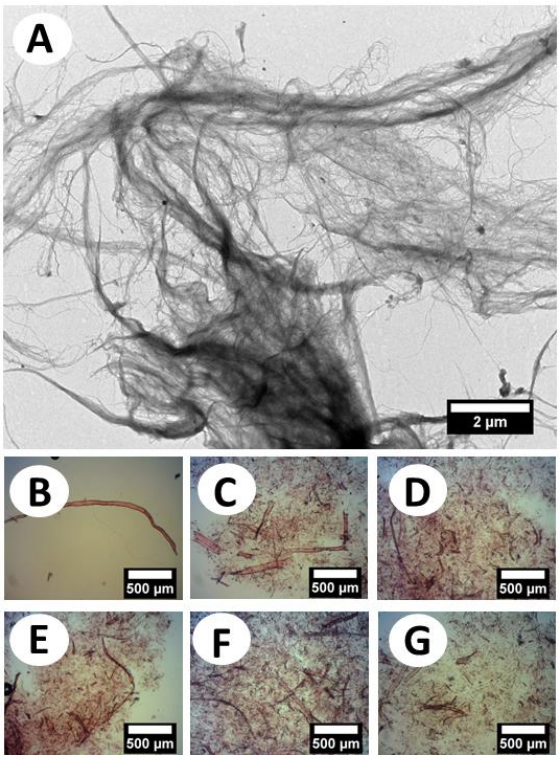

Figure 8. Typical transmission electron microscopic (TEM) and light microscopic (LM) images of UB-Pin B. A) TEM of "blooming tree" nanofibrils (Wang et al., 2012) in gel formation cycle (2 cycles); B) LM in no cycles; C) LM in 1 cycle; D) LM in 2 cycles; E) LM in 3 cycles; F) LM in 4 cycles; G) LM in 5 cycles.

It is observed in Figure 8 the effect of the enzyme B on the UB-Pin nanofibrils/fibers morphology. The TEM image of nanofibrils (Figure 8A) shows the higher presence of thinner cellulose nanofibrils in a "blooming tree" structure; they are formed due to different cellulose crystallinities. This difference can be related to growth stress under the conditions of the growing of cell walls (Stamm, 1964). Typical LM images of fibers during fibrillation (Figures 8 B-G) show a significant decrease in intact fibers after gel formation in the 2nd cycle. UB-Pin A also showed a gel-like consistency at 2 cycles.

With TEM images, diameters of 200 nanofibrils were measured by ImageJ software (Schindelin et al., 2012) in order to classify the suspensions formed from the treatments with and without the addition of enzyme. It is observed in Figure 9 the diameter distribution of the main treatments. Diameters of UB-Euc nanofibrils were concentrated in the range of 15-30 nm whereas UB-Pin had a higher content of nanofibrils of lower than or equal to 15 nm. Nanofibrils with mean diameter lower than 30 nm have potential as reinforcement in composites (Tonoli et al., 2016).

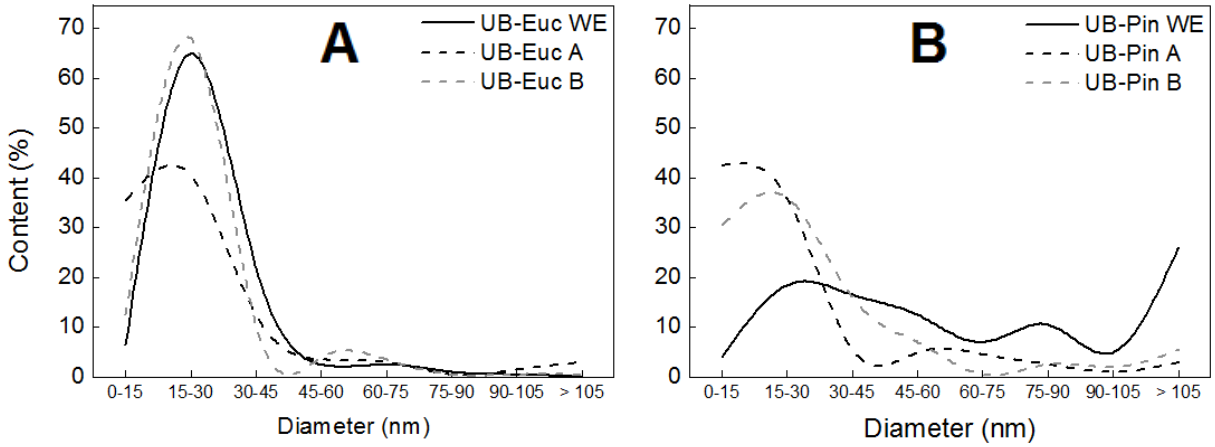

Figure 9. Distribution of cellulose nanofibrils diameter for (A) UB-Euc and (B) UB-Pin.

The average diameter for UB-Euc WE nanofibrils was 26 nm with range between 14-78 nm, with 71.5% of nanofibrils lower than 30 nm (Figure 9A). UB-Euc A presented average diameter of 18 nm (9 - 57 nm) and 80% of them were lower than 30 nm. UB-Euc A also showed higher content of not efficiently fibrillated fibers, with 8% of particles higher than 105 nm of diameter. UB-Euc B led to the average diameter of 22 nm (13 – 66 nm) with 81% diameters lower than 30 nm. Since CTMP did not produce a gel-like dispersions, it was not measured its diameters considering that most of its particles were in microscale instead of nanoscale.

For UB-Pin (Figure 9B), it was observed for WE an average diameter of 58 nm with range between 19 - 296 nm with only 22% of the diameters lower than 30 nm. It was observed bigger particles in the TEM image, increasing average diameter, which indicates a not well-fibrillated suspension. UB-Pin A produced nanofibrils with average diameter of 17 nm (8 - 94 nm), whose 79% of them were lower than 30 nm. UB-Pin B presented 23 nm (4 - 114 nm) of average diameter with 67% of diameter lower than 30 nm. Even though UB-Pin B pretreatment led to lower energy consumption, its suspension was not as fibrillated as UB-Pin A. This may have happened due to longer fibers of enzyme B pretreated pulps.

3.4 Suspension visual aspects

During fibrillation, with the evolution of the number of cycles through the grinder, the suspension reaches a gelatinous appearance. This gel-like consistency indicates the presence of cellulose micro/nanofibrils. In suspension, the turbidity of the supernatant increases as the amount of dispersed nanofibrils increases. Cellulose nanofibrils are dispersed in the supernatant due to its lightness while larger particles decant (McKee et al., 2014). Figure 10 shows the evolution of turbidity of the supernatant of suspensions of untreated (WE) cellulosic nanofibrils and pretreated with enzymes A and B, for each cycle through the grinder.

It was observed that all treatments presented an increase in turbidity as the number of cycle increases. UB-Euc WE supernatant presented lower turbidity, in gel formation cycle than at the 5^{th} cycle, UB-Euc B presented higher value of turbidity among UB-Euc samples. This may have occurred due to higher mean diameter of UB-Euc B nanofibrils. In the last cycle, UB-Euc A and B presented higher turbidity when compared to gel formation cycle. However, UB-Euc A was significantly higher than UB-Euc B and this indicates higher content of nanofibrils in the supernatant.

CTMP samples presented higher values of turbidity, even though they did not present a gel appearance. This turbidity can be related to high hemicelluloses and lignin content attached to CTMP micro and nanoparticles, as discussed in early sections. Xiao et al. (2001) showed a change in turbidity due to the dissolution of hemicelluloses and lignin in the suspension when applying pre-treatments that modified the cell wall of fibers. CTMP A presented the highest turbidity value with 661 ± 10 NTU at the last cycle, followed by WE treatment, with 572 ± 7 NTU and enzyme B treatment with 415 ± 21 NTU, following the same order of energy consumption. A decrease was observed for CTMP A treatment after cycle 2, as well as for WE treatment after 3 cycles, probably due to an entanglement of

particles as showed in section 3.3. The morphology of the nanofibrils may change with the excessive passage through the grinder, becoming more “blooming trees” (Wang et al., 2012).

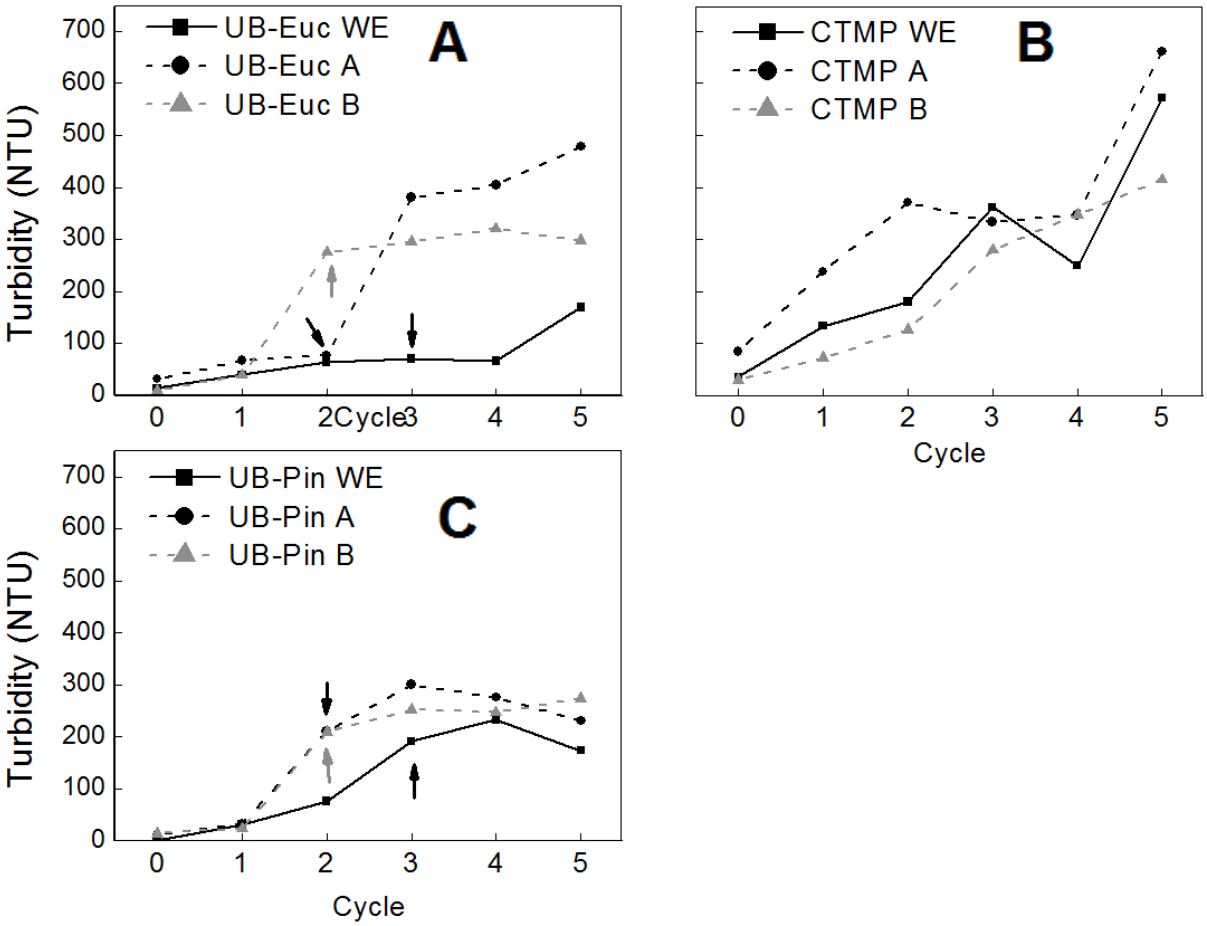

Figure 10. Evolution of turbidity of the supernatant of nanofibrils suspensions with the number of cycles through the grinder: (A) UB-Euc; (B) CTMP; and (C) UB-Pin cellulose nanofibrils. Arrows mark gel formation.

After the third cycle, UB-Pin A decreased its turbidity while the WE suspension decreased after the 4th cycle. Turbidity of enzymatically treated pulps showed similar results at gel formation cycle. Nanofibrils in supernatant were more evident for both enzyme pretreatments when compared to control (untreated) presenting higher turbidity values. In the last cycle, UB-Pin B presented higher turbidity values compared to UB-Pin A and both of them were higher than UB-Pin WE. These results may indicate the success in the use of enzymatic treatment to enhance fibrillation.

The stability of the samples for each grinding cycle is shown in Figure 11. For UB-Euc and UB-Pin fibers it was noted that lower sedimentation occur with the increase of cycles through the grinder. This may correlate with a presence of smaller particles (mixture of

fragments of hemicelluloses, lignin and cellulose nanofibrils) that remain suspended while fibers and fragments tend to sink to the bottom of the vessel.

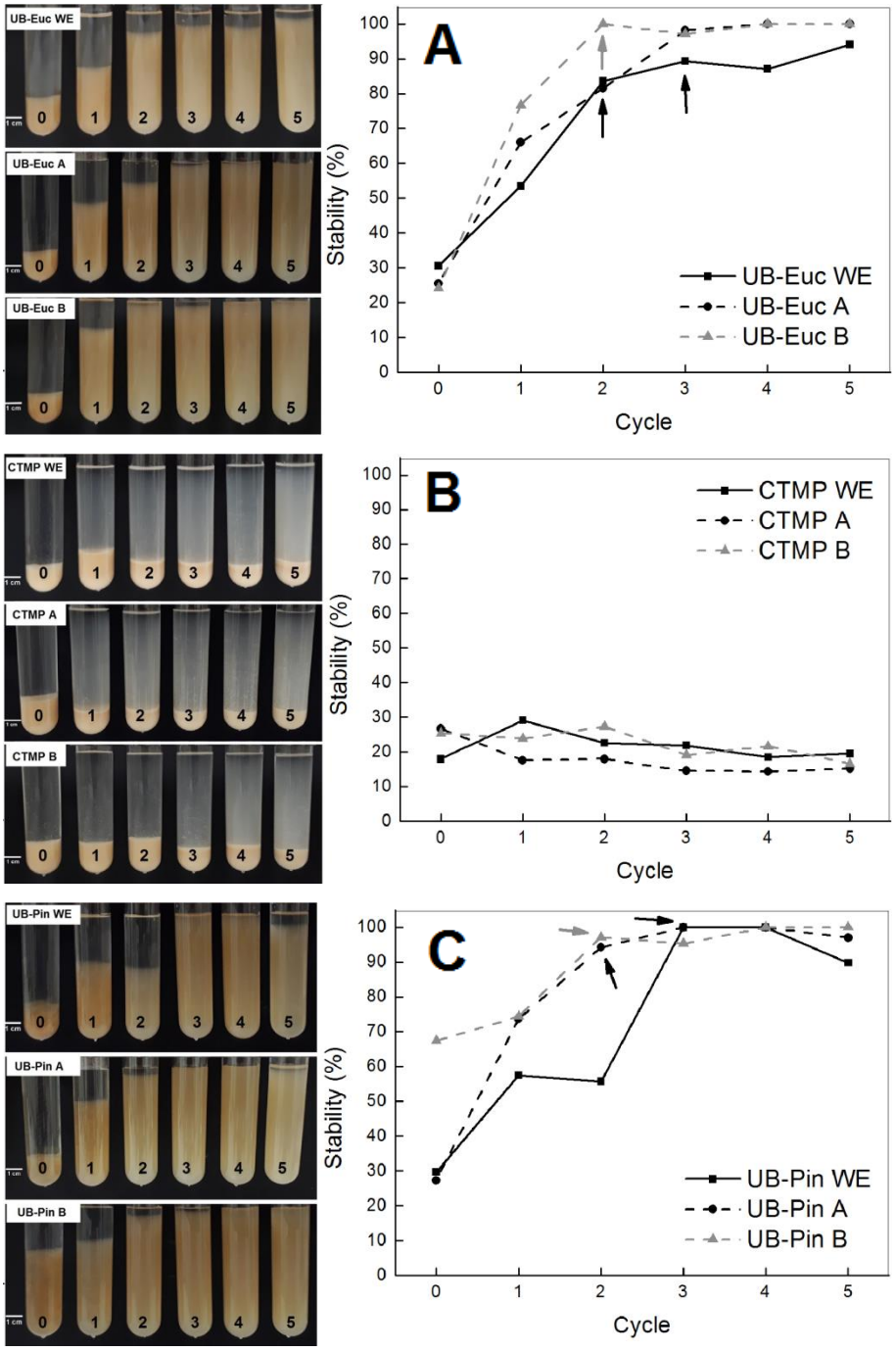

Figure 11. Evolution of the stability of the cellulose nanofibrils with the cycles through the grinder, after 48 h decantation in water for: (A) UB-Euc; (B) CTMP; and (C) UB-Pin. Arrows mark the gel formation cycles for each treatment.

Guimarães Júnior et al. (2015) concluded in their study that with the increase of degree of fibrillation, suspensions of nanofibrils would become more stable in water, being evident mainly in the cycle in which there is gel formation, which led to lower decantation.

As shown in Figure 11A, with the increase of number of cycles, control samples of UB-Euc showed increased stability of the nanofibrils. However, complete stabilization in water was not observed. The cause of non-stabilization is the presence of non-nanoscale material, which led the fragments in suspension to decant (McKee et al., 2014). In the cycle that a gel appearance was formed in the suspension, the stability of the nanofibrils was 89%. One additional cycle caused stability to fell to 87%, rising again in the last cycle, with 94%. The decrease in the fourth cycle sample should be related to nanofibrils flocculation caused by nanofibrils interlacing forming "net" or "blooming trees" structures.

UB-Euc A also presented an increase in suspension stability as cycle increases. In 2 cycles (gel formation cycle), the suspension exhibits 82% of stabilization, and finding complete stability at 4 and 5 cycles. UB-Euc B suspension was stabilized at gel formation cycle (2 cycles), slightly decreasing in the 3rd cycle to 97% and then increasing again to 100%.

Figure 11B shows the stability of CTMP suspensions in water. Larger particles in suspension may have caused decantation in the CTMP suspension. As no gel-like suspension was reached, it was expected that there would be no complete water-stabilization. However, with the increase in the number of cycles through the grinder, the increase of turbidity of the supernatant of the samples was observed. This may have happened due to the increased percentage of nanofibrils in the supernatant, increasing their turbidity. It is known that nanoscale materials are lighter, thus increasing their turbidity (McKee et al., 2014).

The water stabilization of unbleached *Pinus* samples is presented in Figure 11C. As the degree of fibrillation of the suspension increased, the increase of stabilization was observed for all treatments. For control treatment, complete stabilization in water was observed in the cycle where there was the gel formation (3 cycles). But on 5th cycle, the stabilization drop from 100% to 90%. The entanglement of nanofibrils in this cycle should have caused this decrease in stability. Similar pattern was observed for UB-Pin A suspension. In UB-Pin A gel-like formation cycle (2nd cycle), suspension was not fully stabilized but reached 94% of water-stability, completely stabilizing after 3 cycles and having a slight decrease in the last cycle as well. Nanofibrils from enzyme B pretreatment presented 97% of stability in gel formation cycle (2nd cycle) and complete stabilization at the 4th and 5th cycle through the grinder.

3.5 Zeta potential

Zeta potential results are presented in Table 3. According to Mirhosseini et al. (2008), charge values in the surface of nanofibrils higher than 25 mV, in module, is considered a stable suspension. Zeta potential is an important indicator of colloidal dispersion, which higher values in modulus indicate higher dispersion of nanocellulose in water (Tonoli et al., 2012).

Table 3. Average and standard deviation values of zeta potential in different cycles. Results in mV.

	Cycle	UB-Euc	CTMP	UB-Pin
WE	**Gel formation**	-45.6 ± 2 [a]	-45.3 ± 1.4 [a]	-37.3 ± 1.7 [a]
	5	-17.3 ± 1.3 [b]	-25.5 ± 2.4 [b]	-14.7 ± 1.3 [b]
A	**Gel formation**	-44.7 ± 1.5 [a]	-44.1 ± 1.5 [a]	-35 ± 0.7 [a]
	5	-14.7 ± 1.7 [b]	-22.1 ± 1.1 [b,c]	-14.1 ± 0.9 [b]
B	**Gel formation**	-41.3 ± 1.6 [a]	-43.4 ± 3.9 [a]	-37.6 ± 0.3 [a]
	5	-14.9 ± 1.9 [b]	-18.5 ± 1 [c]	-12.4 ± 2.3 [b]

For CTMP there was no gel forming in any cycle and it is used the 2nd cycle for cooperation. Same letters in the columns imply that values do not differ according to Tukey's statistic test at 5%.

Nanofibrils extracted from UB-Euc or CTMP presented zeta potential values higher than UB-Pin. For treatment A and treatment B of all pulps, zeta potential tends to have a small decrease. Bhardwaj, Kumar and Bajpai (2004) reported -32.8 mV for unbleached Kraft *Eucalyptus* pulp, Smolin et al. (2008) found -43.7 mV for CTMP zeta potential, and for *Pinus* Kraft pulp, ColloidMetrix (nd) found -29.5 mV.

Even though CTMP did not form gel in its suspension, zeta potential after 2 cycles presented similar results with UB-Euc. Once gel is formed, after 5 cycles through grinder, zeta potential of CTMP suspensions presented higher values of zeta potential than both UB-Euc and UB-Pin.

High values observed for *Eucalyptus* compared to *Pinus* nanofibrils can be explained by the presence of carboxyl and methyl-glucouronic acid groups present in the xylans, main hemicelluloses of hardwoods (Winuprasith and Suphantharika, 2013), since it increases zeta potential values (Klemm et al., 2011).

Five cycles during mechanical fibrillation caused the decrease of zeta potential values for all treatments. This may occur due to an extraction of hemicelluloses during fibrillation (Dufresne et al., 1997) or the entanglement of nanofibrils particles that could contribute to changes of zeta potential measurement (Siqueira et al., 2009).

3.6 Tensile properties of films composed of nanofibrils

Figure 12 presents a typical stress-strain curve of the films. Table 4 shows the main results of the tensile test of nanofibril film samples. As CTMP did not form a gelatinous suspension, it was not possible to form a film from the micro/nanofibrils suspension.

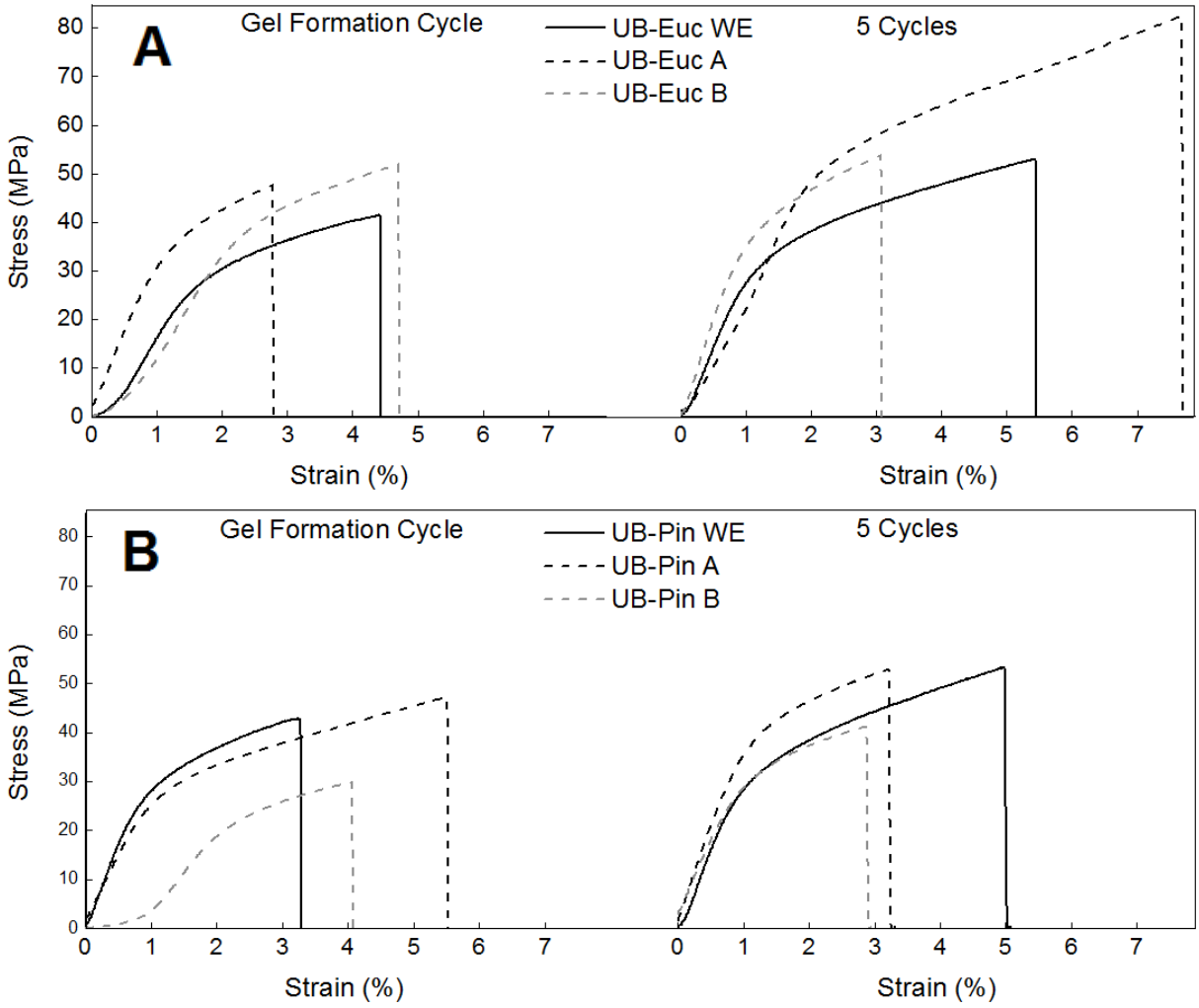

Figure 12. Typical stress-strain curves of films at gel formation and 5 cycles for: (A) UB-Euc; and (B) UB-Pin.

Comparing films on gel formation cycle, UB-Euc A presented the highest tensile strength for *Eucalyptus* pulp, with 42.3 ± 5.0 MPa. UB-Euc A generated nanofibrils with smaller diameters than UB-Euc B and this may have caused a stronger bonding between nanofibrils pretreated with enzyme B due to the higher surface area that improved the interlacing between nanofibrils. Comparing films of the gel formation cycle to the ones at the 5^{th} cycle, it was observed that the increase in tensile strength is lower than 50% for most samples while energy consumption could surpass 100% with the increase of cycles from the point of gel formation. The film that presented the highest tensile strength was UB-Euc A that

also had the highest supernatant turbidity from UB-Euc samples. Young's modulus kept similar to UB-Euc A and B for both gel formation cycle and the 5th cycle. The difference is observed for both treatments in the last cycle. For strain at rupture, it was visualized that with the increase of fibrillation cycles the strain values also increased.

Table 4. Average and standard deviation values of tensile properties of the films in different cycles.**

	Cycle	Tensile strength (MPa)	Young's modulus (GPa)	Strain at rupture (%)
UB-Euc WE	**3***	35.1 ± 5.3 ^{d,e}	2.7 ± 0.4 ^{b,c}	2.4 ± 1.1 ^{c}
	5	49.2 ± 5.2 ^{a,b,c,d}	3.1 ± 0.4 ^{b,c}	4.3 ± 0.9 ^{a,b,c}
UB-Euc A	**2***	42.3 ± 5.0 ^{c,d,e}	2.8 ± 0.2 ^{b,c}	2.8 ± 0.7 ^{b,c}
	5	61.6 ± 21.3 ^{a}	3.2 ± 1.0 ^{a,b}	5.2 ± 3.3 ^{a}
UB-Euc B	**2***	37.2 ± 8.5 ^{d,e}	2.8 ± 0.5 ^{b,c}	2.2 ± 1.5 ^{c}
	5	51.6 ± 4.5 ^{a,b,c}	3.5 ± 0.7 ^{a,b}	3.4 ± 0.6 ^{a,b,c}
UB-Pin WE	**3***	45.2 ± 9.3 ^{b,c,d,e}	2.7 ± 0.7 ^{b,c}	4.7 ± 1.6 ^{a,b}
	5	57.2 ± 6.7 ^{a,b}	4.0 ± 0.8 ^{a}	2.7 ± 0.9 ^{b,c}
UB-Pin A	**2***	40.4 ± 5.1 ^{c,d,e}	2.7 ± 0.1 ^{b,c}	3.3 ± 1.3 ^{a,b,c}
	5	46.6 ± 9.9 ^{b,c,d,e}	4.0 ± 0.3 ^{a}	2.1 ± 1.0 ^{c}
UB-Pin B	**2***	27.3 ± 1.7 ^{e}	1.8 ± 0.3 ^{c}	3.3 ± 0.9 ^{a,b,c}
	5	36.0 ± 4.5 ^{d,e}	2.4 ± 0.4 ^{c}	3.6 ± 1.2 ^{a,b,c}

*Gel formation cycle. ** Same letters in the columns do not differ according to Tukey's statistic test at 5%.

UB-Pin samples followed similar behavior to UB-Euc. UB-Pin WE presented 45.2 ± 9.3 MPa of tensile strength in gel formation cycle and UB-Pin A 40.4 ± 5.1 MPa. UB-Pin B showed the lowest tensile strength (27.3 ± 1.7 MPa) at 3 cycles (gel formation cycle). This may have occurred due to the fact that UB-Pin B presented higher nanofibril average diameter, when compared to UB-Pin A, as presented in previous sections, decreasing the contact surface area between nanofibrils. With the increase in cycles, an increase in strength was also observed for UB-Pin WE, enzymes A and B pretreatments. UB-Pin WE films increased 20% with the 5 cycles, while A and B films increased 13% and 24%, respectively. These samples presented lower supernatant turbidity as well as decreased water stability at 5 cycles, as presented in early sections. Low turbidity indicates few nanofibrils in the supernatant. For Pinus, the strain at rupture seems to be lower in films formed from the cycle that the gel was formed.

The values of Young's modulus and tensile strength found for cellulose nanofibrils are comparable to other commercial materials. For instance, polyester presents Young's modulus of 0.31 ± 0.12 GPa and tensile strength of around 27.7 ± 7.2 MPa (Glória et al., 2017).

4 CONCLUSIONS

The chemical composition and anatomical characteristics of the pulp fibers were not affected by the application of enzymatic pretreatment, consequently, it did not promote excessive hydrolysis of the pulps. In addition, enzymatic pretreatment triggered the reduction of energy consumption for cellulose nanofibrils extraction of Kraft pulps. Chemithermomechanical (CTMP) pulps were difficult to fibrillate and it was not possible to see a gelatinous suspension as observed for the other pulps. Thus, enzymatic pretreatment did not have any significant effect to promote CTMP fibrillation. It was possible to extract nanofibrils of CTMP fibers, but in small contents; most of the particles of CTMP suspension presented microsized particles instead of nanosized ones. CTMP also showed decreased water stability and higher supernatant turbidity, caused by bigger particles in the suspension but fragments of hemicelluloses, lignin and cellulose nanofibrils. On the other hand, enzyme A and B pretreatments promoted more fibrillated nanofibrils at low energy consumption, reaching up to 67% of savings. *Eucalyptus* sp. showed intact fibers even after gel cycle, indicating that *Pinus* sp. was more efficient to fibrillate. In addition, the increase of water stability of the suspensions was caused by smaller average diameters, which increased interlacing between cellulose nanofibrils, also causing a slight increase of tensile strength. Thus, the enzymatic pretreatment proved to be a sustainable alternative for extraction of nanofibrils, generating cellulose nanofibrils with smaller mean diameters at low energy consumption.

ACKNOWLEDGMENTS

This study was financed in part by the Coordenação de Aperfeiçoamento de Pessoal de Nível Superior – Brasil (CAPES) – Finance Code 001, by Conselho Nacional de Desenvolvimento Científico e Tecnológico (CNPq) and Fundação de Amparo à Pesquisa do Estado de Minas Gerais (FAPEMIG). Authors are also thankful for Wood Science and Technology graduation program, Federal University of Lavras (UFLA), Brazil, and Klabin S.A for the provision of cellulosic pulps and part of their characterizations.

REFERENCES

ABITBOL, T. et al. Nanocellulose , a tiny fiber with huge applications. **Current Opinion in Biotechnology**, v. 39, n. I, p. 76–88, 2016.

ARANTES, V.; GOURLAY, K.; SADDLER, J. N. The enzymatic hydrolysis of pretreated pulp fibers predominantly involves "peeling/erosion" modes of action. **Biotechnology for Biofuels**, v. 7, p. 87, 2014.

ASTM. American Society For Testing And Materials. **ASTM D828-16**: Standard Test Method for Tensile Properties of Paper and Paperboard Using Constant Rate of Elongation Apparatus. Philadelphia, 2016.

BALLESTEROS, J. E. M.; SANTOS, V.; MARMOL, G.; FRIAS, M.; FIORELLI, J. Potential of the hornification treatment on *Eucalyptus* and pine fibers for fiber-cement applications. **Cellulose**, v. 24, n. 5, p. 2275-2286, 2017.

BHARDWAJ, N. K.; KUMAR, S.; BAJPAI, P. K. Effects of processing on zeta potential and cationic demand of Kraft pulps. **Colloids and Surfaces A: Physicochemical Engineering Aspects**, v. 246, p. 121–125, 2004.

BIAN, H.; CHEN, L.; WANG, R.; ZHU, J. Green and low-cost production of thermally stable and carboxylated cellulose nanocrystals and nanofibrils using highly recyclable dicarboxylic acids. **Journal of Visualized Experiments,** p. 119, 2017.

BUFALINO, L.; MENDES, L. M.; TONOLI, G. H. D.; RODRIGUES, A.; FONSECA, A.; CUNHA, P. I.; MARCONCINI, J. M. New products made with lignocellulosic nanofibers from Brazilian amazon forest. In: IOP CONFERENCE SERIES: MATERIALS SCIENCE AND ENGINEERING, **Anuais…** v. 64, n. August, p. 1–5, 2014.

BURGUER, L. M.; RICHTER, H. G. Anatomia da madeira. **Nobel**, São Paulo, 154 p., 1991.

CASTRO, A. M.; PEREIRA JR. N. Produção, propriedades e aplicação de celulases na hidrólise de resíduos agroindustriais. **Química Nova,** v. 33, n. 1, p. 181-188, 2010.

CLARKE, K.; LI, X.; LI, K. The mechanism of fiber cutting during enzymatic hydrolysis of wood biomass. **Biomass & Bioenergy**, v. 35, p. 3943–3950, 2011.

CLARO, P.; DE CAMPOS, A.; CORRÊA, A.; RODRIGUES, V.; LUCHESI, B.; SILVA, L.; TONOLI, G. H. D.; MATTOSO, L.; MARCONCINI, J. Curaua and eucalyptus nanofiber films by continuous casting: mixture of cellulose nanocrystals and nanofibrils. **Cellulose**, v. 26, p. 2453-2470, 2019.

CUNHA ARANTES, A. C.; SILVA, L. E.; WOOD, D. F.; DAS GRAÇAS ALMEIDA, C.; TONOLI, G. H. D.; DE OLIVEIRA, J. E.; DA SILVA, J. P.; WILLIAMS, T. G.; ORTS, W. J.; BIANCHI, M. L. Bio-based thin films of cellulose nanofibrils and magnetite for potential application in green electronics. **Carbohydrate Polymers** , v. 207, p. 100-107, 2018.

COLLOIDMETRIX. Comparing three zeta potential analyzers for pulp characterization - Stabino® comes out first for titration and size range. **Application note – Colloid Analysis,** nd. <https://www.colloid-metrix.de/fileadmin/pdf_applications/ZP_comparison%20_3instruments_EN.pdf>

COLODETTE, J.L.; GOMES, F.J.B. Branqueamento de Polpa Celulósica. Viçosa: **Editora UFV**, p. 353-406, 2015.

DIAS, M. C. Alkaline pre-treatments and different parameters as facilitators for obtaining cellulose nanofibrils. 2017. 62 p. Dissertação (Mestrado em Ciência do Solo)-Universidade Federal de Lavras, Lavras, 2017.

DOMUN, N.; HADAVINIA, H.; ZHANG, T.; SAINSBURY, T.; LIAGHATA, G. H.; VAHIDA, S. Improving the fracture toughness and the strength of epoxy using nanomaterials – a review of the current status. **Nanoscale**, v. 7, p. 10294-10329, 2015.

DUFRESNE, A.; CAVAILLE, J.; VIGNON, M.R. Mechanical behavior of sheets prepared form sugar beet cellulose microfibrils. **Journal of Applied Polymer Science**, v. 64, n. 6, p. 1185-1194, 1997.

FARDIM, P.; DURÁN, N. Modification of fibre surfaces during pulping and refining as analysed by SEM, XPS, and ToF-SIMS. **Colloids and Surfaces A**, v. 223, p. 263-276, 2003.

FILSON, P. B.; DAWSON-ANDO, B. E.; SCHWEGLER-BERRY, D. Enzymatic-mediated production of cellulose nanocrystals from recycled pulp. **Green Chemistry : an International Journal and Green Chemistry Resource**, v. 11, n. 11, p. 1808–1814, 2009.

FONSECA, A. S. ; PANTHAPULAKKAL, S.; KONAR, S. K.; SAIN, M.; BUFALINO, L.; RAABE, J.; MIRANDA, I. P. A.; MARTINS, M. A.; TONOLI, G. H. D. Improving cellulose nanofibrillation of non-wood fiber using alkaline and bleaching pre-treatments. **Industrial Crops and Products**, v. 131, p. 203-212, 2019.

GLÓRIA, G. O.; TELES, M. C. A.; LOPES, F. P. D. L.; VIEIRA, C. M. F. V.; MARGEM, F. M. M.; GOMES, M. A. G.; MONTEIRO, S. N. Tensile strength of polyester composites reinforced with PALF. **Journal of Materials Research and Technology**, v. 6, n. 4, p. 401-405, 2017.

GOLDSCHIMID, O. Ultraviolet spectra. In: SARKANEN, K. V.; LUDWIG, C. H. Lignins: occurrence, formation, structure and reations. New York: **John Wiley & Sons**, p. 241-266, 1971.

GOMIDE, J. L.; DEMUNER, B. J. Determinação do teor de lignina em material lenhoso: método Klason modificado. **O Papel,** v. 47, p. 36-38, 1986.

GUIMARÃES JUNIOR, M.; BOTARO, V. R.; NOVACK, K. M.; NETO, W. P. F.; MENDES, L. M.; TONOLI, G. H. D. Preparation of Cellulose Nanofibrils from Bamboo Pulp by Mechanical Defibrillation for Their Applications in Biodegradable Composites. **Nanoscience and Nanotechnology**, v. 15, p. 1–18, 2015.

GUNAWARDHANA, T.; BANHAM, P.; RICHARDSON, D. E.; PATTI, A. BATCHELOR, W. Upgrading waste whitewater fines from a *Pinus* radiata thermomechanical pulping mill. **Nordic Pulp & Paper Research Journal**, v. 32, n. 4, p. 656-665, 2017.

GUPTA, R.; LEE, Y. Mechanism of cellulase reaction on pure cellulosic substrates. **Biotechnology & Bioengineering**, v. 102, n. 6, p. 1570–1581, 2009.

HABIBI, Y.; LUCIA, L. A.; ROJAS, O. J. Cellulose nanocrystals: Chemistry, selfassembly, and applications. **Chemical Reviews**, v. 110, n. 6, p. 3479–3500, 2010.

HE, M.; YANG, G.; CHEN, J.; JI, X.; WANG, Q. Production and characterization of cellulose nanofibrils from different chemical and mechanical pulps. **Journal of Wood Chemistry and Technology**, v. 38, p. 149–158, 2018.

HENNIGES, U.; VEIGEL, S.; LEMS, E.; BAUER, A.; KECKES, J.; PINKL, S.; GINDL-ALTMUTTER, W. Microfibrillated cellulose and cellulose nanopaper from Miscanthus biogas production residue. **Cellulose**, v. 21, n. 3, p. 1601-1610, 2014.

HENRIKSSON, M.; HENRIKSSON, G.; BERGLUND, L. A.; LIDSTROM, T. An environmentally friendly method for enzyme-assisted preparation of microfibrillated cellulose (MFC) nanofibers. **European Polymer Journal**,v. 43, n. 8, p. 3434–3441, 2007.

KANMANI, P.; ARAVIND, J.; KAMARAJ, M.; SURESHBABU, P.; KARTHIKEYAN, S. Environmental applications of chitosan and cellulosic biopolymers: A comprehensive outlook. **Bioresource Technology**, v. 242, p. 295–303, 2017.

KLEMM, D.; KRAMER, F.; MORITZ, S.; LINDSTRÖM, T.; ANKERFORS, M.; GRAY, D.; DORRIS, A. Reviews: Nanocelluloses: A New Family of Nature-Based Materials. **Angewandte Chemie International Edition**, v.50, p.5438 – 5466, 2011.

LE, H. Q.; DIMIC-MISIC, K.; JOHANSSON, L. S.; MALONEY, T.; SIXTA, H. Effect of lignin on the morphology and rheological properties of nanofibrillated cellulose produced from gamma-valerolactone/water fractionation process. **Cellulose**, v. 25, p. 179–194, 2018.

LI, X.; CLARKE, K.; LI, K.; CHEN, A. The pattern of cell wall deterioration in lignocellulose fibers throughout enzymatic cellulose hydrolysis. **Biotechnology Progress**, v. 28, n.6, p. 1389–1399, 2012.

LOPES, T.A.; BUFALINO, L.; JÚNIOR, M.G.; TONOLI, G. H. D.; MENDES, L. M. Eucalyptus wood nanofibrils as reinforcement of carrageenan and starch biopolymers for improvement of physical properties. **Journal of Tropical Forest Science**, v. 30, p. 292-303, 2018.

LU, Z.; FAN, L.; ZHENG, H.; LU, Q.; LIAO, Y.; HUANG, B. Preparation: Characterization and optimization of nanocellulose whiskers by simultaneously ultrasonic wave and microwave assisted. **Bioresource Technology**, v. 146, p. 82–88, 2013.

MATOS, L. C.; ROMPA, V. D.; DAMÁSIO, R. A. P.; MARCONCINI, J. M. TONOLI, G. H. D. Incorporação de Nanomateriais e emulsão de ceras no desenvolvimento de papéis multicamadas. **Scientia Forestales**, Piracicaba, v. 47, n. 122, p. 1-15, jun. 2019

MCKEE, J.; HIETALAT, S.; SEITSONEN, J.; LAINE, J.; KONTTURI, E.; IKKALA, O. Thermoresponsive nanocellulose hydrogels with tunable mechanical properties. **ACS Macro Letters**, v. 3, n. 3, p. 266-270, 2014.

MENDONÇA, M. C. Pré-tratamentos alcalinos como facilitadores da obtenção de nanofibrilas de polpas celulósicas não branqueadas. 2018. 66 p. Dissertação (Mestrado em Engenharia de Biomateriais)-Universidade Federal de Lavras, Lavras, 2018.

MIRHOSSEINI, H.; TAN, C.P.; HAMID, N.S.A.; YUSOF, S. Effect of Arabic gum, xanthan gum and orange oil contents on ζ-potential, conductivity, stability, size index and pH of orange beverage emulsion. **Colloids and Surfaces A: Physicochem. Eng. Aspects**, v.315, p.47–56, 2008.

MIRMEHDI, S.; HEIN, P. R. G.; DE LUCA SARANTÓPOULOS, C. I. G.; DIAS, M. V.; TONOLI, G. H. D. Cellulose nanofibrils/nanoclay hybrid composite as a paper coating: Effects of spray time, nanoclay content and corona discharge on barrier and mechanical properties of the coated papers. **Food Packing and Shelflife**, v. 15, p. 87-94, 2018.

MOON, R. J.; MARTINI, A.; NAIM, J.; SIMONSEN, J.; YOUNGBLOOD, J. Cellulose nanomaterials review: Structure, properties and nanocomposites. **Chemical Society Reviews,** v. 40, n. 7, p. 3941–3994, 2011.

NIE, S.; SAO, S.; WANG, S.; QIN, C. Absorbable organic halide (AOX) reduction in elemental chlorine-free (ECF) bleaching of bagasse pulp from the addition of sodium sulphide. **BioResources** v. 11, p. 713–723, 2016.

OSONG, S. H.; NORGREN, S.; ENGSTRAND, P. Processing of wood-based microfibrillated cellulose and nanofibrillated cellulose, and applications relating to papermaking: a review. **Cellulose**, v. 23, n. 1, p. 93-123, 2016.

PÄÄKKÖ, M.; ANKERFORS, M.; KOSONEN, H.; NYKÄNEN, A.; AHOLA, S.; ÖSTERBERG, M.; RUOKOLAINEN, J.; LAINE, J.; LARSSON, P. T.; IKKALA, O.; LINDSTRÖM, T.Enzymatic Hydrolysis Combined with Mechanical Shearing and High-Pressure Homogenization for Nanoscale Cellulose Fibrils and Strong Gels. **Biomacromolecules**, v. 8, p. 1934-1941, 2007.

PÉREZ, S., SAMAIN, D. Structure and Engineering of Celluloses. **Advances in Carbohydrate Chemistry and Biochemistry.** p. 25 – 116. 2010.

RABELO, S. C. Avaliação do desempenho do pré-tratamento com peroxide de hidrogênio alcalino para a hidrólise enzimática do bagaço de cana-de-açúcar. 2007. Dissertação de mestrado. Universidade Estadual de Campinas (Unicamp) Campinas, 2007.

RAMOS, L. P. The chemistry involved in the pretreatment of lignocellulosic materials. **Química Nova**, v. 26, p. 863-871, 2003.

RESENDE, N. S.; GONÇALVES, G. A. S.; REIS, K. C.; TONOLI, G. H. D.; BOAS, E. V. B. V. Chitosan/Cellulose Nanofibril Nanocomposite and Its Effect on Quality of Coated Strawberries. **Journal of Food Quality**, v. 2018, p. 1-13, 2018.

SANTOS, A. M. P.; YOSHIDA, M. P. Embalagens. Recife: **Edufre,** 152p. ISBN 978-85-7946-090-6, 2011.

SCATOLINO, M. V.; FONSECA, C. S.; DA SILVA GOMES, M.; ROMPA, V. D.; MARTINS, M. A.; TONOLI, G. H. D.; MENDES, L. M. How the surface wettability and modulus of elasticity of the Amazonian paricá nanofibrils films are affected by the chemical changes of the natural fibers. **European Journal of Wood and Wood Products** , v. x, p. 1-14, 2018.

SCHINDELIN, J.; ARGANDA-CARRERAS, I.; FRISE, E.; KAYNIG, V.; LONGAIR, M.; PIETZSCH, T.; PREIBISCH, S.; RUEDEN, C.; SAALFELD, S.; SCHMID, B.; TINEYEZ, J. Y.; WHITE, D. J.; HARTENSTEIN, V.; ELICEIRI, K.; TOMANCAK, P.; CARDONA, A. Fiji: an open-source platform for biológica-imagem analysis. **Nature methods**, v. 9, n. 7, p. 676:682.

SILVA, M. J. F. Avaliação de pré-tratamentos enzimáticos na obtenção de nanofibrilas celulósicas de *Eucalyptus* sp. e *Pinus* sp. 2018. 127 p. Dissertação (Mestrado em Ciência da Madeira) - Universidade Federal de Lavras, Lavras, 2018.

SIQUEIRA, G.; BRAS, J.; DUFRESNE, A. Cellulose whiskers versus microfibrils: Influence of the nature of the nanoparticle and its surface functionalization on the thermal and mechanical properties of nanocomposites. **Biomacromolecules**, v. 10, p. 425–432, 2009.

SMOLIN, A. S.; SHABIEV, R. O.; YAKKOLA, P. The research of zeta potential and cationic demand of chemical and mechanical pulps. **The Chemistry of Plant Raw Materials Academic Journal**, n. 1, p. 177-184, 2009.

SPENCE, K. L.; VENDITTI, R. A.; ROJAS, O. J.; HABIBI, Y.; PAWLAK, J. J. A comparative study of energy consumption and physical properties of microfibrillated cellulose produced by different processing methods. **Cellulose**, v. 18, n. 4, p. 1097–1111, 2011.

STAMM, A.J. Wood and cellulose science. **The Ronald Press Company**, New York, p 549, 1964.

TAPPI. Technical Association of The Pulp And Paper Industry. Test Method T 233 cm-95. Fiber length of pulp by classification. Atlanta, 1995.

TAPPI. Technical Association of The Pulp And Paper Industry. Test Methods TAPPI T 222 om-02. Atlanta, 2006.

TIAN, X.; LU, P.; SONG, X.; NIE, S.; LIU, Y.; LIU, M. Enzyme-assisted mechanical production of microfibrillated cellulose from Northern Bleached Softwood Kraft Pulp. **Cellulose**, v. 24, n. 9, p. 3929–3942, 2017.

TONOLI, G. H. D.; HOLTMAN, K. M.; GLENN, G.; FONSECA, A. S.; WOOD, D.; WILLIANS, T.; SA, V. A.; TORRES, L.; KLAMCZYNSKI, A.; ORTS, W. J. Properties of cellulose micro/nanofibers obtained from *Eucalyptus* pulp fiber treated with anaerobic digestate and high shear mixing. **Cellulose**, v. 23, n. 2, p. 1239–1256, 2016.

TONOLI, G. H. D.; TEIXEIRA, E. M.; CORREA, A. C.; MARCONCINI, J. M.; CAIXETA, L. A.; PEREIRA DA SILVA, M. A.; MATTOSO, L. H. C. Cellulose micro/nanofibres from *Eucalyptus* Kraft pulp: Preparation and properties. **Carbohydrate Polymers**, v. 89, p. 80-88, 2012.

WALLIS, A. F. A.; WEARNE, R. H.; WRIGHT, P. J. Chemical analysis of polysaccharides in plantation eucalypt woods and pulps. **Appita Journal**, v. 49, n. 4, p. 258-262, 1996.

WANG, Q. Q.; ZHU, J. Y.; GLEISNER, R.; KUSTER, T. A.; BAXA, U.; MCNEIL, S. E. Morphological development of cellulose fibrils of a bleached *Eucalyptus* pulp by mechanical fibrillation. **Cellulose**, v. 19, n. 5, p. 1631-1643, 2012.

WINTER, H. T.; CERCLIER, C.; DELORME, N.; BIZOT, H.; QUEMENER, B.; CATHALA, B. Improved colloidal stability of bacterial cellulose nanocrystal suspensions for the elaboration of spin-coated cellulose-based model surfaces. **Biomacromolecules**, v. 11, n. 11, p. 3144-3151, 2010.

WINUPRASITH, T.; SUPHANTHARIKA, M. Microfibrillated cellulose from mangosteen (Garcinia mangostana L.) rind: Preparation, characterization, and evaluation as an emulsion stabilizer. **Food Hydrocolloids**, v.32, p.383-394, 2013.

ZHU, H.; LUO, W.; CIESIELSKI, P. N.; FANG, Z.; ZHU, J. Y.; HENRIKSSON, G. Wood derived materials for green electronics, biological devices, and energy applications. **Chemical Reviews**, v. 116, n. 16, p. 9305–9374, 2016.

ZHU, J. Y.; SABO, R.; LUO, X. Integrated production of nano-fibrillated cellulose and cellulosic biofuel (ethanol) by enzymatic fractionation of wood fibers. **Green Chemistry**, London, v. 13, n. 5, p. 1339, 2011.

QUARTA PARTE

CONCLUSÕES DESTA DISSERTAÇÃO

Foram comparados pré-tratamentos para obtenção de nanofibrilas a um baixo consumo energético. A comparação entre extração e caracterização de nanofibrilas ocorreu entre enzima A (A), enzima B (B), oxidação mediada por 1-oxil-2,2,6,6-tetrametilpiperidina (TEMPO; T) e sem a adição de enzima (WE).

O pré-tratamento enzimático mostrou que as enzimas A e B não causaram alteração significativa na composição química e também nas características anatômicas. Isso indica que a aplicação de enzimas não modifica a qualidade das fibras. Ainda assim, a atividade enzimática de endoglucanase provocou uma diminuição no diâmetro mediano das nanofibrilas. Essa diminuição no diâmetro médio aumentou a estabilidade da suspensão de nanofibrilas em água e aumentou a turbidez do sobrenadante. As nanofibrilas extraídas de polpas branqueadas pré-tratadas com enzimas apresentaram diâmetros menores, com valores próximos a 19 nm, próximos as nanofibrilas pré-tratadas com o tratamento TEMPO, com mediana de 17 nm. A extração de nanofibrilas de polpas pré-tratadas com enzimas apresentou menor consumo energético.

A polpa CTMP parece não ter sido afetada pela atividade enzimática, já que não apresentou uma consistência gelatinosa. Seu teor de lignina foi superior ao de polpas Kraft. A lignina provavelmente inibiu a atividade da endoglucanase sobre a cadeia de celulose.

A atividade da enzima A provocou diminuição significativa do consumo de energia para fibrilação de polpas Kraft branqueadas, alcançando 58% de economia. A enzima B, por outro lado, diminuiu o consumo de forma mais significativa para polpas de *Pinus* não branqueada. A suspensão tratada pela oxidação mediada por TEMPO apresentou nanofibrilas individualizadas enquanto que nanofibrilas provindas de polpa pré-tratada com enzima apresentou estruturas com diferentes diâmetros e fibras ainda em desconstrução. Entretanto, tal diâmetro médio foi inferior ao observado para polpa não tratada com enzima. O pré-tratamento enzimático também foi capaz de aumentar a estabilidade das suspensões em água para ambas as polpas branqueadas e não branqueadas, bem como gerar um aumento na turbidez de nanofibrilas no sobrenadante. Isso indica maior quantidade de nanofibrilas do que os tratamentos em que não foi utilizado enzima.

O presente trabalho mostrou que a utilização de pré-tratamento enzimático diminui o consumo energético, mantendo características químicas e anatômicas das fibras e nanofibrilas.

Entretanto, para trabalhos futuros sugere-se a aplicação de diferentes enzimas e dosagens de enzimas avaliando o custo-benefício do aumento da dosagem nas características morfológicas das nanofibrilas. Ainda, seria adequado realizar a caracterização da resistência de filmes em diferentes graus de fibrilação, para entender como excessivas desfibrilações agem sobre suas propriedades mecânicas. Ainda, estudos devem ser realizados para superar a dificuldade de desfibrilação de polpas CTMP. Neste caso, o uso de enzimas para a lignina pode ser uma alternativa interessante para ser testada como pretratamento para melhorar a fibrilação.

Vale ressaltar ainda a importância de se aprofundar o estudo da caracterização de nanofibrilas de celulose, verificando grau de desfibrilação, por exemplo. A turbidez é uma caracterização que pode ser mais bem explorada pela modificação da metodologia, verificando diferentes diluições. Existe ainda uma variedade de coquetéis enzimáticos no mercado para serem testados, sintetizados ou purificados.

APÊNDICE

Tabela 1A – Composição química dos carboidratos de polpas Kraft branqueadas de *Eucalyptus* sp. e *Pinus* sp.

Amostra	Carboidratos, %					
	Glicana	Xilana	Manana	Arabinana	Galactana	Carboidratos totais
B-Euc WE	75,2 ± 0,2	12,4 ± 0,1	0,0 ± 0,0	0,0 ± 0,0	0,0 ± 0,0	87,6 ± 0,1
B-Euc A	75,3 ± 0,5	12,5 ± 0,1	0,0 ± 0,0	0,0 ± 0,0	0,0 ± 0,0	87,8 ± 0,5
B-Euc B	75,6 ± 0,1	12,5 ± 0,1	0,0 ± 0,0	0,0 ± 0,0	0,0 ± 0,0	88,0 ± 0,1
B-Pin WE	76,1 ± 0,1	7,7 ± 0,1	5,7 ± 0,1	0,4 ± 0,1	0,2 ± 0,1	90,3 ± 0,1
B-Pin A	71,9 ± 0,3	7,3 ± 0,1	6,0 ± 0,1	0,3 ± 0,1	0,2 ± 0,1	85,8 ± 0,3
B-Pin B	74,4 ± 1,2	7,6 ± 0,2	5,8 ± 0,1	0,4 ± 0,1	0,2 ± 0,1	88,4 ± 1,4

Tabela 2A – Composição química dos carboidratos de polpas Kraft não branqueada de *Eucalyptus* sp. e *Pinus* sp. e polpa quimiotermomecânica (CTMP) de *Eucalyptus* sp.

	Carboidratos, %					
Amostra	**Glicana**	**Xilana**	**Manana**	**Arabinana**	**Galactana**	**Carboidratos Totais**
UB-Euc WE	58,8 ± 1,1	9,8 ± 0,3	0,25 ± 0,4	0,0 ± 0,0	0,6 ± 0,1	69,5 ± 1,1
UB-Euc A	54,5 ± 0,7	9,4 ± 0,1	0,0 ± 0,0	0,4 ± 0,1	0,6 ± 0,1	64,8 ± 0,9
UB-Euc B	59,5 ± 1,4	10,0 ± 0,3	0,0 ± 0,0	0,0 ± 0,0	0,6 ± 0,1	70,1 ± 1,7
CTMP WE	43,7 ± 1,3	9,6 ± 0,1	0,9 ± 0,1	0,6 ± 0,5	1,0 ± 0,1	55,7 ± 1,1
CTMP A	43,7 ± 0,9	9,1 ± 0,6	0,9 ± 0,1	0,3 ± 0,1	1,0 ± 0,1	55,0 ± 1,6
CTMP B	43,7 ± 0,8	9,3 ± 1,0	0,8 ± 0,1	0,6 ± 0,4	1,0 ± 0,1	55,4 ± 2,1
UB-Pin WE	64,2 ± 0,5	7,2 ± 0,2	4,5 ± 0,2	0,8 ± 0,1	0,6 ± 0,1	77,3 ± 0,9
UB-Pin A	62,9 ± 1,1	7,5 ± 0,1	5,0 ± 0,1	0,8 ± 0,1	0,7 ± 0,1	76,9 ± 1,4
UB-Pin B	65,0 ± 1,3	7,3 ± 0,3	4,9 ± 0,1	0,8 ± 0,1	0,6 ± 0,1	78,7 ± 1,6

Tabela 3A – Composição de lignina solúvel e insolúvel de polpas Kraft não branqueadas de *Eucalyptus* sp. e *Pinus* sp. e polpa quimiotermomecânica (CTMP) de *Eucalyptus* sp.

Amostra	Lignina insolúvel, %	Lignina solúvel, %
UB-Euc WE	19,1 ± 0,2	3,2 ± 0,2
UB-Euc A	19,9 ± 1,1	3,9 ± 1,0
UB-Euc B	20,0 ± 0,3	3,0 ± 0,2
CTMP WE	31,0 ± 0,6	3,0 ± 0,2
CTMP A	32,7 ± 1,9	3,1 ± 0,1
CTMP B	32,7 ± 1,5	3,1 ± 0,2
UB-Pin WE	13,4 ± 3,0	0,9 ± 0,3
UB-Pin A	13,0 ± 0,3	0,5 0,1±
UB-Pin B	13,3 ± 1,3	0,4 ± 0,1